

CLIENT
THE OCEAN CLEANUP



PROJECT
FLOATING BARRIER HYDRODYNAMICS

DOCUMENT TITLE
3D MODEL TEST RESULTS

PROJECT NUMBER 15020

DOCUMENT NUMBER 15020-TOC-H-AR-001-02

CLIENT DOCUMENT NUMBER 15020-TOC-H-AR-001

DATE: APRIL 10, 2016



mocean



ADVANCED OFFSHORE TECHNOLOGY



REPORT ISSUE STATUS

02	09/04/16	FINAL ISSUE	MAP	WVS	WVS	JEK
01	29/03/16	ISSUED FOR REVIEW	MAP	WVS	WVS	JEK
00a	15/02/16	ISSUED FOR INFORMATION	MAP	WVS	WVS	JEK
Rev.	Issue Date	Reason for Issue	Made by	Docu. Chk	Num. Chk	Appr.

REVISION HISTORY

02	Minor changes
01	Updated for comments
00	Issued to inform
Rev.	Revision info

Executive Summary

Early November 2015 two weeks of 3D scale model tests have been carried out at MARIN's Offshore Basin, one of the worlds most renowned test facilities for floating structures. With the test setup it was possible to simulate barrier lengths of up to 3600m using a prototype length of 360m long, with a scale of approximately 1/18, leading to a scale model of approximately 20m long. Tests were conducted mostly in regular waves, as the response in these waves enables to efficiently understand the system dynamic characteristics and load response. Also a number of irregular wave tests have been carried out; one test that closely resembles a Pacific Ocean sea state, with long waves and relatively mild current, and one test that is similar to a North Sea storm condition, governed by short and steep waves with high current.

In order to learn as much as possible about the system, various configurations are tested: a low, high and secondary mooring concept. This indicates the location of the tension wire in the system: placed underneath the floater, at the ballast weight location or externally, i.e. by usage of an external subsea wire. Furthermore, the high mooring concept has been tested for increased pretensions, in order to simulate a boom much longer than the actual barrier in the tank. By considering the model as a section of a virtually longer barrier span, the loads for this virtual barrier can be derived by simulating the loads of the adjoining structures by increased pretension in the mooring lines.

This report presents the main results and findings from this test campaign, which was the first model testing campaign of its kind; with a 3D floating barrier subject to waves and currents from various directions. Before the tests were carried out there were many unknowns with respect to the 3D motions of the barrier. For instance, how the system performs in waves: do waves run over the barrier (overtopping)? Do gaps appear underneath the screen (bridging)? Measurements from the various tests are used to:

1. Study the:
 - a. Hydrodynamic Response of a floating barrier system
 - b. Plastic capturing efficiency (bridging and overtopping occurrences)
2. Calibrate and validate numerical models

This report focusses on understanding the physics of the system, such that in a numerical environment parametric variation leading to an optimized design can be performed. As such, even though no extreme Pacific storm has been carried out (this was not feasible in the basin), the situation can be accurately modelled.

The three mooring configurations behave in terms of hydrodynamics highly similar, especially in waves. In high current velocities, the low mooring and secondary mooring boom are subjected to higher loads than the high mooring.

The most important finding of tests is that loads in waves are lower than what was expected. By smart engineering the forces in a Pacific Ocean barrier in storm conditions can be kept lower than expected,



reducing the amount of mooring lines required and greatly impacting the costs. In order to realize this, the system has to be flexible. A flexible system can move along with the 2D wave surface and governing loads are caused by current. Even more so, a flexible system will also show less overtopping and bridging. It is therefore highly recommended that the tension member of the Pacific array in a high or low mooring system is made out of stretchable material such as Polyester or Nylon.

The system responds excellent in long waves: no bridging and overtopping is observed and loads are mild. In the Pacific Ocean 97.5% of the waves are long, promising high workability of the Pacific array.

The wave loading can be decomposed in a low, wave and high frequent component. The low frequent phenomena cause the highest loads and is more dominant in low pretensions. It oscillates with a much lower frequency than the wave frequency. Two types of low frequency motions are observed: transient motions during wave build-up, and low frequent motions in irregular sea states. Wave frequent loads remain low, even in higher pretensions. At a certain threshold the system cannot flexibly follow the waves anymore and wave frequent loads increase. Even though these loads were found to be higher for the highest pretension, relative to the current load they are small. A high frequent component (at twice or three times the wave frequency) is observed in all configurations. It is thought to be caused by a pitching motion (rotation about the length axis) of the floater. The magnitude of this component is relatively low: in some cases equal to the wave frequent component, but in most lower. Even though the magnitude is low, due to the high frequency it may cause local fatigue damage. This effect should be investigated, it may be mitigated by installing an additional tension wire on top of the floater.

Effects such as the low frequent and transient motion, which cause high loads and offsets, or the high frequent pitch, have not been found as such in numerical simulations. The model test campaign has shown to be of key importance in understanding the dynamics of a floating barrier. Furthermore, the results provide confidence in further strengthening the feasibility of an ultra-long floating barrier type of artificial coastline in the Pacific Ocean, in order to retrieve ocean plastics.



Table of Contents

Executive Summary	2
1 Introduction.....	10
1.1 Project Information	10
1.2 Document Scope	12
1.3 References	12
1.3.1 External References.....	12
1.4 Conventions	13
1.4.1 Tank.....	13
1.4.2 Model	14
2 Model Test Setup.....	15
2.1 Model & Mooring Properties	15
2.1.1 Main Dimensions	15
2.1.2 Mooring System	16
2.1.3 Mechanical Properties.....	19
2.1.4 Pretension.....	20
2.2 Instrumentation.....	20
2.2.1 Model Based Instrumentation.....	20
2.2.2 Tank Based Instrumentation	21
2.3 Environmental Criteria.....	22
2.3.1 Current.....	22
2.3.2 Irregular Waves Environmental Combinations.....	23
2.3.3 Regular Waves Environmental Combinations	24
2.4 Load Cases	24
3 Test Programme.....	25
4 Analysis	26
4.1 Frequency Domain Analysis.....	26
4.2 Post-Processing of Results.....	26
4.3 Floating Barrier Response Expectation	27
4.3.1 Hydrodynamic Response.....	27
4.3.2 Overtopping & Bridging.....	31
5 Results	36



5.1	Wave and Current Calibration.....	36
5.1.1	Current Only.....	36
5.1.2	Regular Waves.....	37
5.1.3	Irregular Waves.....	40
5.2	Tests in Current.....	43
5.3	Tests in Regular Waves & Current.....	46
5.3.1	Motions.....	47
5.3.2	Loads.....	64
5.3.3	Bridging and overtopping.....	80
5.4	Tests in Irregular Waves & Current.....	81
5.4.1	Motions.....	83
5.4.2	Loads.....	86
5.4.3	Overtopping and bridging.....	93
6	Performance of Configurations.....	97
7	Conclusion & Recommendations.....	100
7.1	Conclusions.....	100
7.2	Recommendations.....	101
Appendix A -	Stiffness & Weight of the Model.....	102
Appendix B -	Load Cases (Carried Out).....	106
Appendix C -	Overtopping & Bridging.....	110
Appendix D -	Photos.....	114



List of Figures

Figure 1-1: Great Pacific Garbage Patch Location.....	10
Figure 1-2: Artist Impression of Ocean Cleanup Barrier.....	11
Figure 1-3: The Effects of Ocean Plastic Waste to Marine Life	11
Figure 1-4: Tank conventions.....	13
Figure 1-5: Model axis convention.....	14
Figure 2-1: Cross section model.....	15
Figure 2-2: High mooring configuration.....	17
Figure 2-3: Low mooring configuration	17
Figure 2-4: Secondary mooring configuration.....	18
Figure 2-5: Cross section secondary mooring configuration	18
Figure 2-6: High mooring concept with instrumentation.....	21
Figure 2-7: Location of wave and current measurement sensors during calibration	22
Figure 4-1: Example frequency domain plot.....	26
Figure 4-2: Example fluid velocity.....	28
Figure 4-3: Expected response to a regular wave	29
Figure 4-4: Spectral density of system excursion and Morison load in a regular wave	29
Figure 4-5: System excursion and Morison force in two regular waves.....	30
Figure 4-6: Spectral density of system excursion and Morison load in two regular waves	31
Figure 4-7: Example of bridging and overtopping.....	32
Figure 4-8: Quasi-static vertical load component in system under pretension	33
Figure 4-9: Quasi-static vertical load component in system under pretension for a Stokes wave	34
Figure 4-10: Bridging or overtopping expected behaviour example for a single system configuration .	35
Figure 5-1: 0.3m/s current calibrated time signal (upper) and energy density (lower).....	36
Figure 5-2: 1.0m/s current calibrated time signal (upper) and energy density (lower).....	37
Figure 5-3: Regular wave modelling.....	38
Figure 5-4: 225 and 270 degrees SLS wave cases (blue measured and red theoretical)	40
Figure 5-5: 225 and 270 degrees ULS wave cases (blue measured and red theoretical).....	41
Figure 5-6: Wave spectra at various locations and fluid velocity (REF) for ULS 225 sea state	42
Figure 5-7: Decline in fluid velocity (REF) for SLS 225 case	43
Figure 5-8: Centre displacement for all configurations	44
Figure 5-9: Starboard and port side mean tension for all configurations	44
Figure 5-10: Transverse load due to current (total)	45
Figure 5-11: Unit load (transversal load normalized with span).....	46
Figure 5-12: Drag coefficient (constant area assumption)	46
Figure 5-13: 270 degree (parallel to system) regular wave spectral density plots: filter placed at 1.5 rad/s	47
Figure 5-14: Horizontal motion snapshot for 0.3 and 1.0 m/s current cases (equal wave conditions)..	48
Figure 5-15: Surge motion time trace of high mooring low pretension regular wave test	48
Figure 5-16: Low pass surge for high mooring low pretension 3m waves in 0.3 m/s current	50



Figure 5-17: Low pass surge for high mooring low pretension 6m waves in 0.3 m/s current 50

Figure 5-18: H6 T7.3 180 deg surge for different configurations51

Figure 5-19: H6 T7.3 180 deg surge for different configurations (normalized for starting position to see differences between configurations)51

Figure 5-20: H6m T6.5s 225 deg surge for different configurations..... 52

Figure 5-21: H6m T6.5s 225 deg surge for different configurations (normalized for starting position) 52

Figure 5-22: Maximum surge motion for high mooring low pretension cases 53

Figure 5-23: Transient motion maximum..... 53

Figure 5-24: Surge wave frequent response 54

Figure 5-25: Surge high frequent (twice the wave frequency) response 54

Figure 5-26: Wave frequent surge response for various configurations in 0.3 m/s current..... 55

Figure 5-27: Wave frequent surge response for various configurations in 1.0 m/s current 55

Figure 5-28: Transient motions in 0.3 m/s current 56

Figure 5-29: Transient motions in 1.0 m/s current 56

Figure 5-30: Starboard wave frequent accelerations in x-direction 57

Figure 5-31: Starboard high frequent (twice the wave frequency) accelerations in x-direction 57

Figure 5-32: Wave frequent sway motion 58

Figure 5-33: High frequent (twice the wave frequency) sway motion..... 58

Figure 5-34: Wave frequent accelerations in boom direction 59

Figure 5-35: High frequent (twice wave frequency) accelerations in boom direction..... 59

Figure 5-36: Pitch motion of centre cross section 60

Figure 5-37: Time trace of pitch motion for test 802003 (H3m, T5.2s, 270deg)61

Figure 5-38: Mean pitch angle (high mooring, low pretension)61

Figure 5-39: Mean pitch angle (low mooring, low pretension) 62

Figure 5-40: Wave frequent pitch amplitude (high mooring, low pretension)..... 63

Figure 5-41: High frequent pitch amplitude (high mooring, low pretension) 63

Figure 5-42: High frequent pitch amplitude for all configurations in 0.3m/s current 64

Figure 5-43: High frequent pitch amplitude for all configurations in 1m/s current 64

Figure 5-44: Unit load for H6 T6.5 deg225..... 65

Figure 5-45: Unit load for H6 T6.5 deg225 (filtered and normalized to start at zero) 66

Figure 5-46: Unit load for H6 T7.3 deg180 66

Figure 5-47: Unit load for H6 T7.3 deg180 (filtered and normalized to start at zero) 67

Figure 5-48: Transverse wave frequent load component (high mooring low pretension)..... 68

Figure 5-49: Transversal high frequent load component (twice the wave frequency, high mooring low pretension) 69

Figure 5-50: Wave frequent transverse load in 0.3 m/s current for various configurations 69

Figure 5-51: Transverse load in 0.3 m/s as a function of the relative wave velocity squared 70

Figure 5-52: Wave frequent transverse load in 1.0 m/s current for various configurations..... 70

Figure 5-53: Transverse load in 1.0 m/s as a function of the relative wave velocity squared 71

Figure 5-54: Transient transverse peak load in 0.3 m/s current 71



Figure 5-55: Transient transverse peak load in 1.0 m/s current 72

Figure 5-56: Wave frequent unit load amplitude in 0.3 m/s current for various configurations 72

Figure 5-57: Wave frequent unit load amplitude in 1.0 m/s current for various configurations 73

Figure 5-58: High frequency amplitude in port side mooring line..... 73

Figure 5-59: Low frequent subsea mooring wire load time traces (225&180 deg waves)..... 74

Figure 5-60: Wave frequent tension in port side part of submerged mooring line 75

Figure 5-61: High frequent (twice wave frequency) tension in port side part of submerged mooring line 75

Figure 5-62: Time trace of secondary mooring lines tension (0.3 m/s current, 6m 7.3s 225 deg waves) 76

Figure 5-63: Spectral density load (0.3 m/s current, 6m 7.3s 225 deg waves)..... 76

Figure 5-64: Low frequent load of secondary mooring line 5 time traces (225&180 deg waves)77

Figure 5-65: Secondary mooring line linear amplitude (0 m/s current)77

Figure 5-66: Secondary mooring line linear amplitude (0.3 m/s current) 78

Figure 5-67: Secondary mooring line linear amplitude (1.0 m/s current) 78

Figure 5-68: Secondary mooring high freq. amplitude (0 m/s current) 79

Figure 5-69: Secondary mooring high freq. amplitude (0.3 m/s current) 79

Figure 5-70: Secondary mooring high freq. amplitude (1.0 m/s current)80

Figure 5-71: Snapshot of test showing both bridging and overtopping..... 81

Figure 5-72: Typical time trace loads in springs 82

Figure 5-73: Spectral density of load signal (left) and input wave spectrum (right)—ULS 225 degrees high mooring setup..... 82

Figure 5-74: Time trace of starboard unfiltered load, on the left the transient ramp-up time and on the right the filtered signal including selected peaks..... 83

Figure 5-75: Extreme value fit with 95% confidence interval 83

Figure 5-76: Surge motion significant values, including mean current contribution 84

Figure 5-77: Surge motion significant values, current contribution removed..... 85

Figure 5-78: Comparison of displacement contributions: mean, low, wave and high frequency 85

Figure 5-79: Time trace of pitch motion of test 803004 (high mooring, high ballast, medium pretension, ULS 225 deg)..... 86

Figure 5-80: 3hr MPM (low frequency) of port and starboard side loads 87

Figure 5-81: Load contributions (port side)..... 88

Figure 5-82: Normalized loads (port side)..... 88

Figure 5-83: Fitted MPM and extrapolated 3hr MPM of low frequent transverse load..... 89

Figure 5-84: Transverse load contributions..... 89

Figure 5-85: Relative transverse loads 90

Figure 5-86: Time trace of secondary mooring line 3 and 6 in 225deg ULS91

Figure 5-87: Significant amplitude of secondary mooring lines91

Figure 5-88: Load components of highest loaded line (number 3) 92

Figure 5-89: Load components of port side subsea tension line 92



Figure 5-90: Comparison of mean (including pretension) and low frequent 3 hour MPM of subsea mooring line tension..... 93
Figure 5-91: High mooring (low pretension) 270 deg ULS..... 95
Figure 5-92: Low mooring 270 deg ULS 95
Figure 5-93: Secondary mooring 270 deg ULS 96
Figure 6-1: Rough load component ratio in a transient and steady state (irregular seas 1m/s and 6m Hs) condition 97
Figure 7-1: High mooring low pretension 225 deg ULS 114
Figure 7-2: High mooring med pretension 225 deg ULS 115
Figure 7-3: High mooring high pretension 225 deg ULS 115
Figure 7-4: Low mooring 225 deg ULS..... 116
Figure 7-5: Secondary mooring 225 deg ULS 116

List of Tables

Table 2-1: Main dimension properties16
Table 2-2: System mechanical properties19
Table 2-3: Pretensions used in model test 20
Table 2-4: Overview of current cases 23
Table 2-5: Irregular wave parameters 23
Table 2-6: Regular wave parameters 24
Table 5-1: Regular wave calibration summary 39
Table 5-2: Irregular wave calibration summary 40
Table 5-3: Quality of realized wave spectra at various locations 42
Table 5-4: Overtopping and bridging events in irregular waves..... 94
Table 6-1: Configuration hydrodynamic response performance 98
Table 6-2: Configuration plastic holding performance 98
Table 6-3: Pretension hydrodynamic performance 99
Table 6-4: Pretension plastic holding performance 99

1 Introduction

1.1 Project Information

The Ocean Cleanup (TOC) is developing a permanent floating barrier, to extract harmful plastic debris from the ocean. The aim of TOC is to install a barrier in the great pacific garbage patch (Figure 1-1) in 2020. Plastic that doesn't beach ends up in one of the five patches, the biggest patch today is found in the Pacific gyre. The system is a passive system that relies on the mean surface current to intercept plastics in the top level of the ocean, see Figure 1-2. This way, substantial amounts of plastic can be removed. This way the system acts as an artificial coastline. It is, as for today, not yet possible to give an accurate estimation of the total amount of plastics that can be removed as this is determined by: the total mass of the great pacific garbage patch, the distribution of the debris over the sea surface and the efficiency of the boom.



Figure 1-1: Great Pacific Garbage Patch Location

The problem is widely acknowledged, as the consequences for coastal communities, the ecosystem, marine life and shipping become more and more visible. Examples of the impact of plastics for marine species are given in Figure 1-3.



Figure 1-2: Artist Impression of Ocean Cleanup Barrier



Figure 1-3: The Effects of Ocean Plastic Waste to Marine Life

1.2 Document Scope

A key aspect to designing of a permanently moored floating barrier is understanding of the hydrodynamic forces that act on such a flexible system. Previously, model testing has been carried out for a simplified 2D boom at Deltares. However, 3D aspects play a crucial role in the motions and loads occurring in a barrier subjected to current and waves. There exists very limited literature on this subject, as no other mission of this scale—100 km long system moored at least 10 years—has been performed. Particularly challenging in terms of hydrodynamics, is that the motions of the barrier disturb the flow, which then again influences the system: the fluid and structure are strongly coupled. In order to better understand this phenomenon, multiple configurations of a floating barrier have been tested at MARIN's Offshore Basin. This basin provides dimensions that can accommodate a 360m section at a scale of 1:18 and has good possibilities to generate different current speeds and wave conditions from different directions. This document presents measurements and more important interpretation of these results:

- The tension in the boom in transverse current and varying wave parameters
- The forces in the suspension points
- The gaps (bridging and overtopping) between boom and water surface

Tests have been carried out for three different configurations: a high, low and secondary mooring. In the first the system is suspended right underneath the cylindrical floater where a tension line runs, in the second the ballast weight is used for this purpose. The secondary mooring system decouples the high loads in current from the dynamic wave induced loads, by having a secondary subsea tension member that connects to the screen at multiple locations. Furthermore, by subjecting the system to a pretension, the barrier behaves as it was part of a much longer system, enabling the possibility to simulate a barrier of more than 2 km with only 360 m boom in the basin. Lastly, the mooring system is not considered in these tests, as it is not possible to have a scaled 4 km mooring system in the basin and more importantly: the mooring design is not sufficiently mature for model testing. This test focusses on flexible barrier hydrodynamics.

The model tests provide understanding of the response of a barrier in waves and current and also serves to calibrate and validate the numerical hydrodynamic models that are being developed to design the barrier and its mooring system. Calibrated models are key to designing a permanent system, as they ensure various sea states can be simulated in order to determine governing loads and motions, which determine the design of the system.

1.3 References

1.3.1 External References

- [ER.1] The Ocean Cleanup Wave and Current Load Model Tests, 28559-1-OB-2.0

1.4 Conventions

1.4.1 Tank

Tank conventions are provided in Figure 1-4.

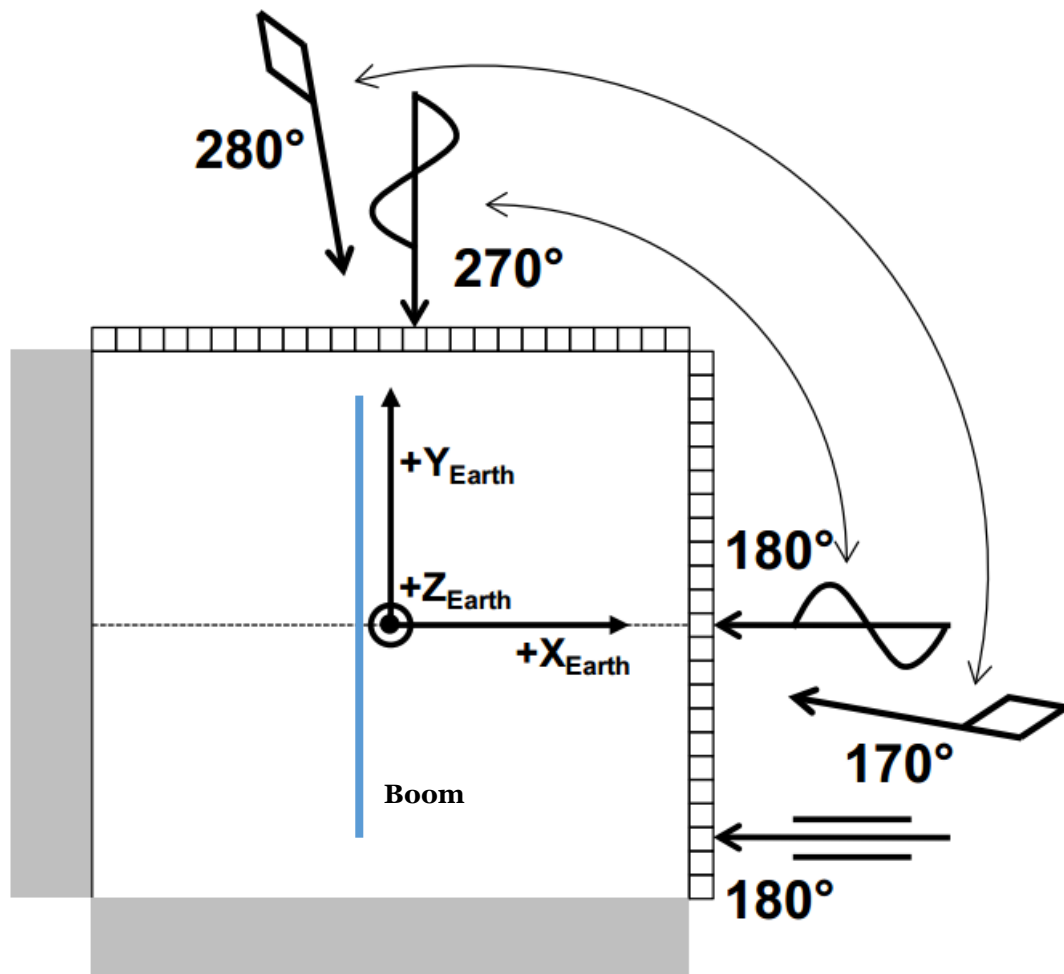


Figure 1-4: Tank conventions

1.4.2 Model

Model axes conventions are shown in Figure 1-5. Port side corresponds with the upper part of Figure 1-4 (positive surge points towards the current outlet, sway towards the wave maker side of the basin).

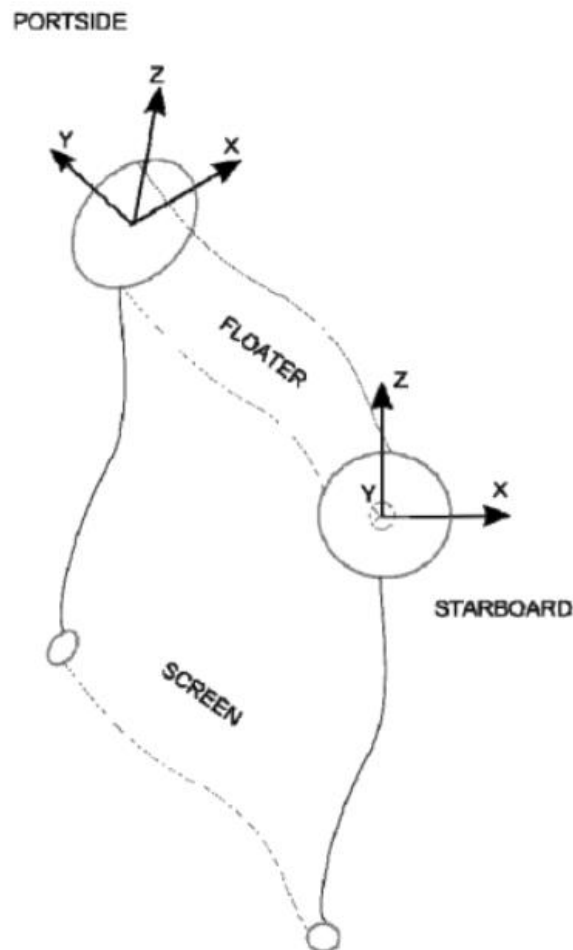


Figure 1-5: Model axis convention

Barrier motions are expressed relative to any point on the floater (as the system is flexible and deforms consequently). In the figure above, the six (6) motion components are indicated as follows:

- surge x : translation along x-axis, positive in positive x direction
- sway y : translation along y-axis, positive in positive y direction
- heave z : translation along z-axis, positive in positive z direction
- roll ϕ : rotation around x-axis, positive with positive y down
- pitch θ : rotation around y-axis, positive with positive x down
- yaw ψ : rotation around z-axis, positive x to portside

2 Model Test Setup

2.1 Model & Mooring Properties

2.1.1 Main Dimensions

Three mooring layout or system setups have been tested. The barrier design remains equal, consisting of a flexible floater, a screen and a ballast weight. A schematic cross section of the boom is provided in Figure 2-1.

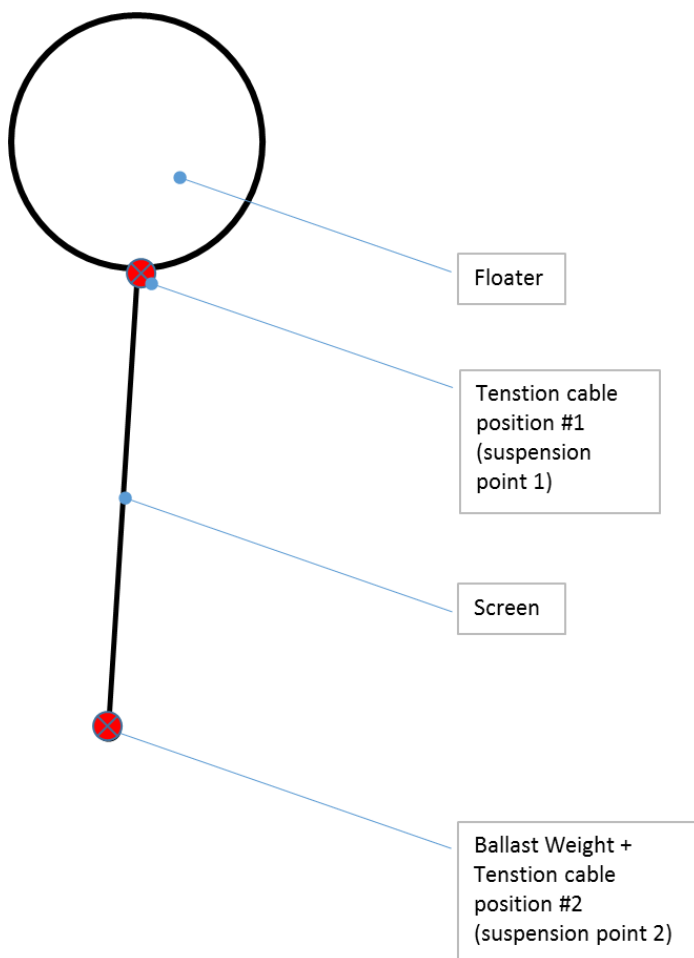


Figure 2-1: Cross section model

The main dimensions (prototype scale) of the barrier (floater diameter, screen length, etc.) are provided in Table 2-1. The barrier is scaled by Froude law, at a geometric scale of 18.8.

Table 2-1: Main dimension properties

Item	Symbol	Value	Unit
Barrier length	L	360	m
Diameter floater	D	1.5	m
Skirt length	L _s	2	m

2.1.2 Mooring System

Three different suspensions will be tested:

1. **High suspension:** on both ends of the boom a connection is made, with the suspension point at the screen/floater connection point.
2. **Low suspension:** also on both ends of the boom, however the suspension point is in this case the ballast chain/wire.
3. **Secondary suspension:** an extra tension cable is suspended to which the lower end of the boom is connected with a cable, every other 60m.

Schematic representations of these three models are presented on the following pages. The distance from the suspension points that are mounted to the basin carriage is also provided in these figures.

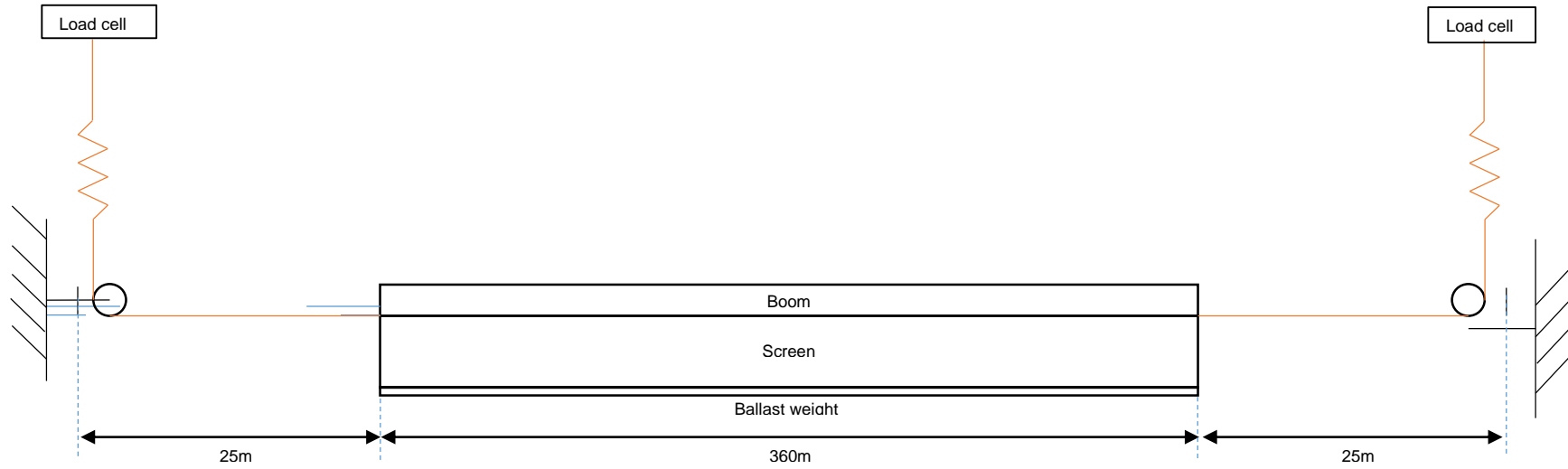


Figure 2-2: High mooring configuration

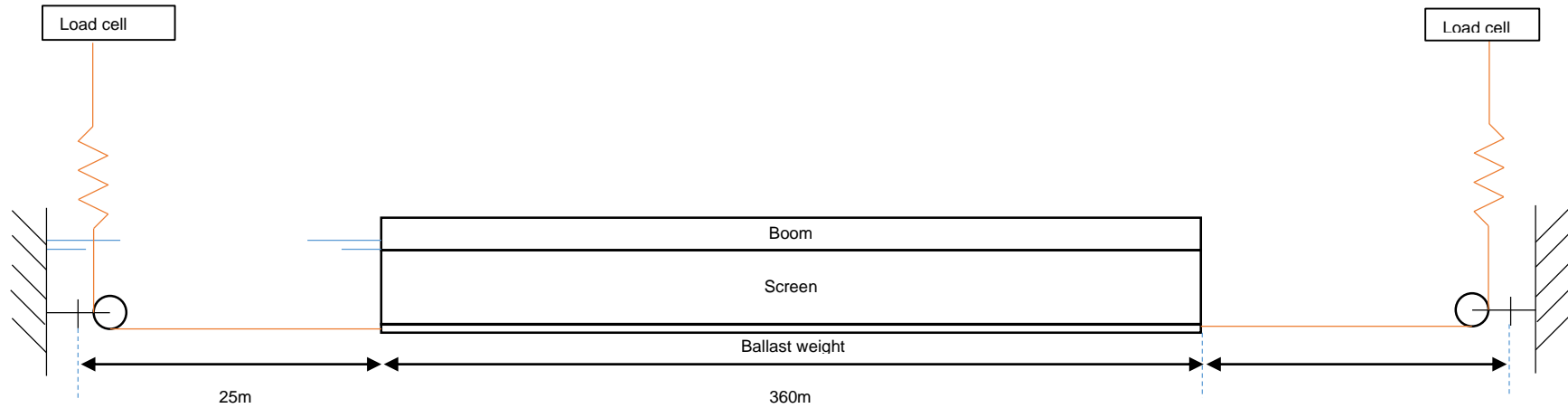


Figure 2-3: Low mooring configuration

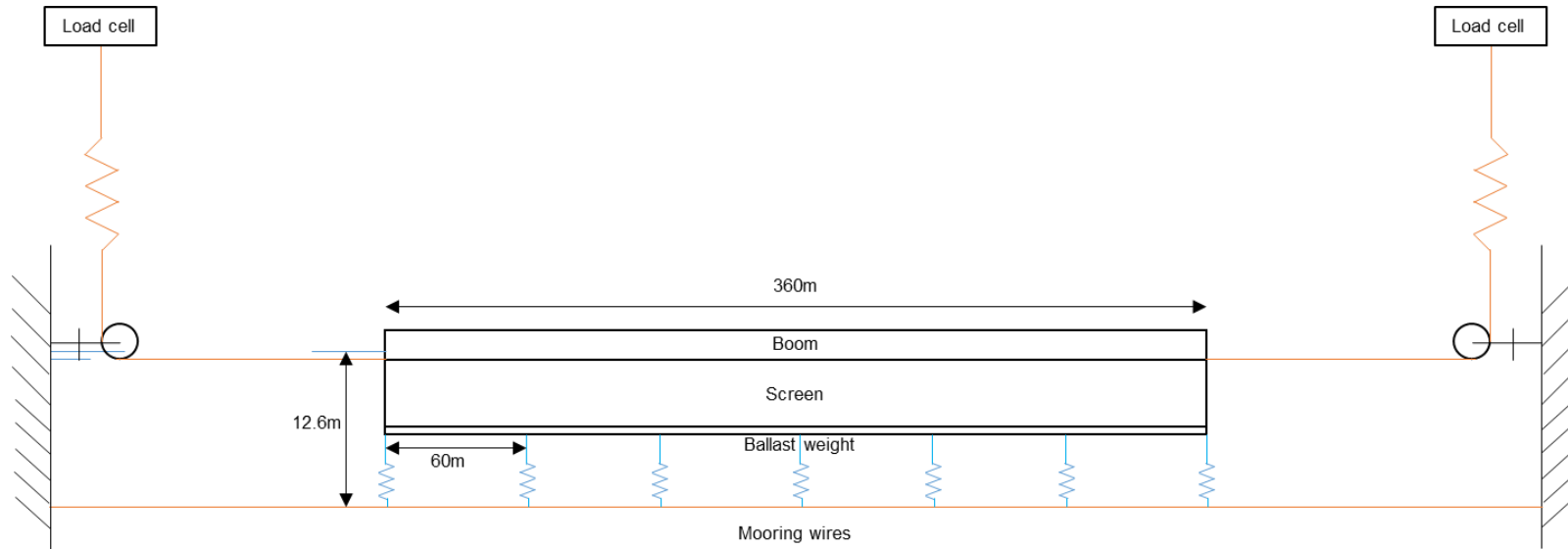


Figure 2-4: Secondary mooring configuration

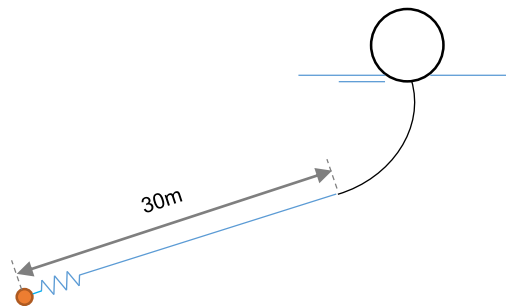


Figure 2-5: Cross section secondary mooring configuration

2.1.3 Mechanical Properties

Mechanical properties of the system can be found in Table 2-2, taken from reference [ER.1].

Table 2-2: System mechanical properties

Item		Symbol	Value	Unit
Unit mass	Floater	M_F	See Appendix A -	kg/m
	Screen	M_S		
	Tension cable	M_{TC}		
	Ballast weight (submerged)	M_{BW}	40/120	
Bending stiffness	Floater	EI_F	See Appendix A -	kNm ²
	Screen	EI_S		
	Ballast weight	EI_{BW}		
	Tension cable	EI_T		
Axial stiffness	Floater	EA_F	See Appendix A -	kN
	Screen	EA_S		
	Ballast weight	EA_{BW}		
	Tension cable	EA_T		
Spring stiffness	Main spring	k_s	17.7	kN/m
	Secondary mooring springs (PS to SB)	k_{ss}	668.2, 657.3, 641.5, 657.3, 641.5, 641.5, 651.9	kN/m
	Subsea mooring springs (PS/SB)	k_{sm}	624.0 / 636.4	kN/m

The system is setup such that the bending stiffness is as low as reasonably possible for multiple reasons. Bending stiffness scales with the scale parameter to the power five. It is very difficult to specify a realistic material to accurately model the flexible boom. Another reason is that the material that will be used for the floater and other components is still unknown.

Axial stiffness in the tension cable is very large; the actual axial stiffness of the system is modelled with the two springs on both sides of the model (see previous section). The axial stiffness of other components other than the tension cable is low in comparison.

Note that the spring stiffness given in Table 2-2 is the spring stiffness of an individual spring. The total system stiffness is given by:

$$F = \frac{EA}{L} \Delta x = 2k_s \Delta x$$

One spring k_s models half of the total system axial stiffness $\frac{EA}{L}$.

2.1.4 Pretension

As described in the previous chapter, by introducing pretension effectively the modelled segment becomes part of a bigger system. This has been validated using numerical tools. Table 2-3 provides three lengths of the total section for which the pretension has been computed. Note that this only holds for high/low mooring, as the secondary mooring interval will be sufficiently small, such that loads are transferred often and mean tension remains low.

Table 2-3: Pretensions used in model test

Section length [m]	Pretension [kN]
400	1
1000	300
4000	1600

2.2 Instrumentation

2.2.1 Model Based Instrumentation

The following properties are measured with respective sensors positioned on the model:

- Displacement (position): 3 DoF optic position measurements are taken on five points on the mid-section of the model.
- Accelerations: 3&6 DoF accelerations measurements by accelerometers and gyrometers.
- Loads: on both sides of the mooring connections of the barrier (3 DoF) and in the secondary mooring lines (1 DoF) loads are measured.
- Angles: the planar orientation of the pulleys that guide the mooring wire to the model is measured with a potentiometer.

Figure 2-6 shows the location of the sensors in the high mooring concept. In the low mooring concept the only change is the connection point of the mooring lines. Note that the secondary mooring lines of the third concept are not shown in this figure.

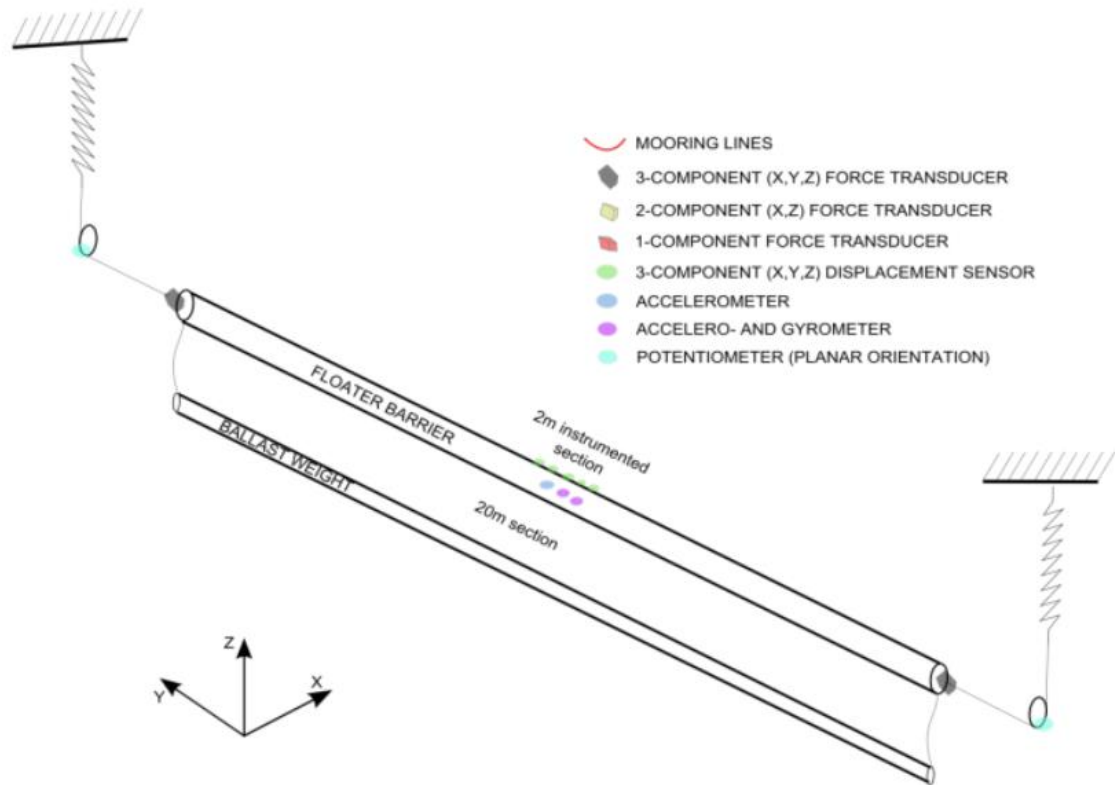


Figure 2-6: High mooring concept with instrumentation

The mid segment, that contains most of the sensors, is consequently heavier. This addition is significant and shall be considered in the validation of the numerical models. Furthermore, a number of wires run from all these sensors to the carriage, suspended in a catenary to the downstream side of the model. The wires are partly suspended in the water. It is expected that the cables exert small disturbances to the motions of the barrier.

2.2.2 Tank Based Instrumentation

The wave and current sensors are placed close to the location of the model. Four more wave sensors are used in order to calibrate phases of the two wave maker sides for the oblique waves. These sensors are not shown here, as they were only used to correct phases and not amplitudes. All other sensors are presented in Figure 2-7.

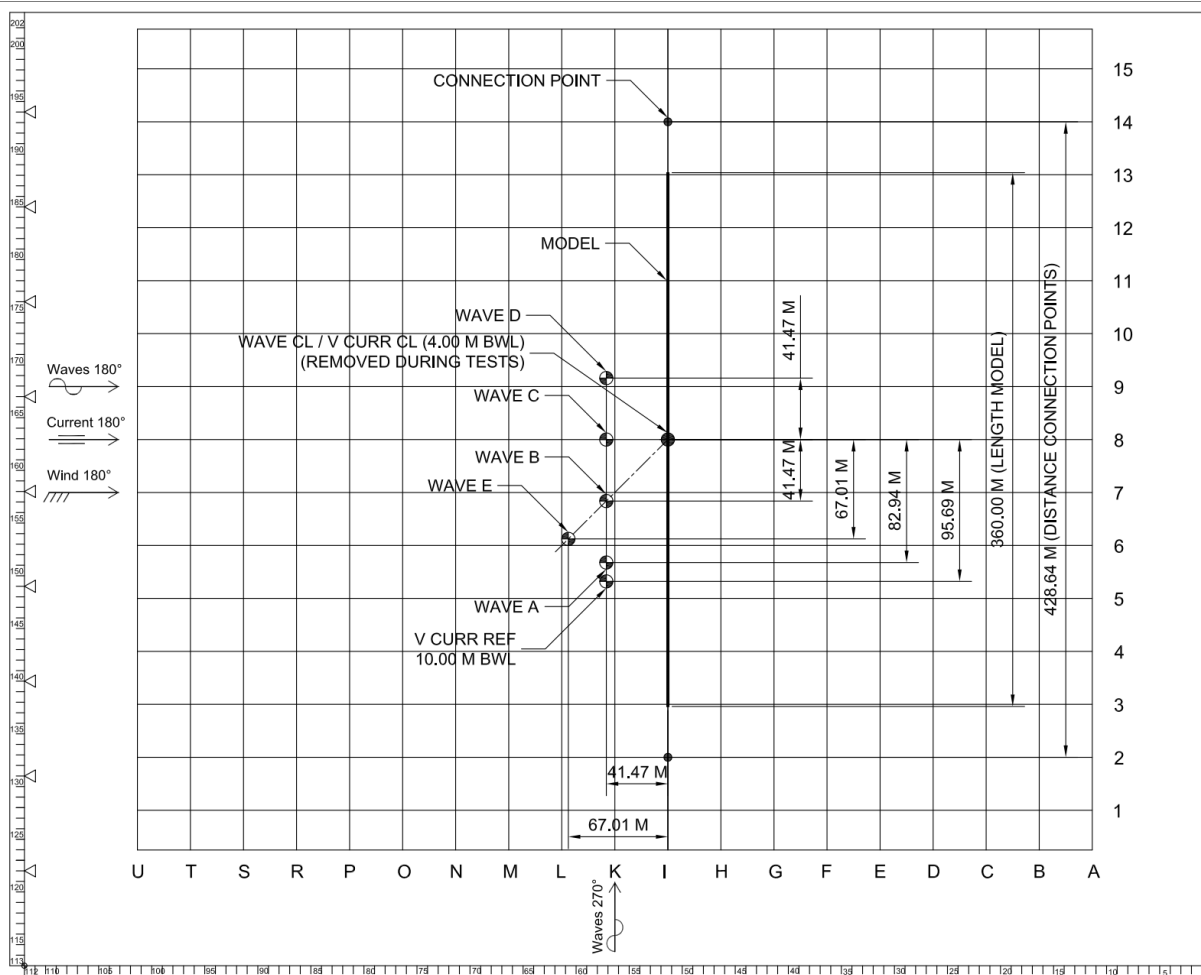


Figure 2-7: Location of wave and current measurement sensors during calibration

2.3 Environmental Criteria

Tests are carried out in current and waves. Two types of waves are tested: regular and irregular waves. Regular waves resemble most a simple sinusoidal waves with a single amplitude and wave length/period. These types of waves do not exist on the ocean, but enable the hydrodynamics of the system to be understood much better. Irregular waves resemble sea states and can be thought to exist of infinite sinusoidal wave components.

2.3.1 Current

Two different current cases will be tested, all having the same relative direction to the model: perpendicular to the boom. An extreme current speed is taken, in order to amplify any unexpected behaviour, this velocity is expected to occur in the North Sea in a five year storm, but in the Pacific Ocean such a speed will not be observed. Also a relatively low current velocity is tested, which is somewhat



higher than the day-to-day velocity in the Pacific: a too low speed leads to a high noise/error ratio and is furthermore difficult to produce in the tank. An overview is provided in Table 2-4.

Table 2-4: Overview of current cases

Case	Velocity	Direction
[-]	[m/s]	[deg]
1	0.30	180
2	1.00	

2.3.2 Irregular Waves Environmental Combinations

The system is tested in a number of irregular sea states. Sea state parameters and corresponding current conditions are provided in Table 2-5. Note that the ULS resembles a North Sea storm conditions, and the SLS the longer swell waves that one would encounter in the Pacific. The steep waves of the ULS are very unlikely to be encountered in the Pacific Ocean. This condition was with the relatively large scale of tests the maximum wave height that could be generated.

Table 2-5: Irregular wave parameters

Limit State	Waves				Current	
	Spectrum	Hs	Tp	Dir	Velocity	Direction
[-]	[-]	[m]	[s]	[deg]	[m/s]	[deg]
ULS	PM	6.25	8.45	270	1.0	180
		6.25	8.45	225	1.0	180
SLS		4.00	13.00	270	0.3	180
		4.00	13.00	225	0.3	180

2.3.3 Regular Waves Environmental Combinations

In order to find linear system response, and bridging and overtopping characteristics, a number of regular wave tests are performed. The wave heights, periods, directions and steepness are given in Table 2-6.

Table 2-6: Regular wave parameters

ID	H	T	Dir	S
[-]	[m]	[s]	[deg]	[-]
2-3	3	6.000	270	0.053
2-4		5.150	270	0.072
2-5		4.600	270	0.091
3-3	6	8.500	270	0.053
3-4		7.290	270	0.072
3-5		6.500	270	0.091
5-3	3	6.000	225	0.053
5-4		5.150	225	0.072
5-5		4.600	225	0.091
6-3	6	8.500	225	0.053
6-4		7.290	225	0.072
6-5		6.500	225	0.091
7-4	6	7.29	180	0.072

During testing it was decided to limit the number of regular wave tests, as in the longer regular waves response was predictable—the system followed the waves well.

2.4 Load Cases

An overview of load cases can be found in Appendix B - .

3 Test Programme

The tests to be carried out are:

- Decay tests (in surge only, by giving the model an initial displacement)
- Current load tests (no waves)
- Regular wave tests (combined with current)
- Irregular wave tests (combined with current)

The order of the tests is as follows:

- Static load tests (in order to test sensors)
- Decay tests (surge)
- Current tests (no waves) with velocities (0.3 & 1.0 m/s as per Table 2-6) as per Table 2-4.
- Regular waves with no current (wave ID 5-4, 6-4 and 7-4)
- 13 Regular waves from Table 2-6 with the 2 current velocities from Table 2-6. In total 26 tests.
- Irregular wave tests with currents as described in Table 2-6.

The test program is to be carried out with three configurations:

- High mooring with three pretensions and low spring stiffness
- Low mooring with pretension corresponding to 360m and low spring stiffness
- Secondary mooring with pretension corresponding to 360m

The total test programme is presented in Appendix B - .Not all cases have been carried out due to time restrictions. For instance the high mooring with high pretension is not tested in 0.3 m/s currents. Furthermore, the highest pretension was not realized due to time constraints: a value of approximately 880 kN instead of 1600 kN was realized.

4 Analysis

4.1 Frequency Domain Analysis

In the post-processing of the results use is made of Fourier transforms, to transform the measured signals into the frequency domain. This is relevant, as it shows at which frequencies a response is present and the magnitude of said response. For instance, moored tankers show a large low-frequent response outside of the wave spectra frequencies. This indicates non-linearity, in this case low-frequent drift due to a structure's ability to cause waves. Figure 4-1 shows an example frequency domain plot, where three signals are shown which shown a peak at approximately 0.8 rad/s, which is also the wave frequency. A small peak can be seen at twice the wave frequency, indicating a second order harmonic.

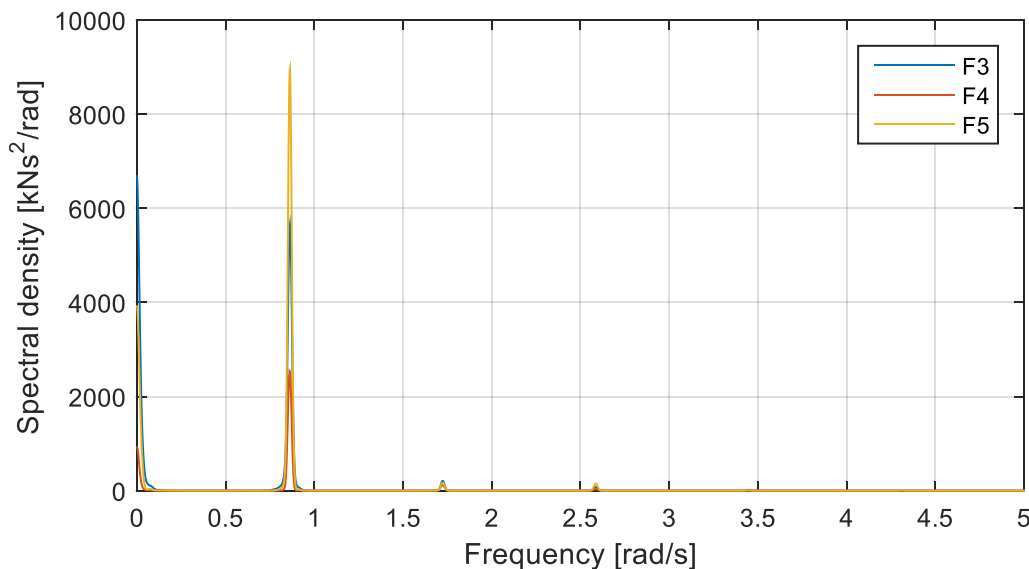


Figure 4-1: Example frequency domain plot

Filtering can be performed in the frequency domain, cutting of certain bands of frequencies.

4.2 Post-Processing of Results

In regular sea states amplitudes can be computed straight forward: amplitudes and mean values can be identified. In irregular sea states, this is not the case. The maximum event corresponds to the realization of the spectrum that was used in the tank. Running a different realization, yields a different extreme. Therefore statistical values are used: significant values and most probable maxima (MPM) that correspond to the duration of a sea state, commonly three hours.

Most probable maximum values are calculated by using a Peak Over Threshold (POT) method. In this method individual peaks are identified (one peak per certain cycle, a peak period or mean zero crossing

period for instance). The peaks are identified if they are over a certain threshold, and a distribution model is fitted; in this case the most general distribution, the Generalized Pareto. In the tank the irregular test was limited to one hour, to safe time. The distribution is fitted over the extremes in this duration and extrapolated to a three hour maximum.

4.3 Floating Barrier Response Expectation

4.3.1 Hydrodynamic Response

As the floating barrier is small with respect to the wave length, it can be expected to behave as a Morison element. Morison's equation describes the forces exerted by a flow on a structure and exists of quadratic drag and linear added mass/inertia:

$$F = \rho C_M V \dot{u} + \frac{1}{2} \rho C_D A u |u|$$

Where the first term denotes the inertia part and the second a drag term. Furthermore:

- ρ is the density
- C_M is the inertia coefficient
- V denotes the volume
- \dot{u} is the derivative of the flow velocity u
- C_D is the drag coefficient
- A reference area of drag

The system thus responds to the fluid velocity. Therefore it is important to know local particle velocity. The velocity is measured on a fixed location, below the water line. We expect the horizontal velocity components of a regular wave to be fairly of the same characteristic, except if a current is present which should lead to a mean increase. The horizontal velocities are written as follows, assuming linear Airy wave theory and deep water:

$$u_x = A(z, \omega, U) \cdot \cos(kx - \omega t)$$

With

$$A = a \cdot k \cdot (\omega - kU) \cdot e^{kz}$$

Where a is the wave amplitude, k the wave number, ω the wave frequency, U current velocity, x and z the respective horizontal and vertical fixed position, and t the time.

Based on this, we would expect the local velocity in a point located slightly below the free surface, to take the shape as shown in Figure 4-2.

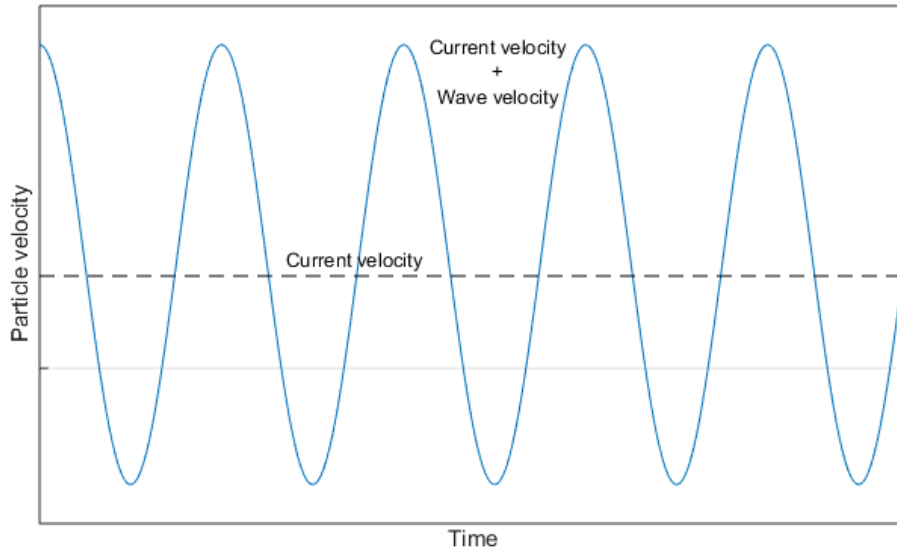


Figure 4-2: Example fluid velocity

Consequently it is expected that the response shows similar characteristics. Low frequent response can be expected, although not in the conventional form of drift. It is unlikely that this system reflects waves that are so much longer than the diameter of the boom and especially due to its flexible nature. However, a non-linear term is present in the waves: Stokes drift. Stokes drift is a constant velocity that a fluid particle experiences, in line with the wave heading. This velocity is as a function of the frequency, for a regular Airy wave the Stokes drift reads:

$$\bar{u}_s \approx \omega k a^2 e^{2kz}$$

In the derivation of this results, higher order terms have been neglected. In irregular seas this will lead to a slowly varying velocity, superimposed of all component loads. In order to prove this statement, a numerical experiment is carried out. The Morison equation is solved for a light object with high drag and low stiffness. At the instantaneous position the velocity and acceleration of wave particles is used to calculate loading on the boom. Note that merely a single DoF system is solved, which can be thought to be a 2D boom, neglecting 3D effects.

The equation is solved in the time domain using the Newmark-beta method for time integration. First one wave is taken into consideration, leading to the excursion as shown in Figure 4-3.

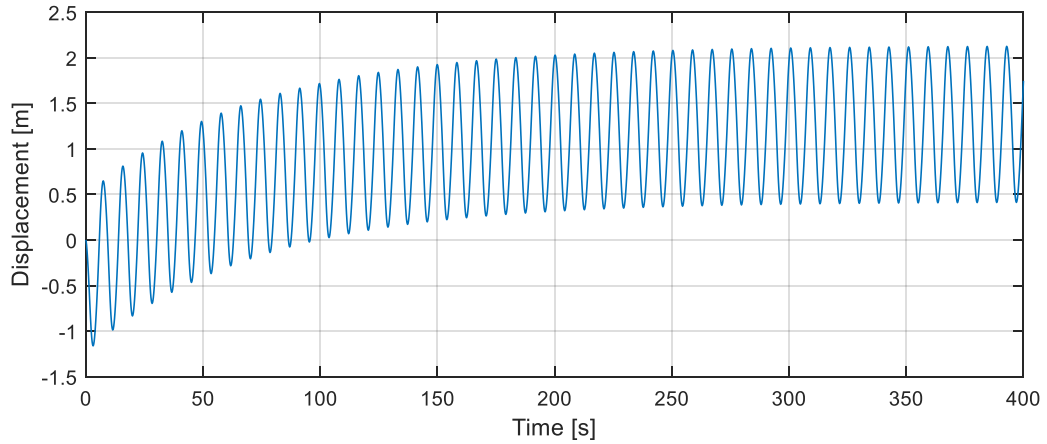


Figure 4-3: Expected response to a regular wave

A transient motion is seen, leading to a steady state response. The transient motion originates from Stokes drift. The spectral response of the excursion and Morison load is shown in Figure 4-4. Higher order harmonics are seen: notably the largest at three time the wave frequency.

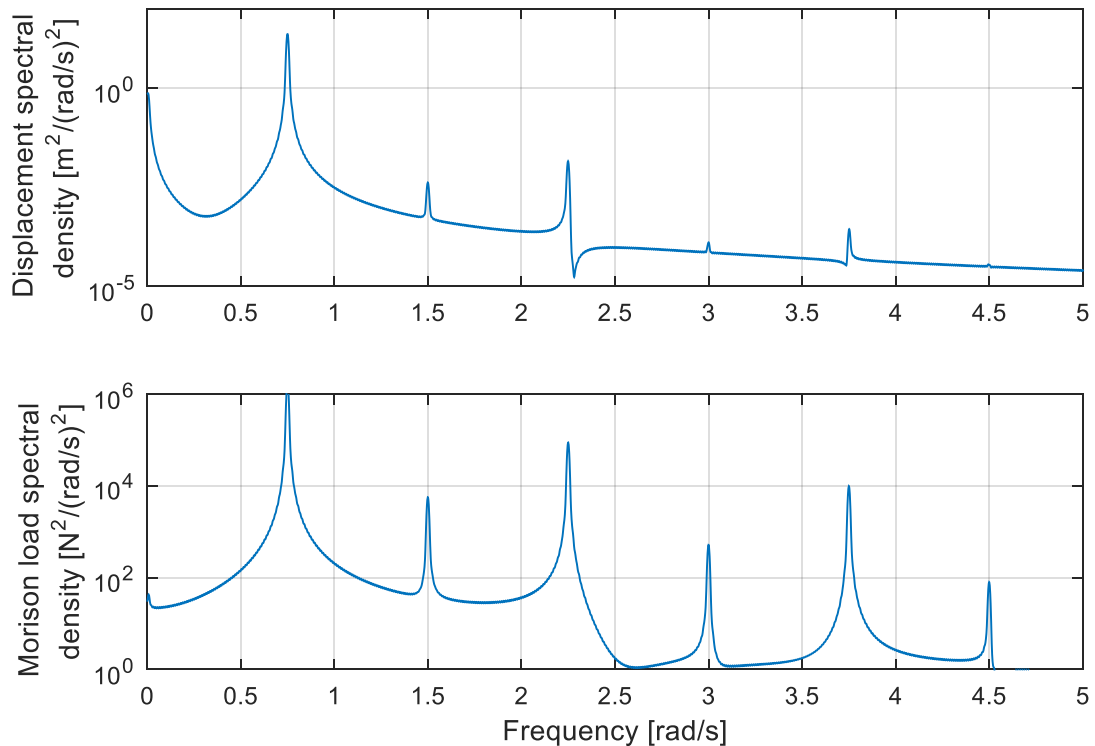


Figure 4-4: Spectral density of system excursion and Morison load in a regular wave

Now a simulation is carried out with two waves with equal amplitude, but different frequencies: 0.5 and 0.75 rad/s. The total velocity can now be written as:

$$V(t, x) = A_1 \cos((kx - \omega_1 t) + A_2 \cos((kx - \omega_2 t)$$

Unfortunately, it is not straightforward to plug this into the Morison equation and find an analytic solution, due to the absolute value present. Resulting time traces of the displacement and the Morison load are provided in Figure 4-5. Also here a similar transient motion is visible. Furthermore, spectral density plots of said signals are given in Figure 4-6. Note that since the figure is plotted on a logarithmic axis, small amplitudes are exaggerated. Multiple observances can be made:

1. Two peaks are present at the wave frequencies, in both excursion and loading. These contain most energy.
2. A small peak is observed at a difference frequency of $0.75 - 0.5 = 0.25$ rad/s. Although the energy is low, if this excites a natural period response can be high. Interestingly, this peak is relatively low in the Morison load, but due to the low stiffness of the system it yields a significant response.
3. Multiple peaks are found in the Morison load time trace at either multitudes of the wave frequency or sum frequencies: 1, 1.25, 1.5, 2, 2.25, 2.5 rad/s and further on. Most energy is in the 2 rad/s peak.

A response is found at the following frequencies, in order of magnitude:

$$\omega_1, \omega_2, (\omega_1 - \omega_2), 2\omega_1, 2\omega_2, (\omega_1 + \omega_2), \dots$$

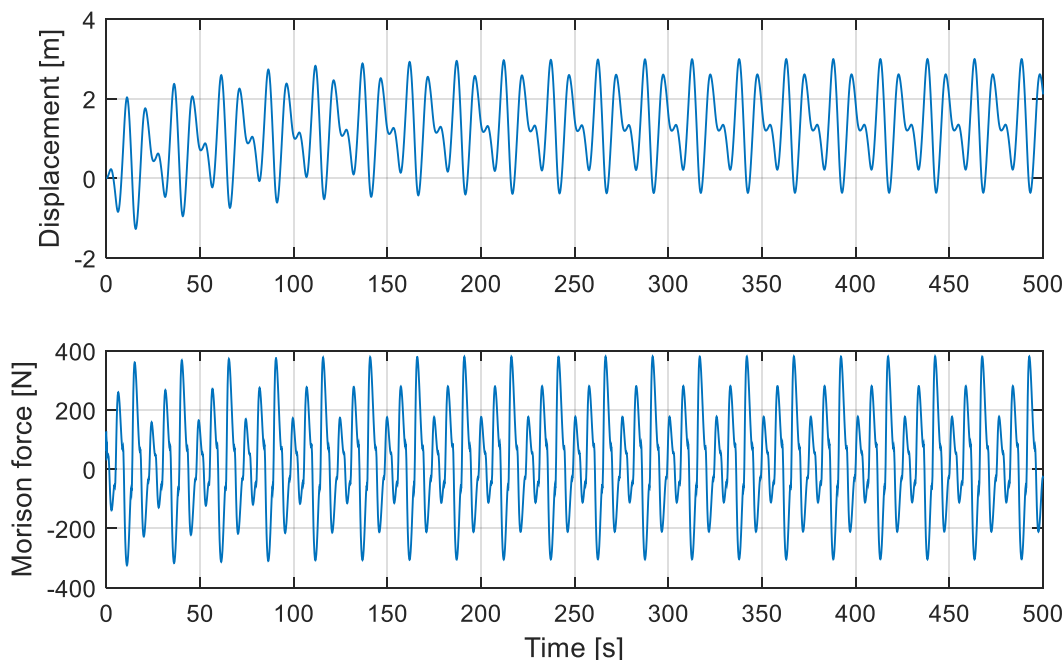


Figure 4-5: System excursion and Morison force in two regular waves

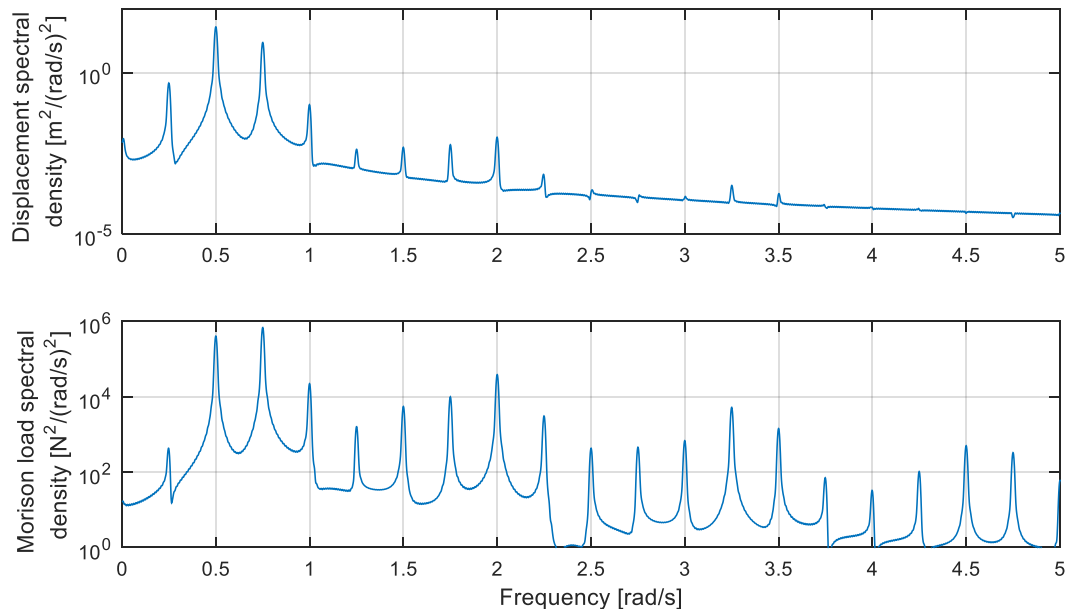


Figure 4-6: Spectral density of system excursion and Morison load in two regular waves

It can be concluded that responses can be expected at different frequencies than the wave frequencies in both regular and irregular waves. It depends on the system characteristics (stiffness, mass, added mass, etc.) at which frequency largest response is found. However, the following can be expected:

- In regular waves response at two and three times the wave frequency, where loading at three times the wave frequency is higher than two times.
- In irregular waves both low and high frequency effects are to be expected. This consists of difference, sum and double frequencies. The difference frequency loading is approximately two orders of magnitude lower than the wave frequency loading, furthermore the difference frequency is again an order lower than the sum frequency loading.

4.3.2 Overtopping & Bridging

Limiting criteria in terms of plastic capturing are bridging and overtopping. When bridging, the screen is lifted out of the water as the floater rests on two wave crests and is not sufficiently flexible to follow the waves. During overtopping, the system is pulled under water in a wave crest, allowing plastic to wash over the barrier. An example is provided in Figure 4-7.

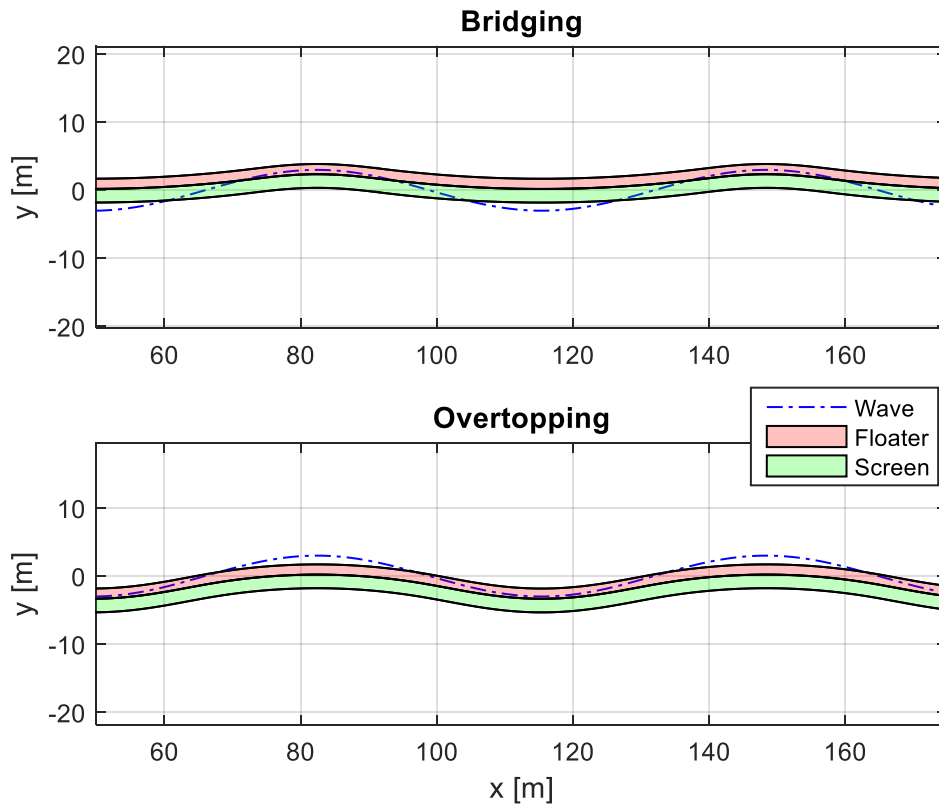


Figure 4-7: Example of bridging and overtopping

Overtopping and bridging are influenced by the following parameters:

1. Buoyancy force: this is the main force that keeps the system afloat. As the system is pulled down, the buoyancy force increases greatly due to the cylindrical shape of the floater. Once the system is half submerged, the increase decreases.
2. Static weight: the static weight of the system consists of ballast chain (which may be submerged) and the weight of the floater. This load is equally distributed over the system and pointing downwards (if the ballast chain is fully submerged—once it is out of the water the weight increases).
3. Pretension force: as the pretension increases, the system gets more resistant towards bending.
4. Dynamic forces: drag in the vertical plane and mass cause the system to respond out of phase with respect to the wave. In a system dominated by stiffness (buoyancy) the dynamic loads will be low. However, then the load pointing downwards is low as well. Note that in the low mooring configuration a vertical component is introduced, where the screen pulls the floater down.

An example of the quasi static vertical loads is presented in Figure 4-8, where the system is subjected to the medium pretension (300 kN) and a wave with 6m height and 6.5s period. Note that the bend

stiffness has been neglected in this case: assuming the bend stiffness is much lower than the resistance to bending due to pretension. The loads have been computed with a finite element numerical model.

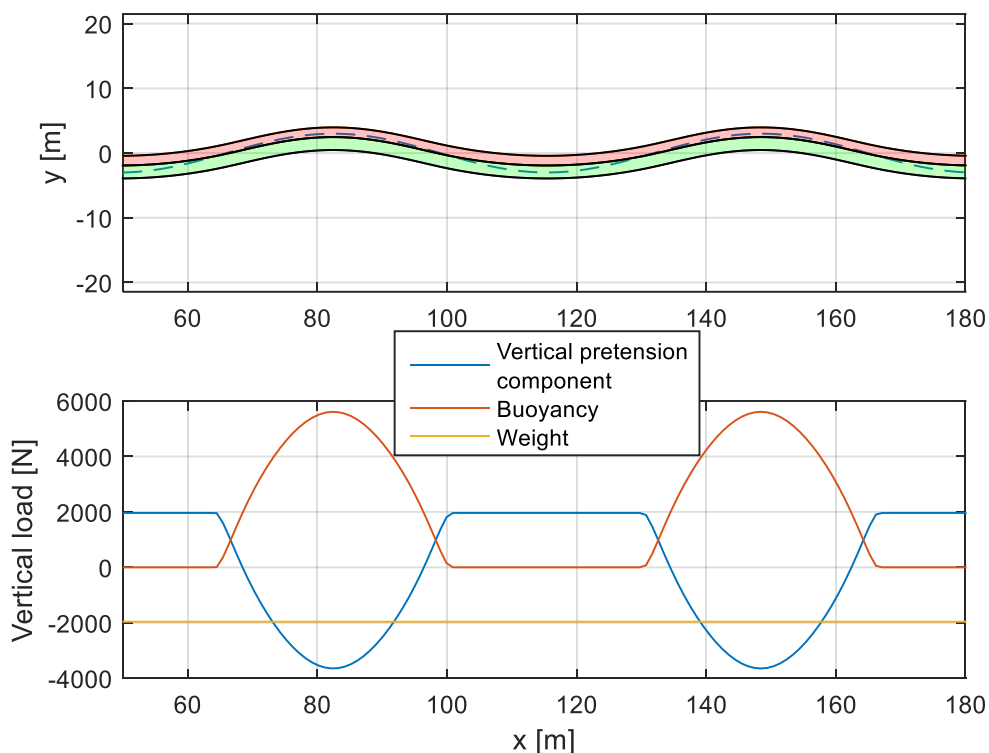


Figure 4-8: Quasi-static vertical load component in system under pretension

Two interesting aspects can be observed: if the system is lifted out of the water, at the trough, the buoyancy load is zero and consequently the vertical component of the pretension load is equal to the constant weight. At the crest, the buoyancy load steeply increases, due to the cylindrical shape of the floater. In order to maintain statics the vertical pretension component decreases.

If the diameter of the floater is large with respect to the weight, then the plastic capturing limiting behaviour is bridging. The other way around holds as well: with large weight and small buoyancy, the system will be pulled into the wave crest easier. Another important aspect is nonlinearity of waves: in the tank steep waves tend to look slightly more trochoid shaped than sinusoidal. This implies wave crests are sharper and higher, and troughs shallower and flatter. The same case as presented in Figure 4-8 is ran with a Stokes 5th order wave. Results are presented in Figure 4-9. The vertical loads are larger; consequently the distance between the wave crest and top of the floater is smaller. It can therefore be expected in waves that get more non-linear, the occurrence of overtopping will increase.

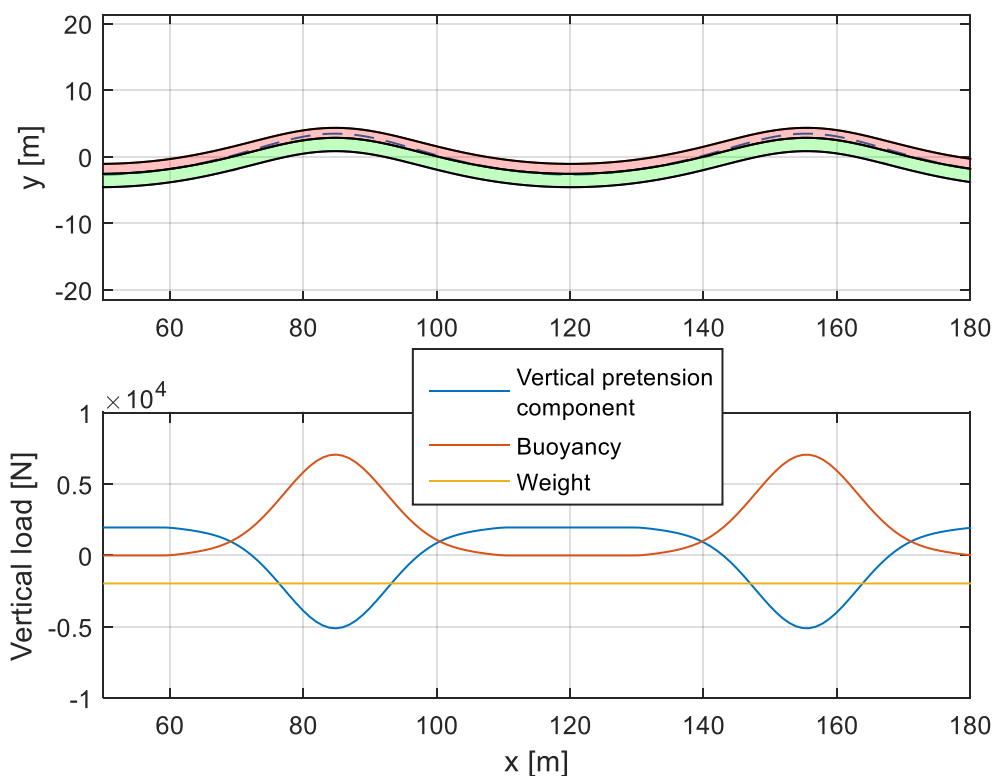


Figure 4-9: Quasi-static vertical load component in system under pretension for a Stokes wave

It is important to be able to compare configurations (span, mooring configuration, dimensions, etc.) quantitatively in terms of overtopping and bridging. The three most governing parameters for a certain configuration are: wave steepness, significant wave height and current velocity. Using these parameters it is envisioned an area of operation can be determined, where no bridging and overtopping occurs. Indeed, this is not something binary, as plastic might already escape once the screen is lifted a meter out of the water. Therefore this should be combined with the local plastic capturing efficiency, which is still being determined numerically and empirically. An example of such a figure can be found in Figure 4-10, where the coloured area is the area in which can be operated. This figure can be generated for different designs (floater dimension, weight, span, etc.) enabling a quantitative comparison and optimizing the design.

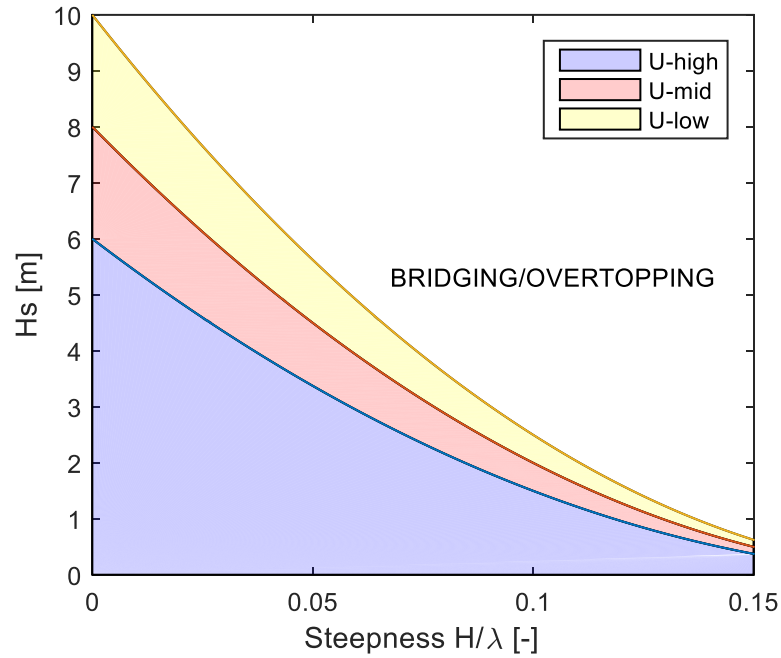


Figure 4-10: Bridging or overtopping expected behaviour example for a single system configuration

5 Results

5.1 Wave and Current Calibration

5.1.1 Current Only

Two current velocities have been tested: 0.3 and 1.0 m/s. Current is calibrated without waves and the obtained signals are used for wave calibration. The time signals and power spectra of these two currents are presented in Figure 5-1 and Figure 5-2 for the centre line (CL) and reference (REF) locations, as shown in Figure 2-7.

In the 0.3 m/s case the mean of the CL signal is 0.307 m/s, slightly lower than that of the REF signal; 0.323 m/s. The signals are, as expected, not entirely constant: the standard deviation of both signals is 0.0166 and 0.0375 m/s. This is small, yet significant—for the REF signal the standard deviation is more than 10% of the mean. In the power spectra a peak can be observed at around 1 rad/s; response of the system can be expected here as well.

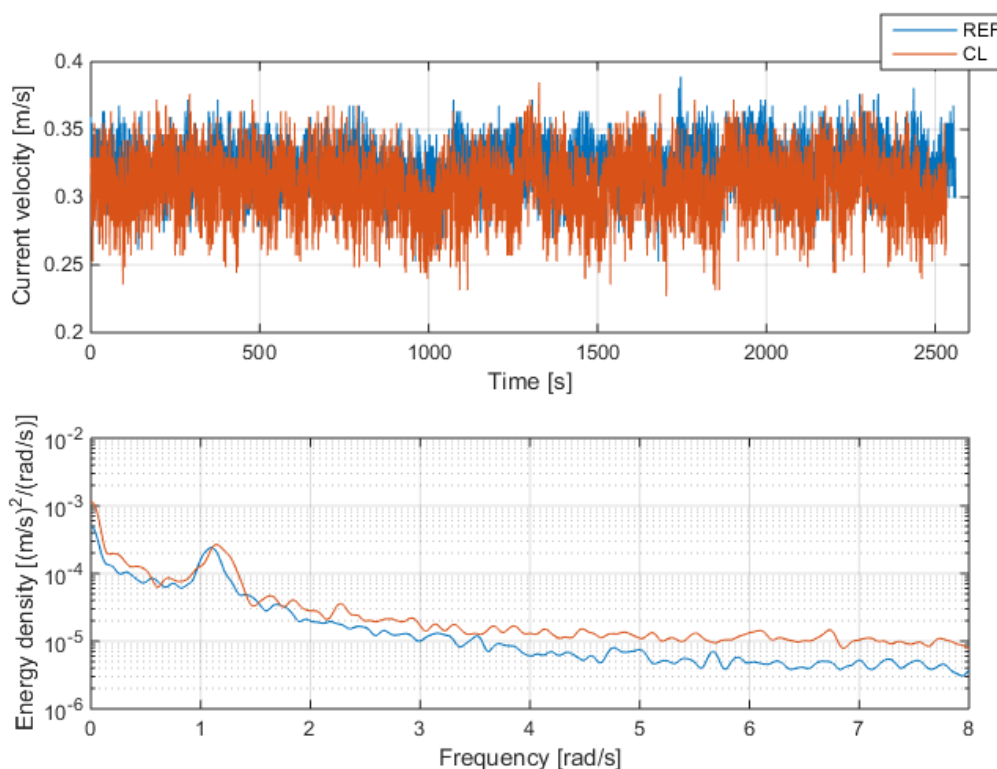


Figure 5-1: 0.3m/s current calibrated time signal (upper) and energy density (lower)

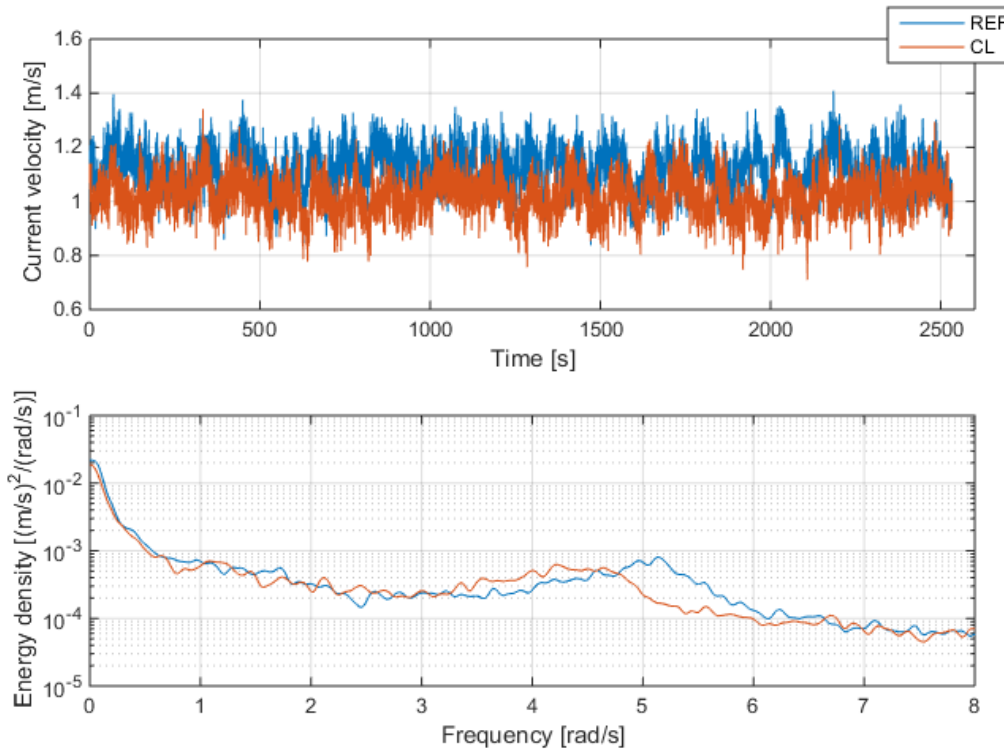


Figure 5-2: 1.0m/s current calibrated time signal (upper) and energy density (lower)

5.1.2 Regular Waves

Regular waves without current are fairly straight forward to calibrate and the error is consequently low. The combination of waves and current is more complex, especially the oblique waves. A phase difference occurs between waves propagating from the two different wave makers that needs to be corrected. Therefore the error between nominal and realized (measured) waves in these cases is larger. An overview of all these cases is presented in Table 5-1.

Steep waves tend to get more nonlinear than relatively long waves. In order to check the nonlinear effects, three periods for the 6m regular wave are shown and compared with a regular Airy and Stokes 5th order wave in Figure 5-3. The longest wave is approximated best by an Airy wave, however, the steeper two waves show more nonlinear behaviour and are better modelled by a Stokes wave.

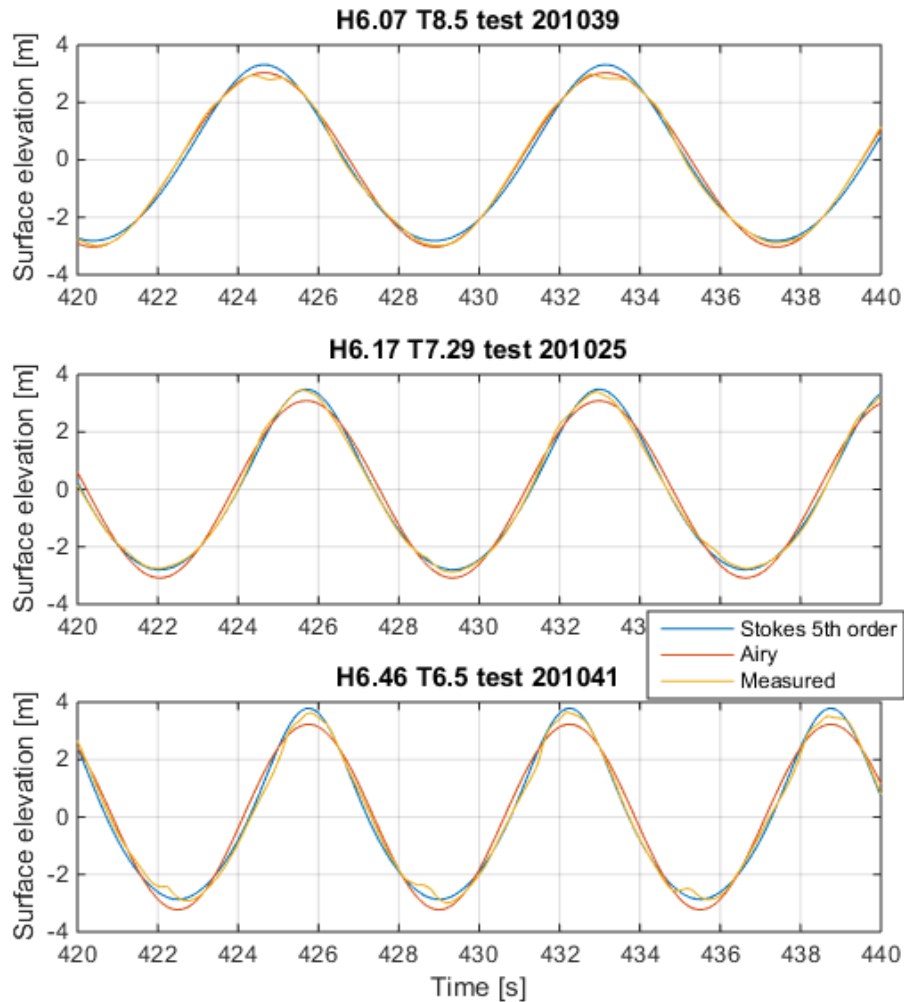


Figure 5-3: Regular wave modelling

The nominal values of these signals are not of great importance: as there is no clear design case yet and the goal of this campaign is to understand the response of the system; it is of more importance to know the exact wave/current input and to be able to compare that to slightly different cases.



Table 5-1: Regular wave calibration summary

MARIN Test No.	Wave type	Regular Sea Characteristics			
		H nominal / measured [m]	Period T [s]	Period T measured [s]	Wave direction [deg]
without current					
201022	Wave 2-3	3.0 / 2.98	6.00	6.016	270
201035	Wave 2-4	3.0 / 3.01	5.15	5.155	
201037	Wave 2-5	3.0 / 3.12	4.60	4.567	
201039	Wave 3-3	6.0 / 6.05	8.50	8.509	
201025	Wave 3-4	6.0 / 6	7.29	7.306	
201041	Wave 3-5	6.0 / 6.29	6.50	6.500	225
201043	Wave 5-3	3.0 / 3.12	6.00	6.015	
201044	Wave 5-4	3.0 / 2.88	5.15	5.150	
201045	Wave 5-5	3.0 / 2.96	4.60	4.569	
201046	Wave 6-3	6.0 / 5.92	8.50	8.504	
201047	Wave 6-4	6.0 / 6.14	7.29	7.308	
201032	Wave 6-5	6.0 / 5.82	6.50	6.494	
201049	Wave 7-4	6.0 / 6.07	7.29	7.305	180
with current 0.3m/s					
202041	Wave 2-3 Case 1	3.0 / 3.05	6.00	6.008	270
202042	Wave 2-4 Case 1	3.0 / 2.86	5.15	5.156	
202045	Wave 2-5 Case 1	3.0 / 2.75	4.60	4.566	
202047	Wave 3-3 Case 1	6.0 / 6.28	8.50	8.510	
202048	Wave 3-4 Case 1	6.0 / 5.71	7.29	7.308	
202049	Wave 3-5 Case 1	6.0 / 5.28	6.50	6.491	225
202046	Wave 5-3 Case 1	3.0 / 3.14	6.00	6.019	
202014	Wave 5-4 Case 1	3.0 / 2.93	5.15	5.154	
202050	Wave 5-5 Case 1	3.0 / 2.97	4.60	4.577	
202035	Wave 6-3 Case 1	6.0 / 6.13	8.50	8.502	
202037	Wave 6-4 Case 1	6.0 / 6.43	7.29	7.303	
202039	Wave 6-5 Case 1	6.0 / 6.3	6.50	6.498	
202051	Wave 7-4 Case 1	6.0 / 5.3	7.29	7.306	180
with current 1.0m/s					
202059	Wave 2-3 Case 2	3.0 / 2.8	6.00	6.014	270
202060	Wave 2-4 Case 2	3.0 / 2.86	5.15	5.157	
202061	Wave 2-5 Case 2	3.0 / 2.69	4.60	4.575	
202062	Wave 3-3 Case 2	6.0 / 6.15	8.50	8.504	
202063	Wave 3-4 Case 2	6.0 / 5.95	7.29	7.306	
202064	Wave 3-5 Case 2	6.0 / 5.48	6.50	6.491	225
202055	Wave 5-3 Case 2	3.0 / 2.48	6.00	6.016	
202056	Wave 5-4 Case 2	3.0 / 2.43	5.15	5.161	
202057	Wave 5-5 Case 2	3.0 / 2.43	4.60	4.572	
202065	Wave 6-3 Case 2	6.0 / 5.69	8.50	8.504	
202053	Wave 6-4 Case 2	6.0 / 5.49	7.29	7.310	
202066	Wave 6-5 Case 2	6.0 / 5.75	6.50	6.505	
202058	Wave 7-4 Case 2	6.0 / 5	7.29	7.311	180



5.1.3 Irregular Waves

Two irregular wave conditions are carried out: SLS and ULS (note that these are not SLS and ULS of the Pacific system, but representative cases within the tank capabilities). The wave parameters are shown in Table 5-2. The theoretical and realized spectra are shown in Figure 5-4 and Figure 5-5.

Table 5-2: Irregular wave calibration summary

MARIN Test No.	Wave type	Irregular Sea Characteristics JONSWAP Type Spectrum				Current	
		Hs nominal / measured [m]	Tp nominal / measured [s]	Dir. [deg]	γ [-]	Vc [m/s]	Dir. [deg]
203007	ULS 225deg	6.25	8.45	225	1.0	1.0	180
204005	ULS 270deg	6.25	8.45	270			
205005	SLS 225deg	4.0	13.00	225		0.3	
206003	SLS 270deg	4.0	13.00	270			

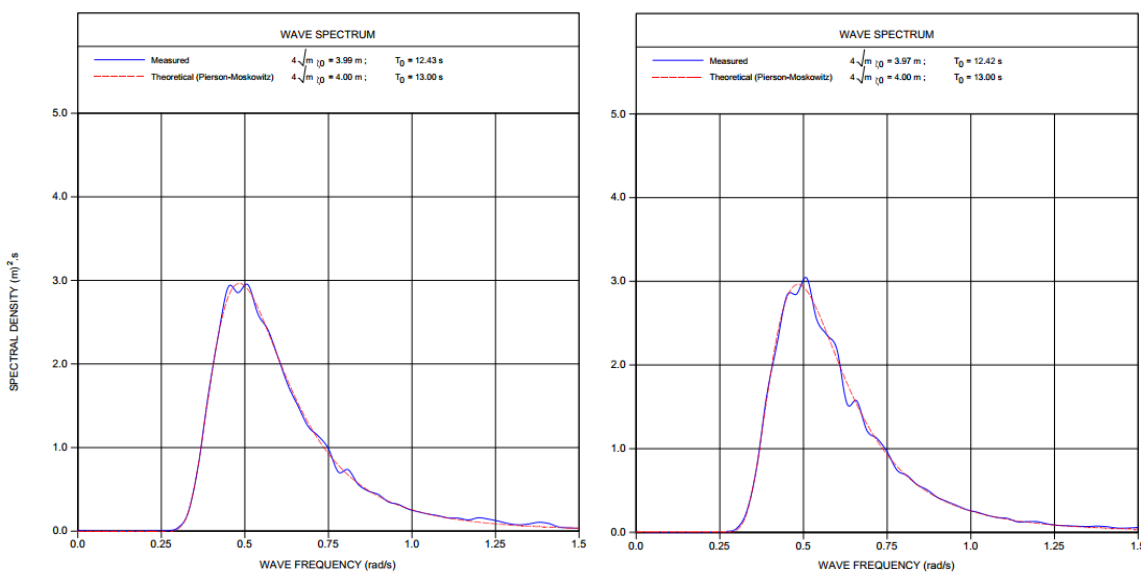


Figure 5-4: 225 and 270 degrees SLS wave cases (blue measured and red theoretical)

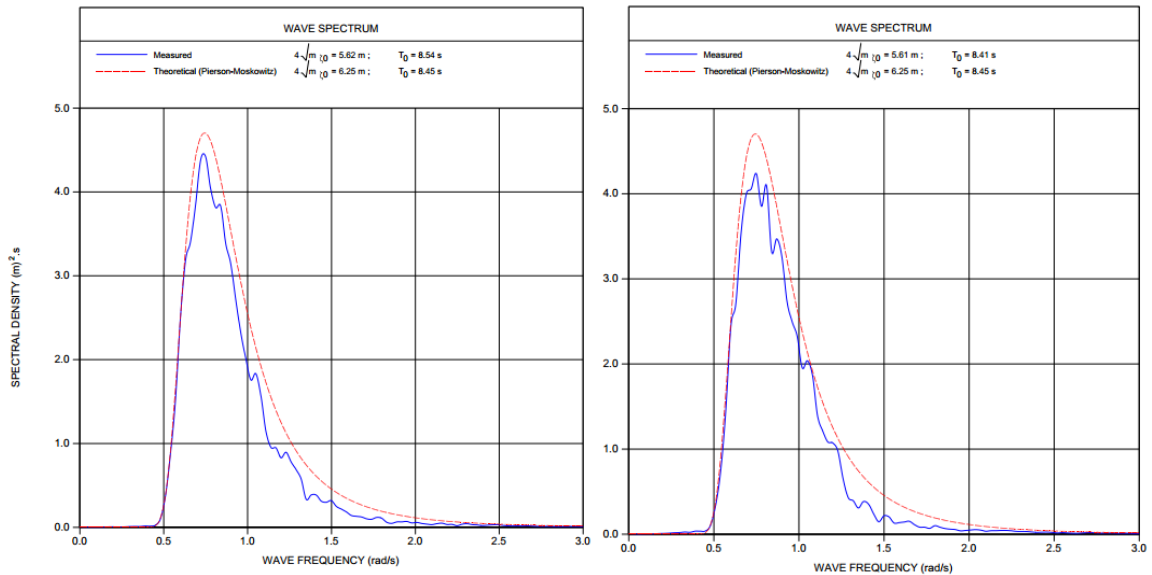


Figure 5-5: 225 and 270 degrees ULS wave cases (blue measured and red theoretical)

A number of observations can be made:

- The SLS condition is a better fit than the ULS
- ULS contains less energy than theoretical: actually H_s 5.62 m instead of 6.5 m.
- Less energy is present in the high frequency range of the ULS spectrum, likely due to wave breaking at higher frequencies (steeper waves).

Wave height measurements were carried out at a number of positions (see Figure 2-7). The spectra for the ULS at 225 degrees is shown for the various positions in Figure 5-6. The spectra show significant differences over the width of the tank. The significant wave heights of the various positions are listed in Table 5-3.

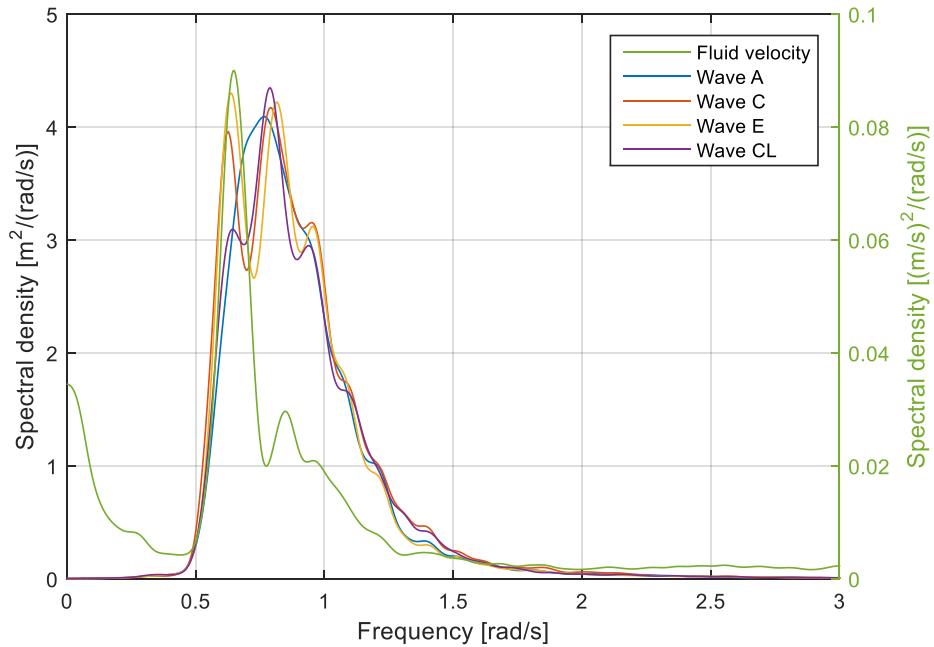


Figure 5-6: Wave spectra at various locations and fluid velocity (REF) for ULS 225 sea state

Table 5-3: Quality of realized wave spectra at various locations

Position	Significant wave height [m]				Normalized [%]			
	ULS		SLS		ULS		SLS	
	225	270	225	270	225	270	225	270
A	6	5,63	4,01	3,86	7,10%	-0,40%	0,80%	-2,00%
C	5,22	5,73	4,04	3,95	-6,90%	1,40%	1,40%	0,30%
E	5,78	5,86	3,95	4,04	3,10%	3,70%	-0,90%	2,70%
Cl	5,61	5,65	3,98	3,93	0,00%	0,00%	0,00%	0,00%

A decline in fluid velocity is observed in the SLS cases (see Figure 5-7), likely leading to lower response in the system. This was communicated with MARIN, who state that it is a sensor issue and not a physical observance from the basin.

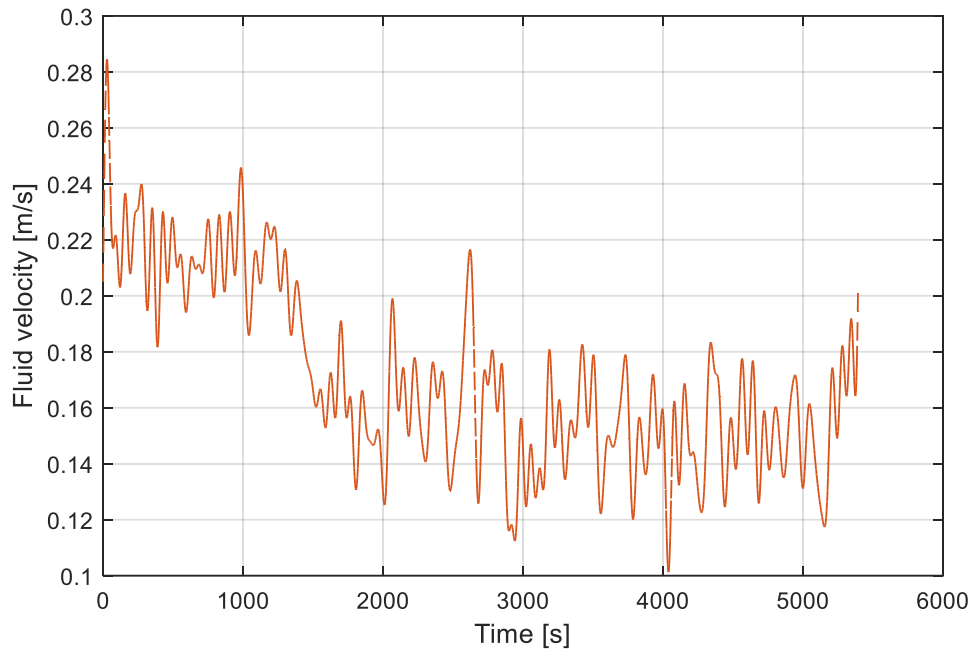


Figure 5-7: Decline in fluid velocity (REF) for SLS 225 case

5.2 Tests in Current

The centre displacement for all configurations in current without waves is shown in Figure 5-8. Unfortunately the results in medium pretension with the original ballast weight were not usable, as the targets rotated out of view of the optical measurement device.

The offset is an important aspect to the working principle of the barrier, as it should concentrate plastic to one central point, meaning the plastic has to be able to travel along the barrier. Too much offset disables this mechanism. A second option is to retrieve plastic at multiple points along the barrier.

The mean excursion reduces as pretension increases. However, as the ballast weight was increased in the high mooring configuration, the screen is pulled down more in 1 m/s current leading again to a higher excursion. The secondary mooring configuration is limited in surge due to the length of the secondary mooring lines.

Limiting offsets can thus be achieved by increasing pretension, by for instance tensioning the system between two mooring buoys. The downside of this option is that overtopping and bridging will occur more often. A second option is working with a secondary tension wire that is relatively stiff and tensioned.

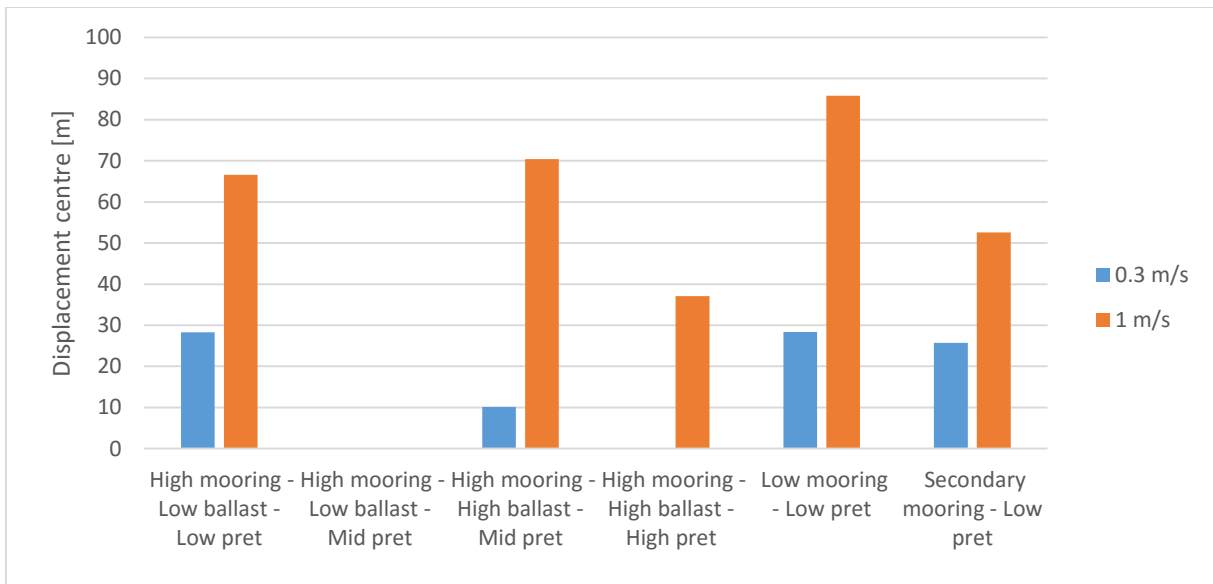


Figure 5-8: Centre displacement for all configurations

Tensions are measured starboard and portside. The mean tensions for the various configurations are shown in Figure 5-9. It should be noted that the pretension configuration has a significant impact on the tension of the mooring line.

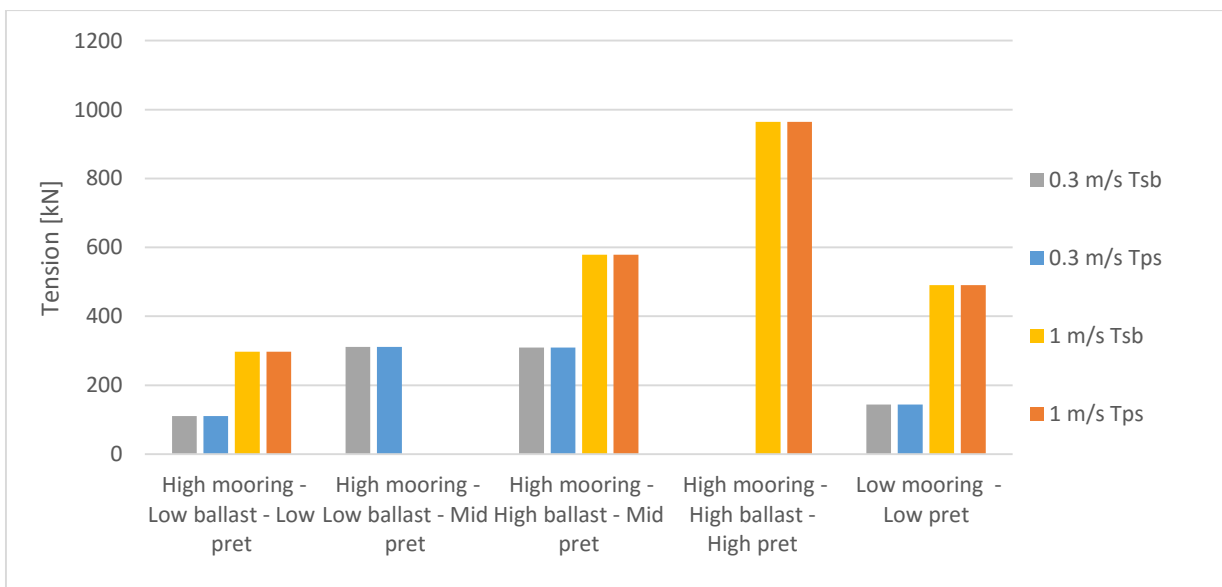


Figure 5-9: Starboard and port side mean tension for all configurations

The transverse load, pointing the current direction, is presented in Figure 5-10. The transverse load in the medium and high pretension is equal to that of the low mooring. As the ballast weight was increased the high mooring system is more similar to that of the low mooring. In 0.3 m/s loads for all

configurations are equal. In 1.0 m/s the transverse load almost doubles if the ballast weight is increased or the connection point fixed at the ballast weight (low mooring). Furthermore, the exposed area of the boom to current is larger for higher pretensions, this effect is not visible as an increase in transversal load.

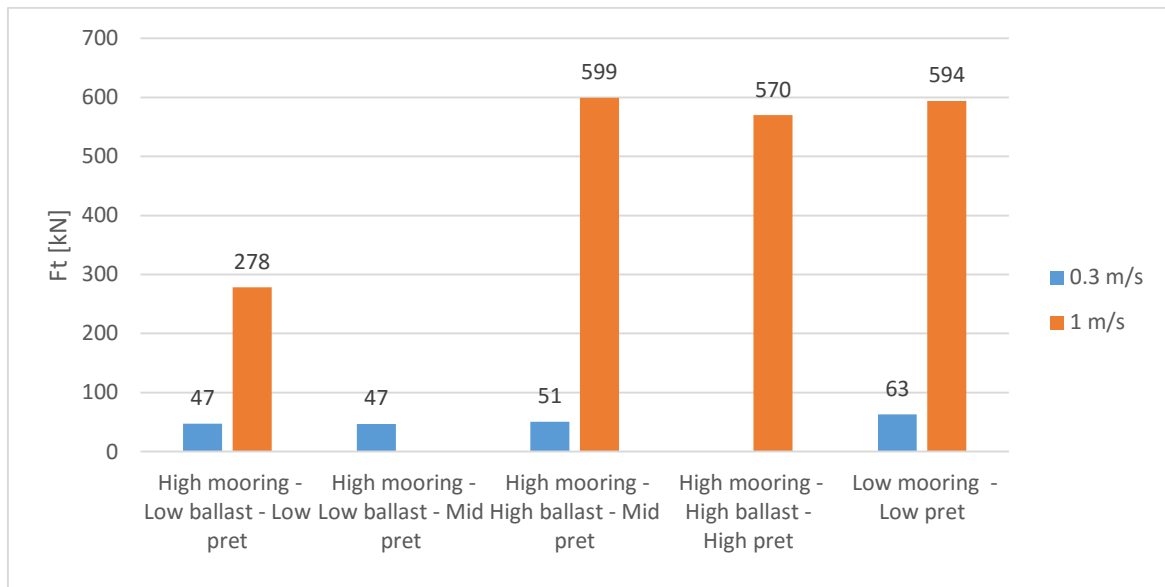


Figure 5-10: Transverse load due to current (total)

The unit load (distributed load per meter span) for various configurations in current only is shown in Figure 5-11. The unit load is a useful figure as it allows for quick comparison and calculation of design loads for a certain length of boom. The unit load is derived by dividing the transversal loads of Figure 5-10 by the span. The span varies per configuration and can be estimated based on the horizontal azimuth of the two connection points and the elongation of the two springs.

Based on the unit load, an effective drag coefficient can be calculated. This is done with a constant area assumption: the projected area remains the same. This is not the case as the screen rotates away from the current in the high mooring configuration. However, the orientation of the screen is unknown. The drag coefficient is presented in Figure 5-12.

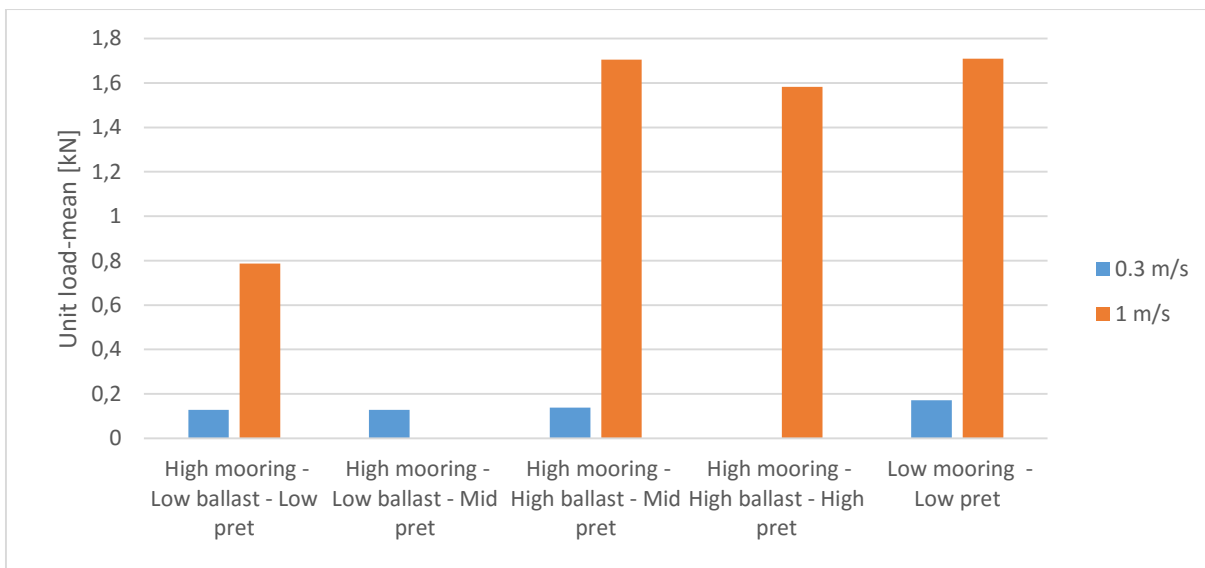


Figure 5-11: Unit load (transversal load normalized with span)

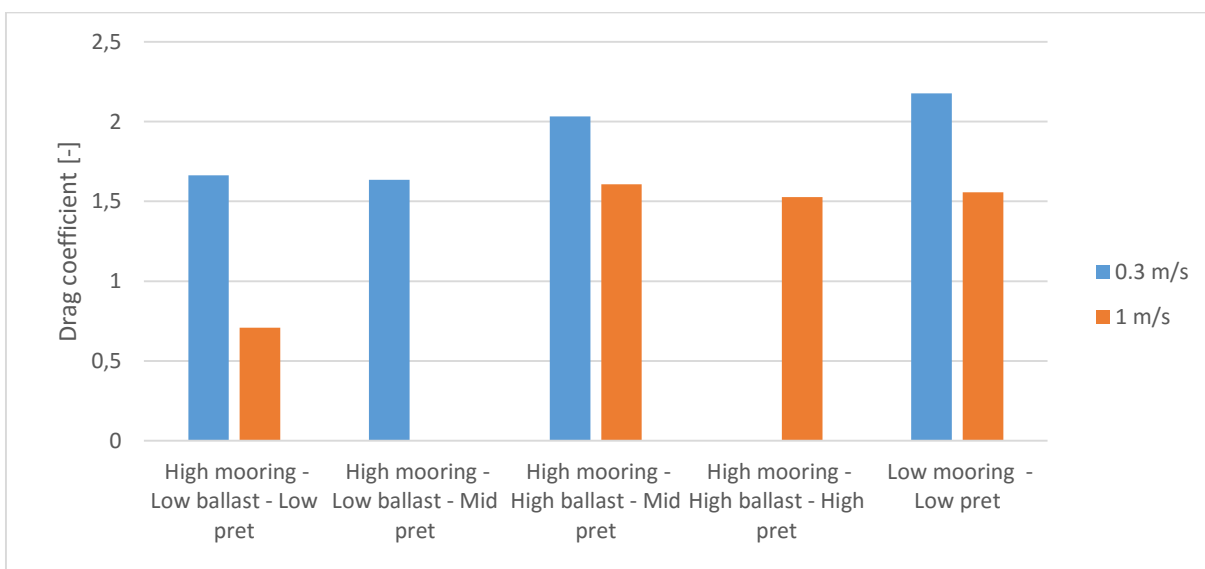


Figure 5-12: Drag coefficient (constant area assumption)

5.3 Tests in Regular Waves & Current

In order to find the linear wave response of the system, a bandpass filter is applied. The low pass frequency is 0.3 rad/s and the high pass frequency is 1.5 rad/s. The high pass frequency is taken relatively low because of higher order effects occurring at twice the wave frequency. These higher order effects are visible in Figure 5-13, where spectral density plots are given of the starboard and port side

loads. In this case even more energy is present in the first higher order harmonic than in the wave frequent component. Note that this frequency domain plot is made of the high mooring low pretension configuration in 270 degree (parallel) waves.

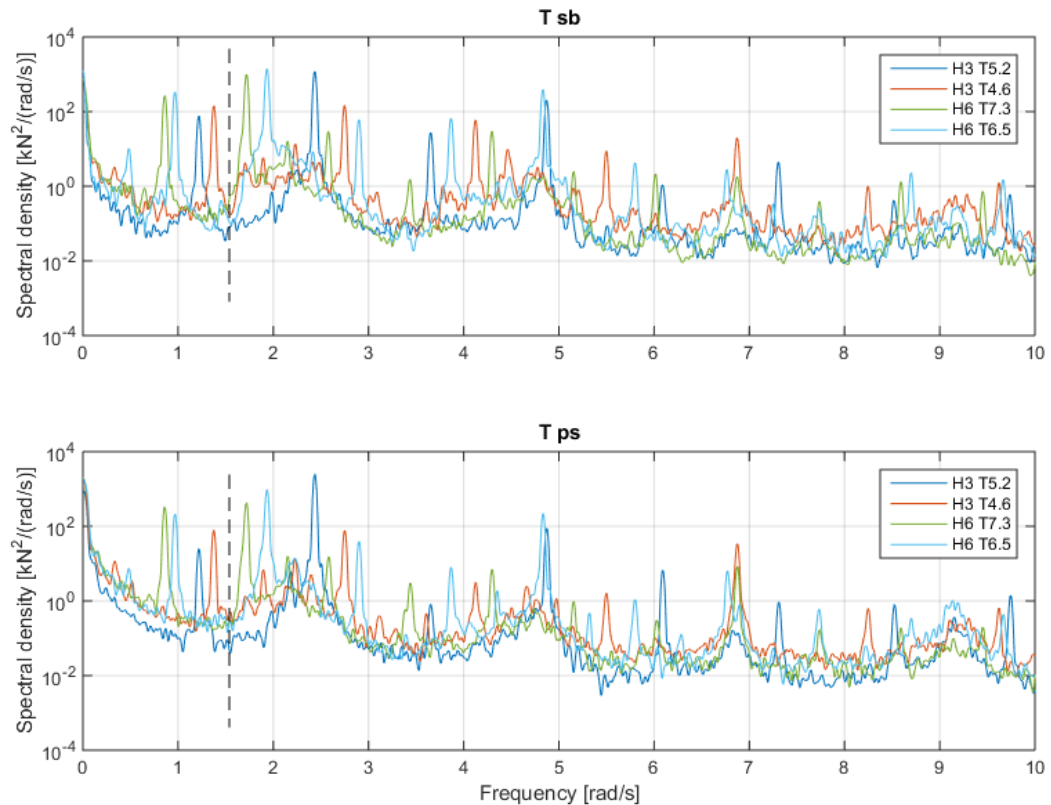


Figure 5-13: 270 degree (parallel to system) regular wave spectral density plots: filter placed at 1.5 rad/s

In order to study the higher order harmonics a second bandpass filter is applied between 1.5 and 3 rad/s.

5.3.1 Motions

A top view is given for the high mooring and low pretension mean positions in 0.3 and 1.0 m/s current, in Figure 5-14.

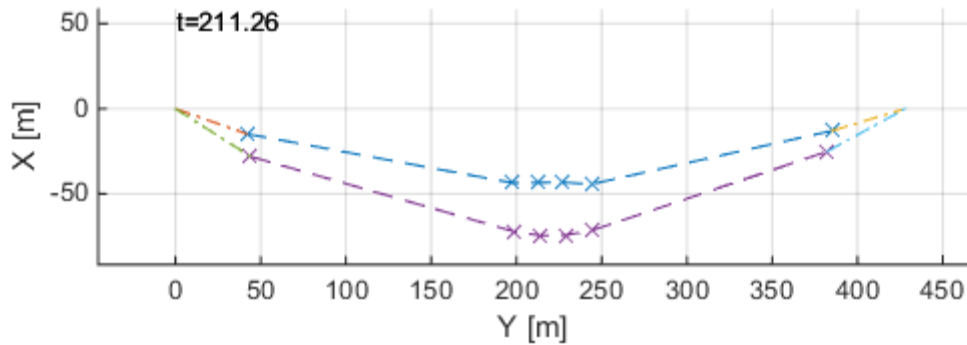


Figure 5-14: Horizontal motion snapshot for 0.3 and 1.0 m/s current cases (equal wave conditions)

5.3.1.1 Surge

The surge motion of the barrier is presented in the centre position. This value is highly transient/ or low frequent: i.e. the motions are dominated by a component that is not linear with the waves. See Figure 5-15 for an example time trace, with a low pass filtered signal overlapped. Note the irregularities in the filtered signal at the beginning and end, which should be ignored. Furthermore, we see a decrease in the mean excursion of the system in waves with respect to its initial position. In various wave conditions the low frequent behavior is different. First a look is taken to the low frequent characteristics, after which wave- and high-frequency behavior is studied.

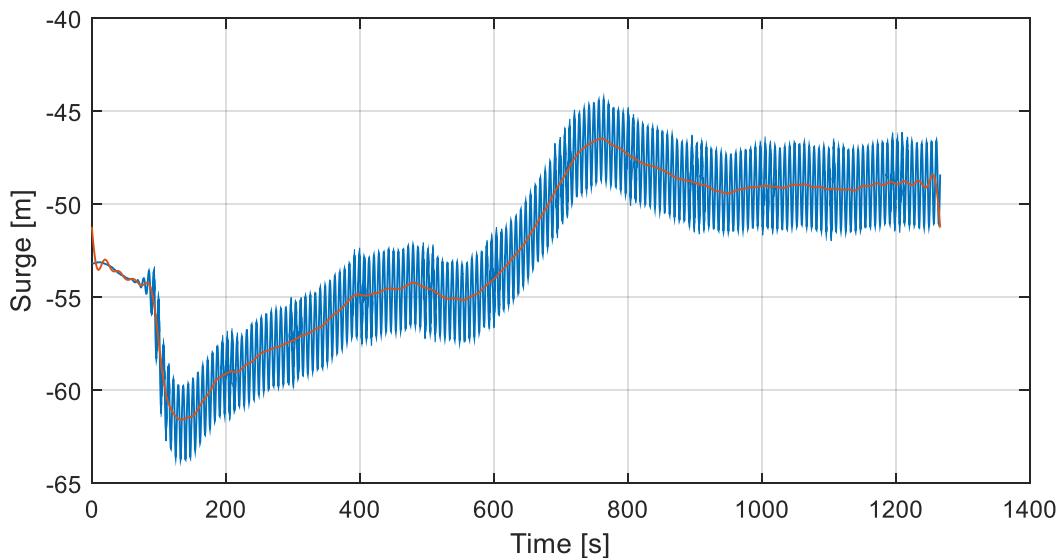


Figure 5-15: Surge motion time trace of high mooring low pretension regular wave test

Multiple wave and current conditions for the high mooring low pretension configuration are shown in Figure 5-16 and Figure 5-17. An error is present in the 6m 6.5s wave from 225 deg in 0.3 m/s current, from approximately 600s. Different configurations for equal wave and current conditions are shown Figure 5-19 and Figure 5-21. Note that the initial position has been set to zero, in order to have an easier comparison for different configurations, as the initial position differs. Low frequent motions are observed in all cases and correlations are present:

- In 225 and 180 deg waves the centre of the systems moves away from the mean current position during the first wave occurrences. The motion builds up to a peak from which a slow decline takes place, which seems to be continuing after the test stops.
- The steep increase and slow decrease of the mean position is observed in all mooring configurations and pretensions. In 0.3 m/s current the decrease is either slower or likely stagnates. In 1.0 m/s the decrease is to approximately to the position the system started the test in. In one case (high mooring, med pretension) the decrease is such that the system moves further back than the position it started in.
- In 0.3 m/s the transient motion is larger than in 1.0 m/s current, the difference is approximately a factor 2. In 1.0 m/s the system is subjected to more tension, leading to a higher resistance to bending. In higher pretensions lower transient motions are observed.
- In 270 deg waves no increase is observed. Even more so, the system slowly moves in the current direction. This can be caused by lowering of the effective drag area of the boom, as the screen compresses part of a wave cycle.
- Possibly the transient loads cause excitation of a very low frequent natural mode.

As these tests were carried out with a regular wave, which consists only of a single wave component with a frequency and amplitude, no slow difference frequency drift can be present. It is concluded this is transient behaviour due to the sudden build-up of waves. It is expected this will not take place in the same order in ocean waves, as build-up of waves is much more gradual. However, during engineering special attention should be paid towards the build-up of a storm in confused seas, instead of simulating merely steady state situations.

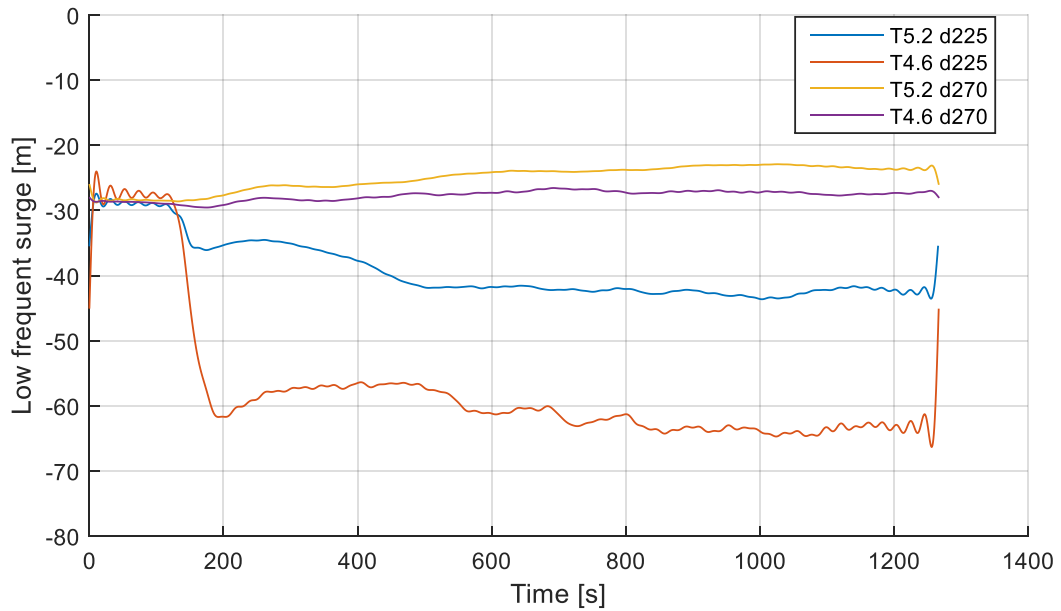


Figure 5-16: Low pass surge for high mooring low pretension 3m waves in 0.3 m/s current

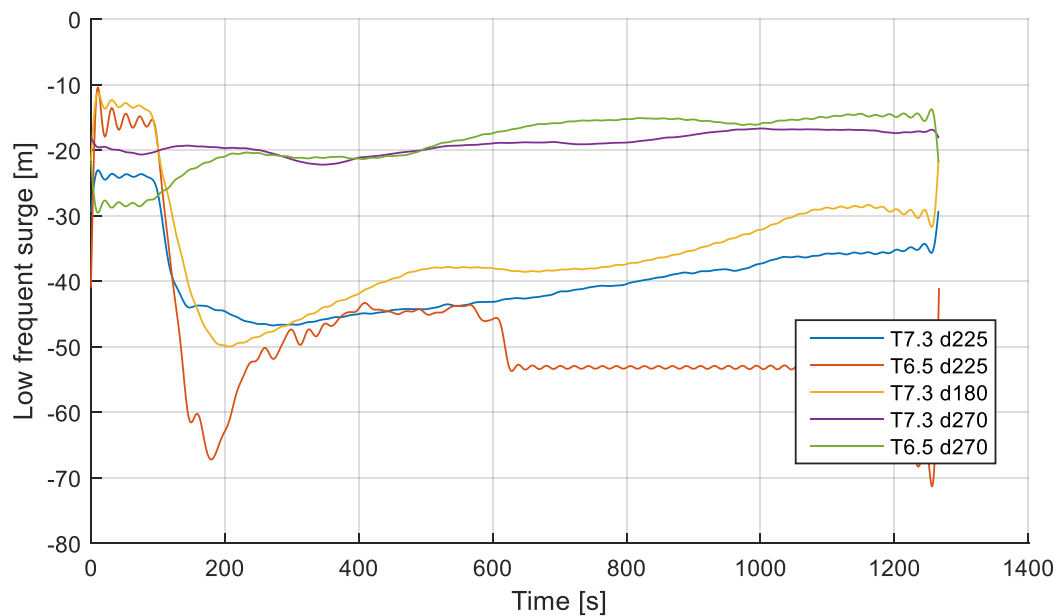


Figure 5-17: Low pass surge for high mooring low pretension 6m waves in 0.3 m/s current

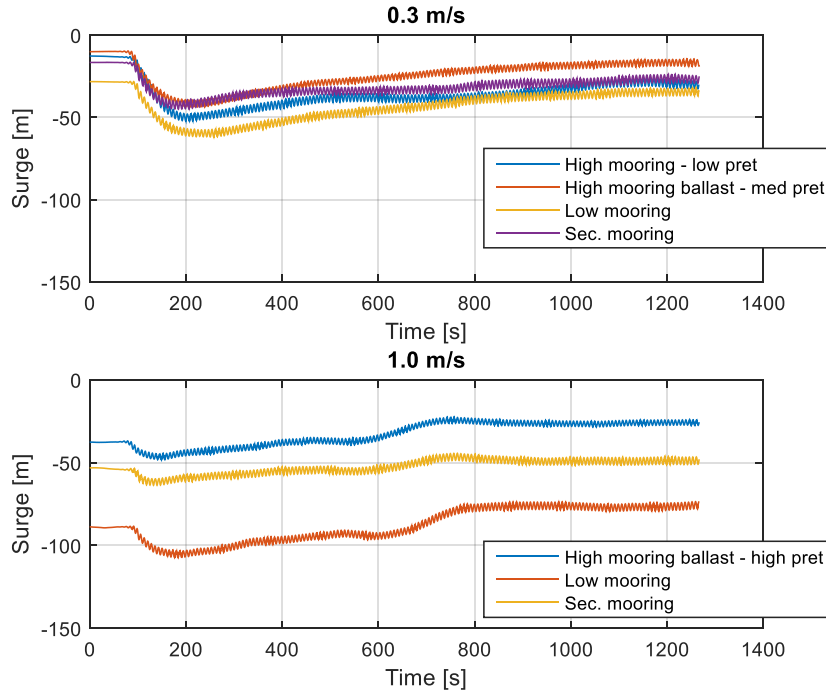


Figure 5-18: H6 T7.3 180 deg surge for different configurations

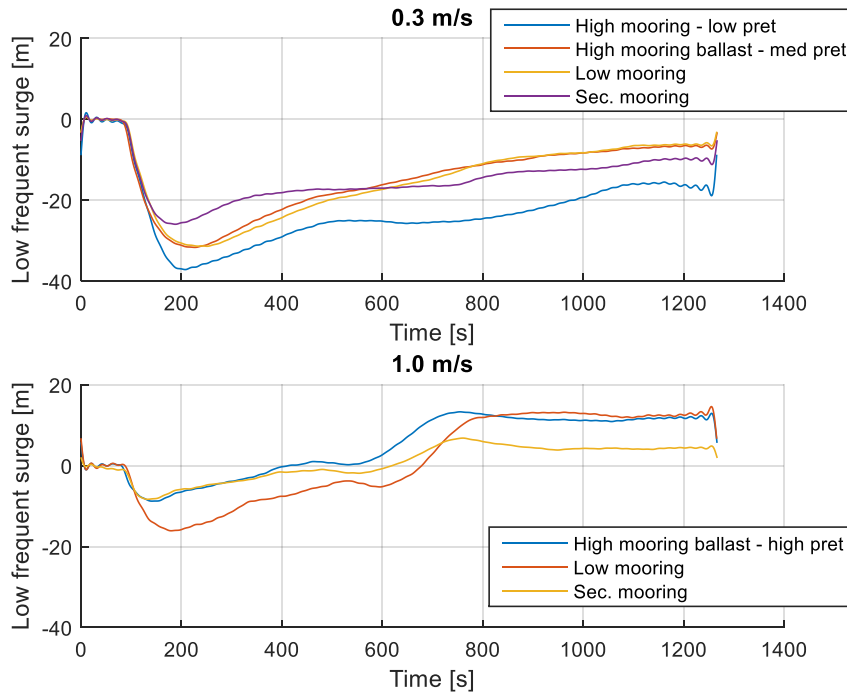


Figure 5-19: H6 T7.3 180 deg surge for different configurations (normalized for starting position to see differences between configurations)

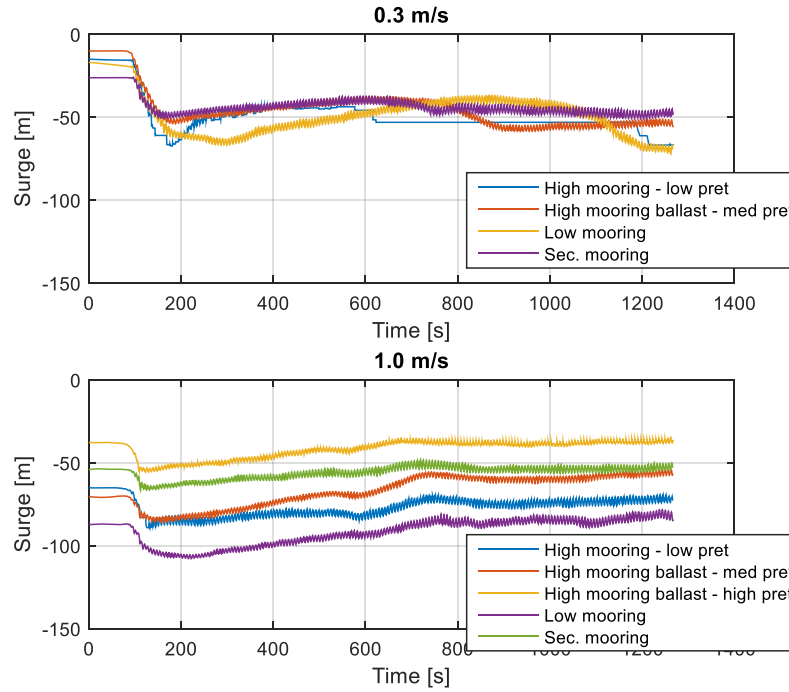


Figure 5-20: H6m T6.5s 225 deg surge for different configurations

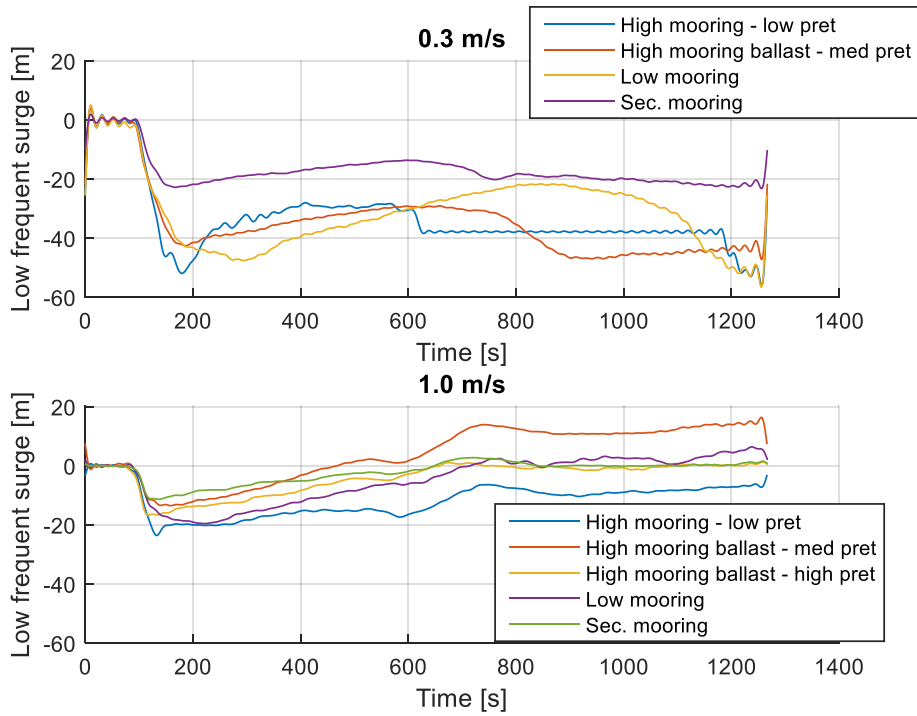


Figure 5-21: H6m T6.5s 225 deg surge for different configurations (normalized for starting position)



Maximum surge motions for all regular waves and current conditions of the high mooring low pretension configuration are shown in Figure 5-22. Wave and high frequent amplitudes can be found in Figure 5-24 and Figure 5-25. Furthermore, results for different configurations are presented in Figure 5-26 and Figure 5-27.

The wave frequent surge amplitude is low relative to the deflection due to current and even more so to the low frequent motion. High frequency surge is even smaller, but may lead to high accelerations as accelerations increase with respect to the motion in frequencies larger than 1 rad/s.

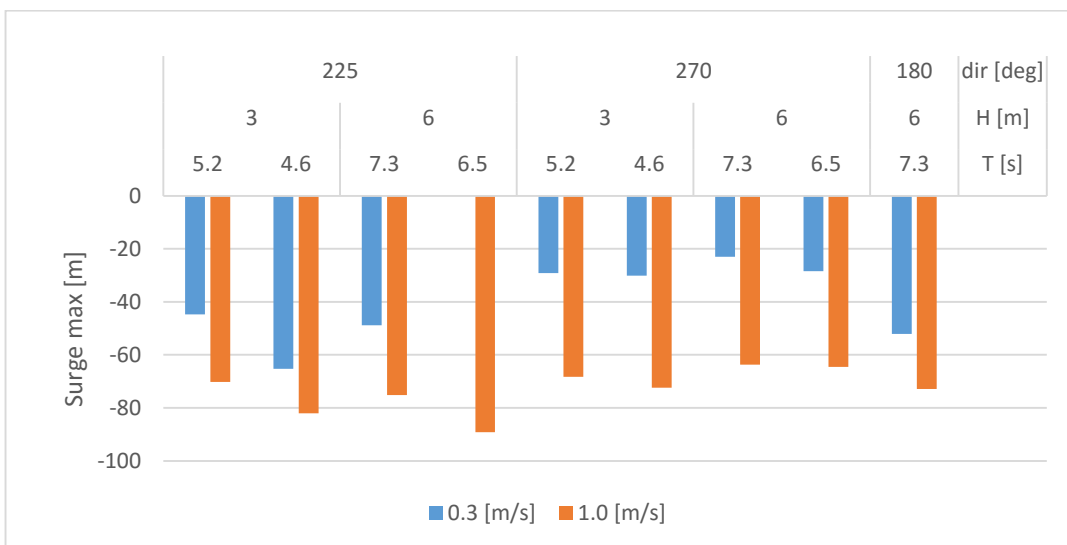


Figure 5-22: Maximum surge motion for high mooring low pretension cases

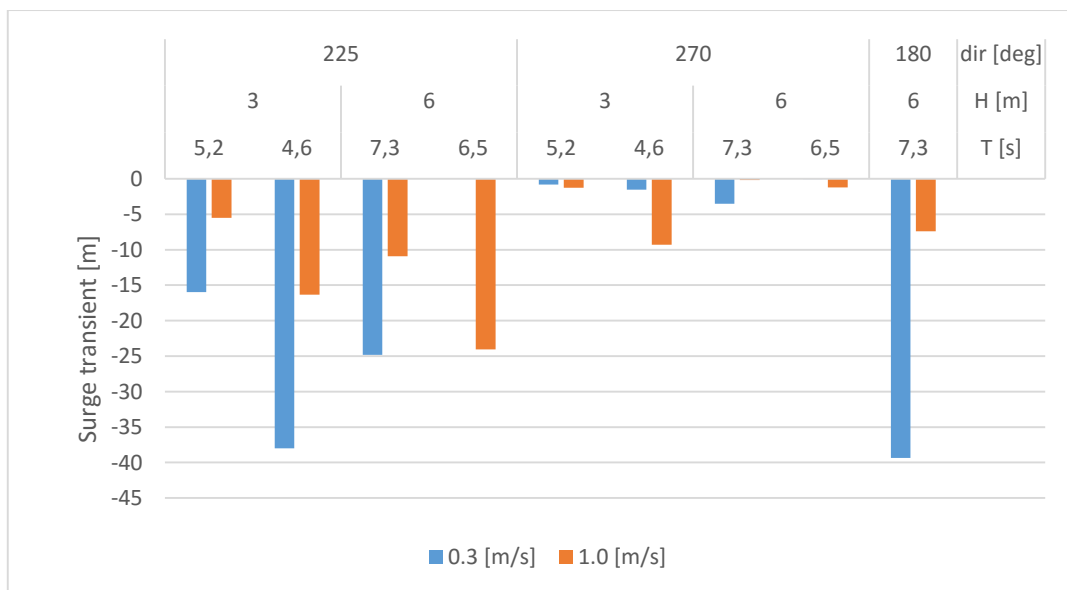


Figure 5-23: Transient motion maximum

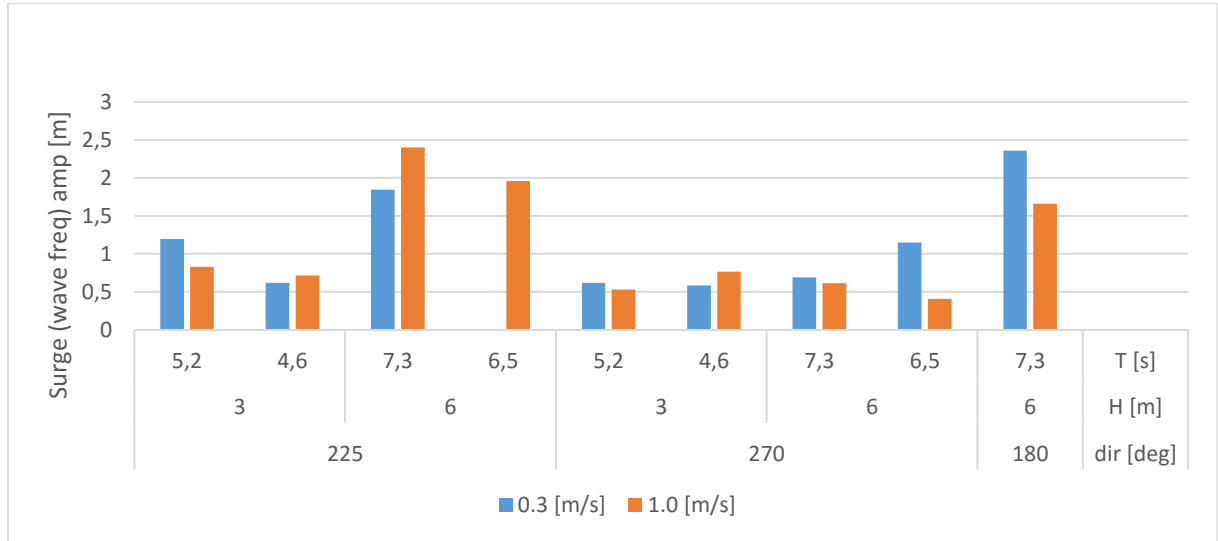


Figure 5-24: Surge wave frequent response

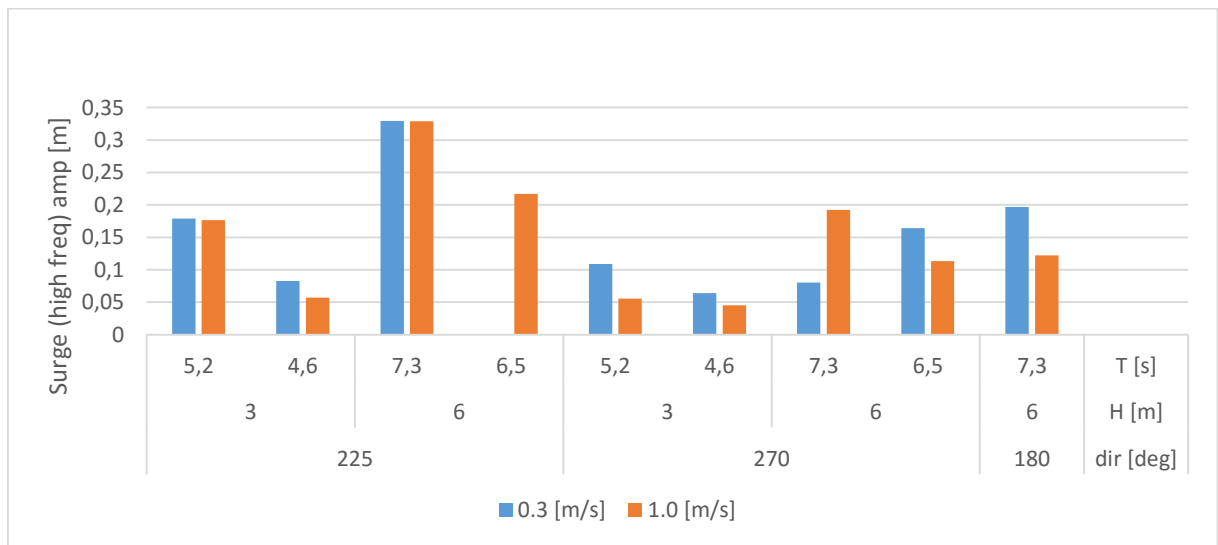


Figure 5-25: Surge high frequent (twice the wave frequency) response

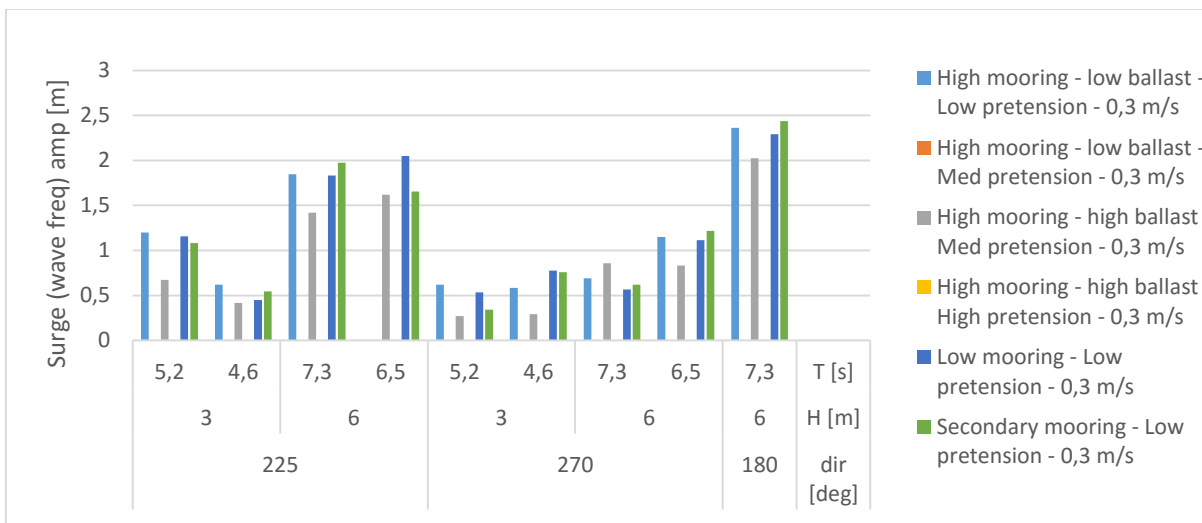


Figure 5-26: Wave frequent surge response for various configurations in 0.3 m/s current

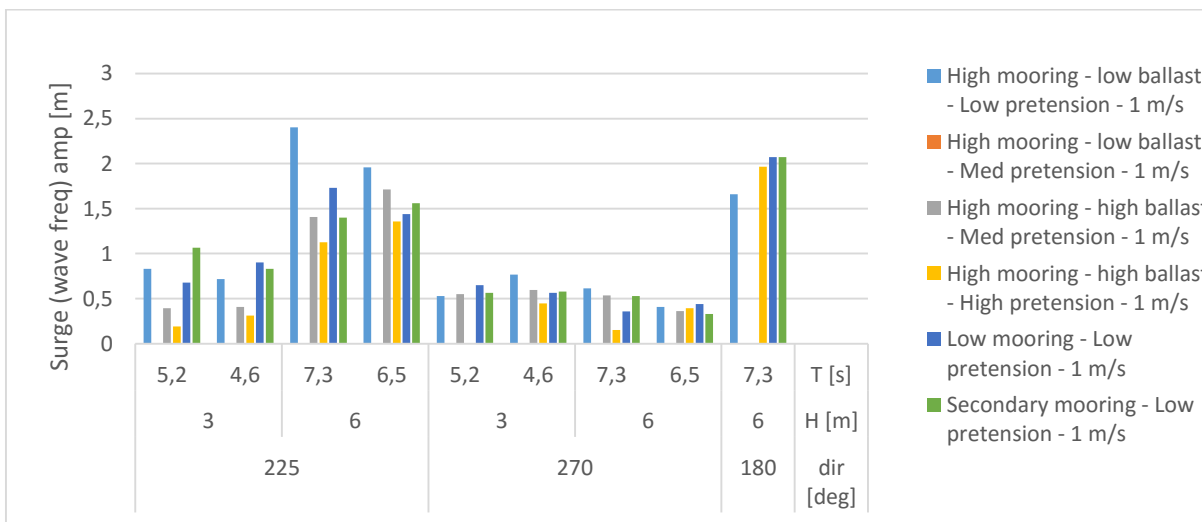


Figure 5-27: Wave frequent surge response for various configurations in 1.0 m/s current

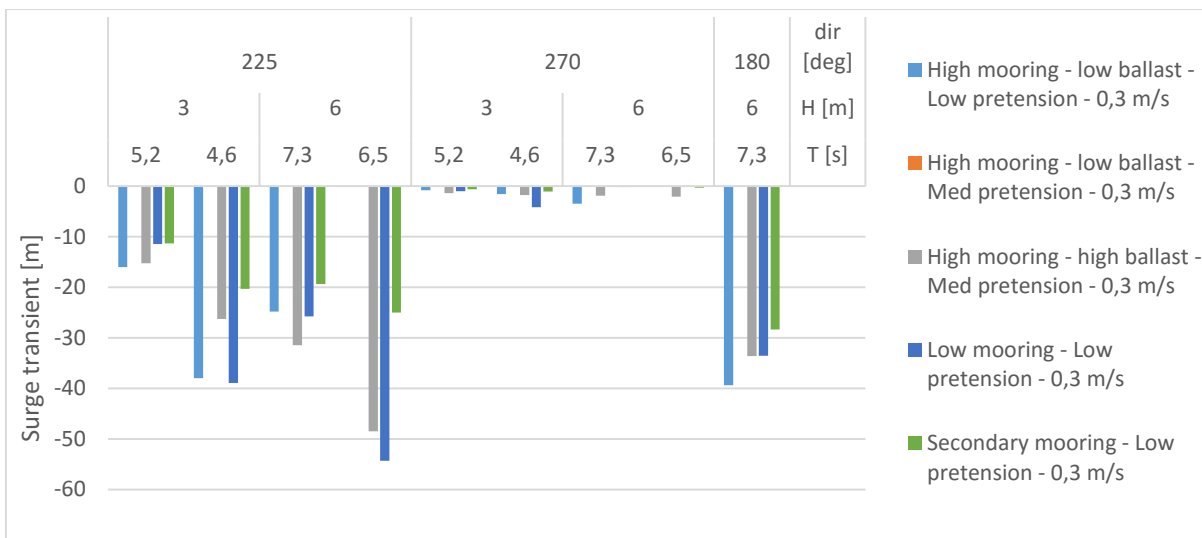


Figure 5-28: Transient motions in 0.3 m/s current

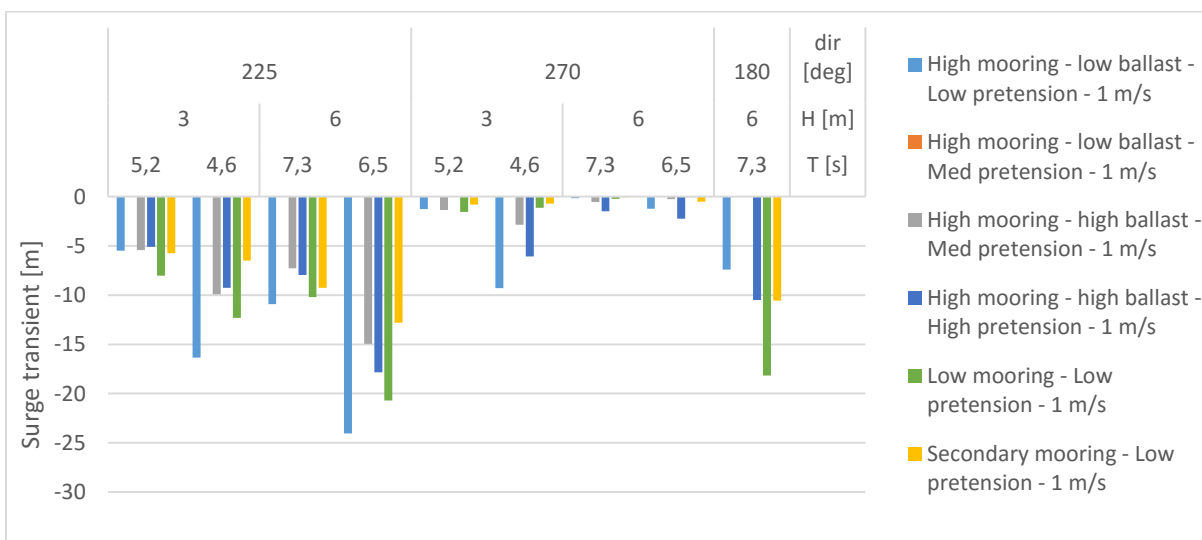


Figure 5-29: Transient motions in 1.0 m/s current

Starboard accelerations are used as this sensor proved to be more reliable. Results are presented in Figure 5-30 and Figure 5-31. Accelerations are measured in a model fixed reference frame. Due to rotation of the floater about the local y-axis the x-axis points partly towards the water surface. In some cases rotations larger than 90 degrees are found and the x and z-axis are consequently swapped. This means a gravity component is included (which is in the case of the results presented filtered out).

High accelerations in 225 degrees, 6m and 7.3s observed. This might be a natural mode. However, due to the many errors present in the acceleration sensors it is not unlikely that it is a sensor error. According to reference [ER.1] the sensor should, however, operate well in this test case.

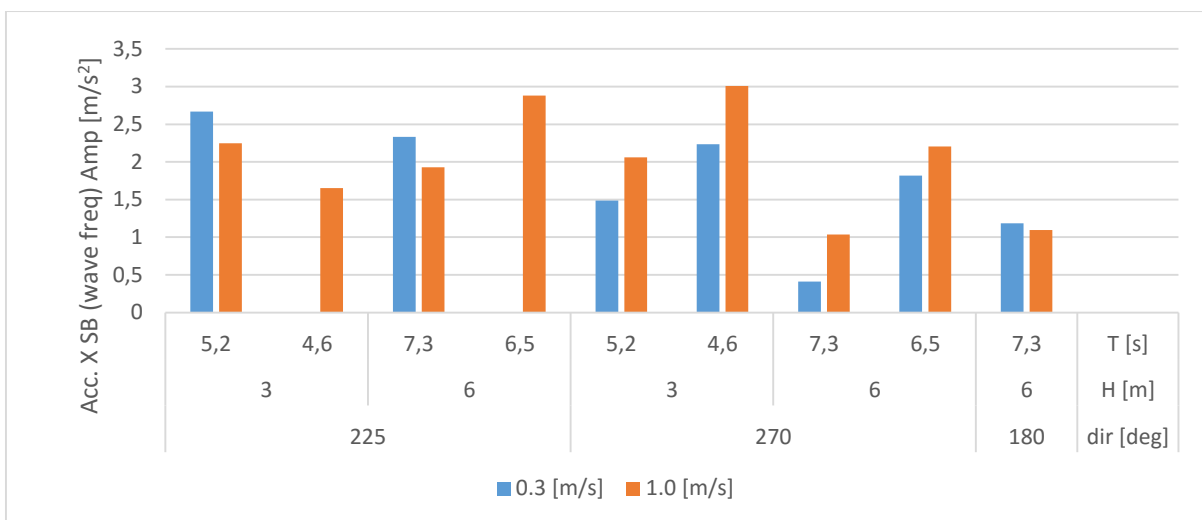


Figure 5-30: Starboard wave frequent accelerations in x-direction

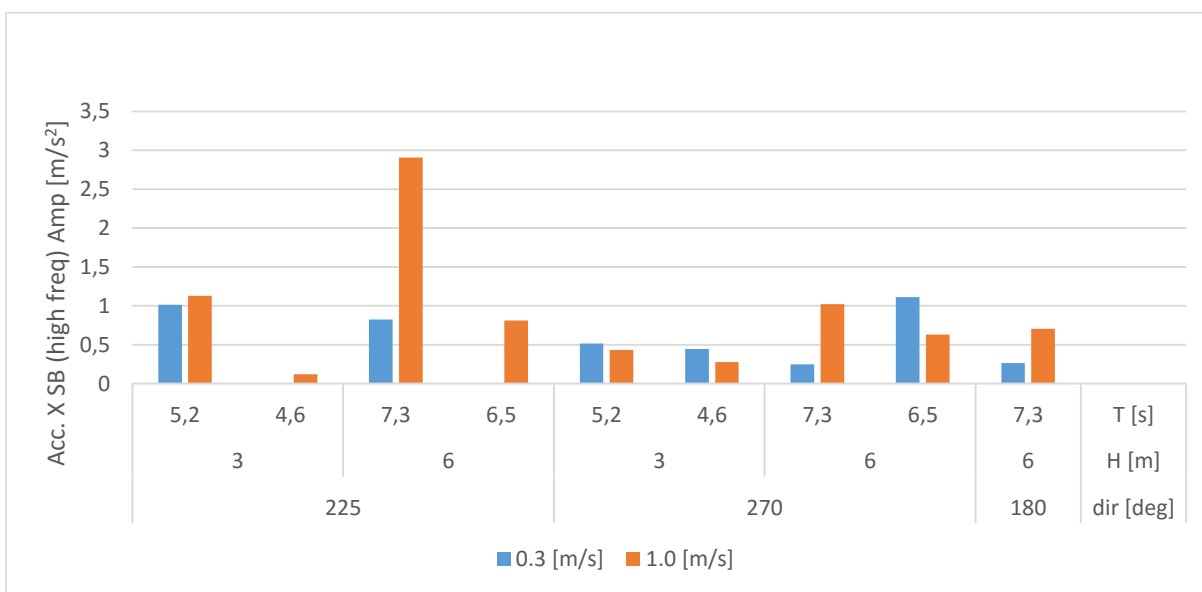


Figure 5-31: Starboard high frequent (twice the wave frequency) accelerations in x-direction

5.3.1.2 Sway

Sway motions and accelerations, having once wave and twice the wave frequency, are shown in Figure 5-32 to Figure 5-35 for the high mooring and low pretension. Overall, the sway motion is low, and the high frequency component is unlikely to cause the large high frequent component observed in the loads.

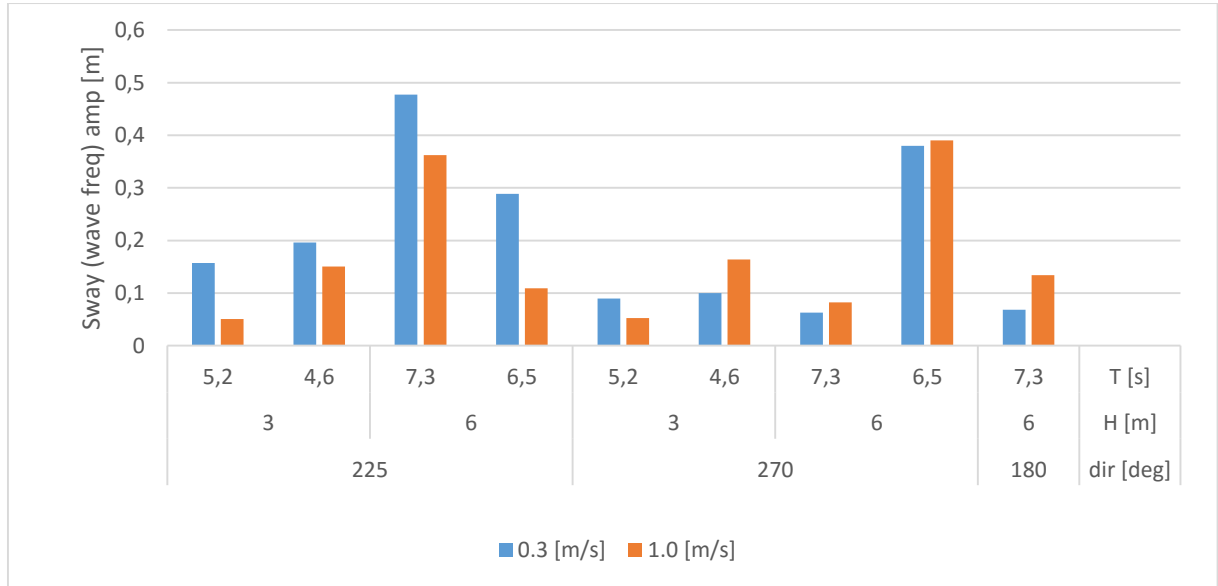


Figure 5-32: Wave frequent sway motion

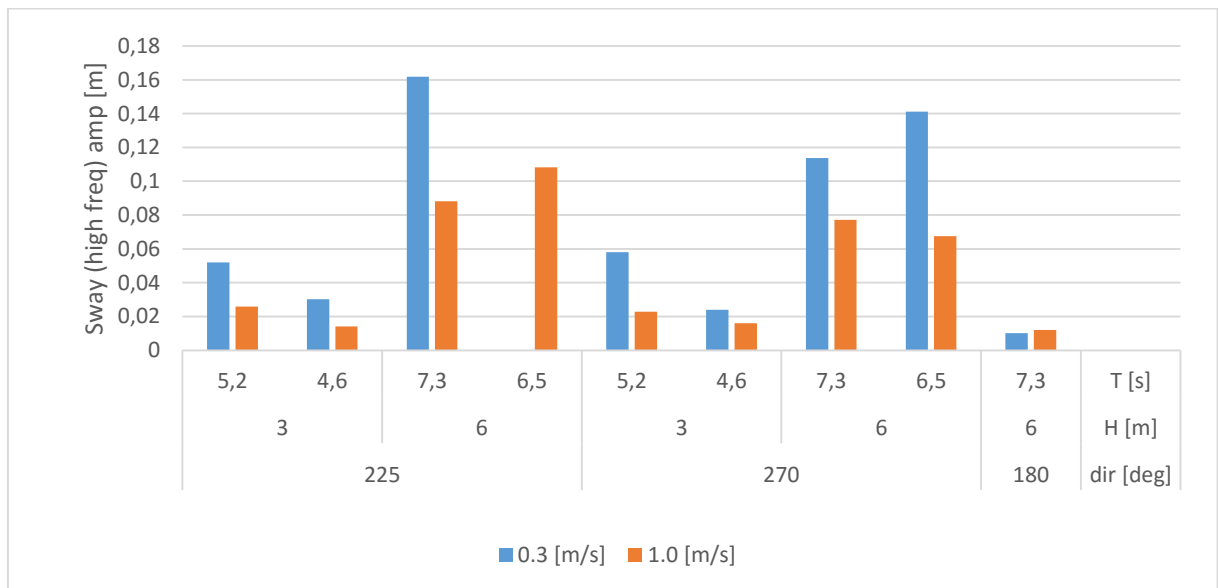


Figure 5-33: High frequent (twice the wave frequency) sway motion

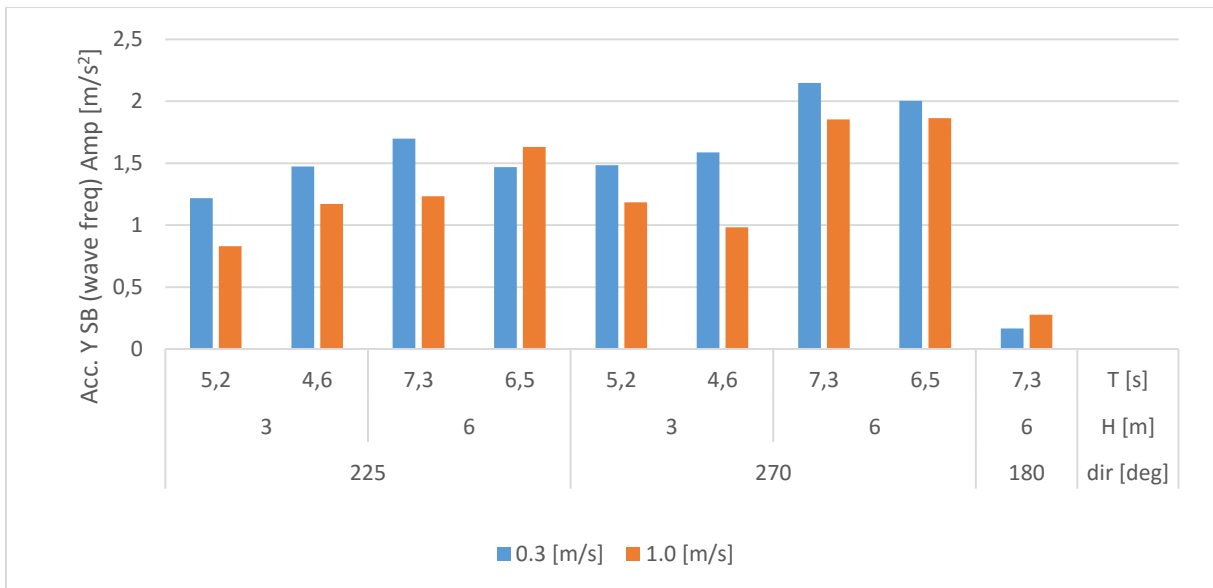


Figure 5-34: Wave frequent accelerations in boom direction

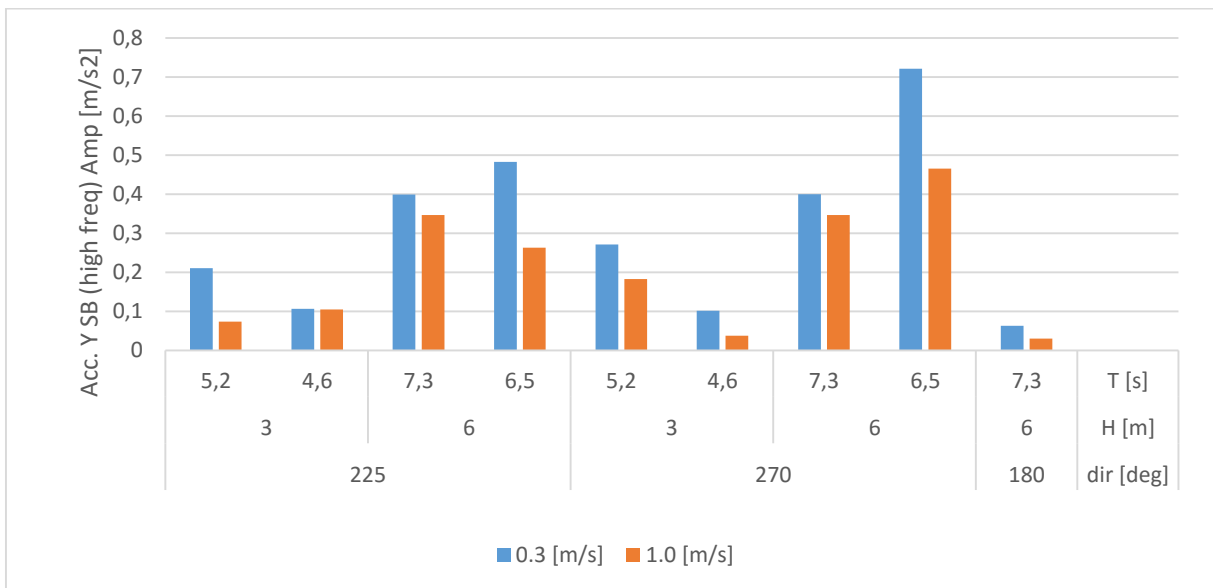


Figure 5-35: High frequent (twice wave frequency) accelerations in boom direction

5.3.1.3 Pitch

The pitch motion (around the axial axis of the system) is stronger with a frequency twice the wave frequency. This motion causes the loads in that frequency. The motion of the centre cross section is shown below.

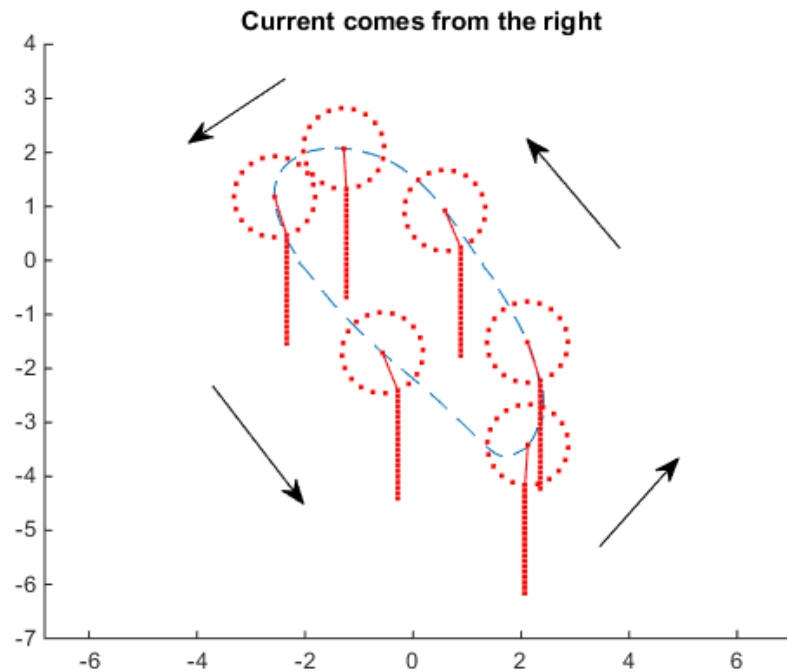


Figure 5-36: Pitch motion of centre cross section

Note that the motion of the screen is unknown, this is visualized as a line always pointing downwards; which in reality will have an orientation depending on the mooring (this is for visualization purposes only). The wave conditions are regular oblique 6m waves. The path is not circular but closer to elliptic, it is unknown at this stage why this is the case.

Some of the pitch time traces show very inconsistent and non-linear behavior. See for instance the center pitch of test 802003, high mooring low pretension with a 3m and 5.2s regular parallel wave in 0.3m/s current in Figure 5-37. The pitch drops to around 30 degrees, after some time it drops even further to 90 degrees.

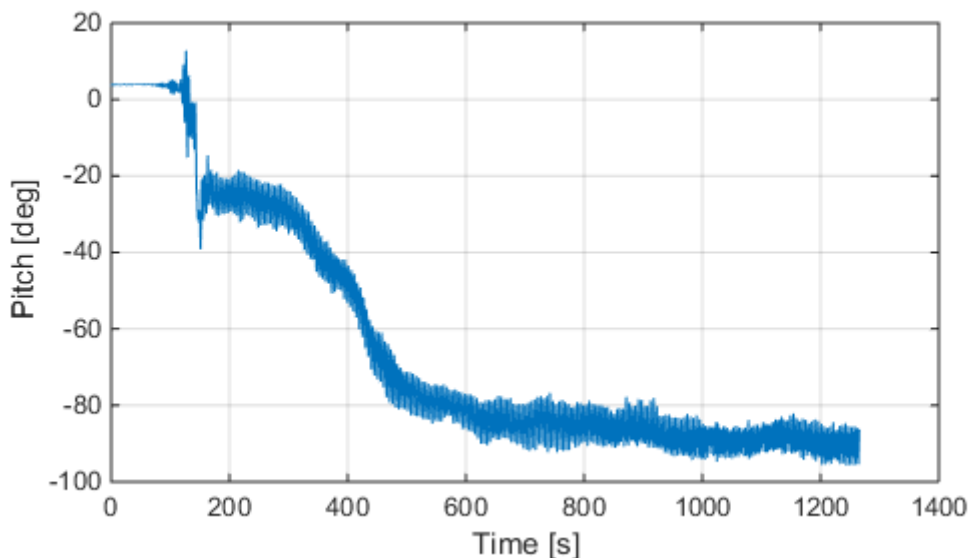


Figure 5-37: Time trace of pitch motion for test 802003 (H3m, T5.2s, 270deg)

The mean pitch angle for various regular wave tests in the high mooring low pretension setup is shown in Figure 5-38. A negative pitch angle corresponds to a rotation away from the current. Note that for the large rotations over 90 degrees the sensor becomes invisible for the carriage based sensing system. These cases have been removed from the database. The barrier rotates in some cases a large angle away from the current heading. This is remarkable, as the force exerted on the screen causes a moment in the opposite direction. It might be caused by wave loading on the cylindrical floater.

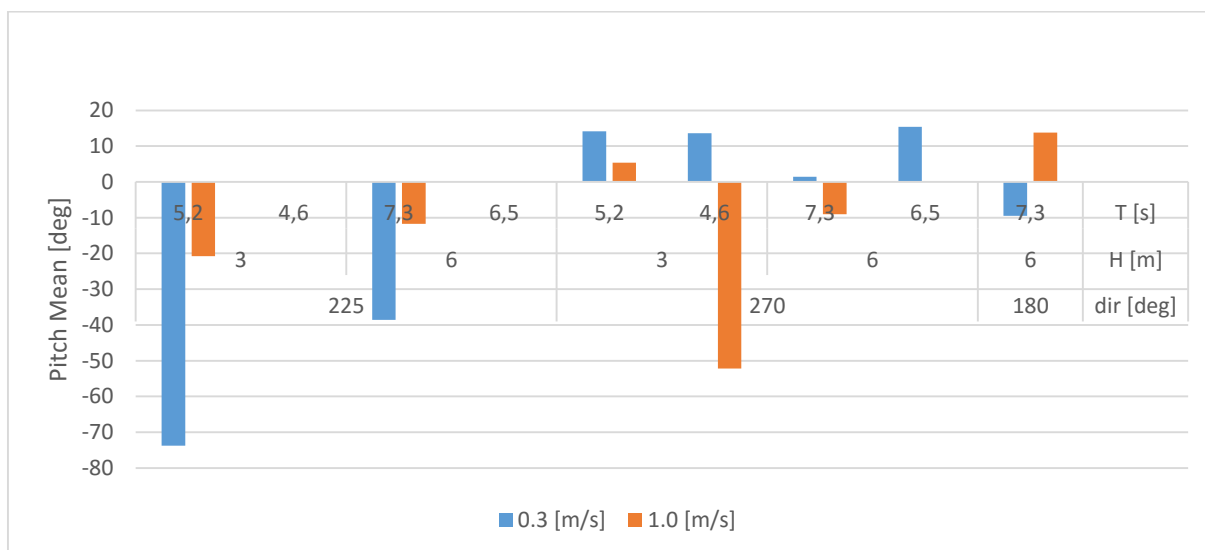


Figure 5-38: Mean pitch angle (high mooring, low pretension)

The low mooring mean pitch angle is shown in Figure 5-39. In this setup a small negative angle is expected, as the moment about the tension wire rotates the floater away from the current direction. However, also in this setup sometimes angles close to -90 degrees are seen, meaning the floater is lifting the screen effectively. Care should be taken with these numbers as they are indicative, since the process is not a steady-state one (see Figure 5-37). A mean angle of -45 degrees could still indicate that somewhere in the test the angle is -90 degrees for a significant duration.

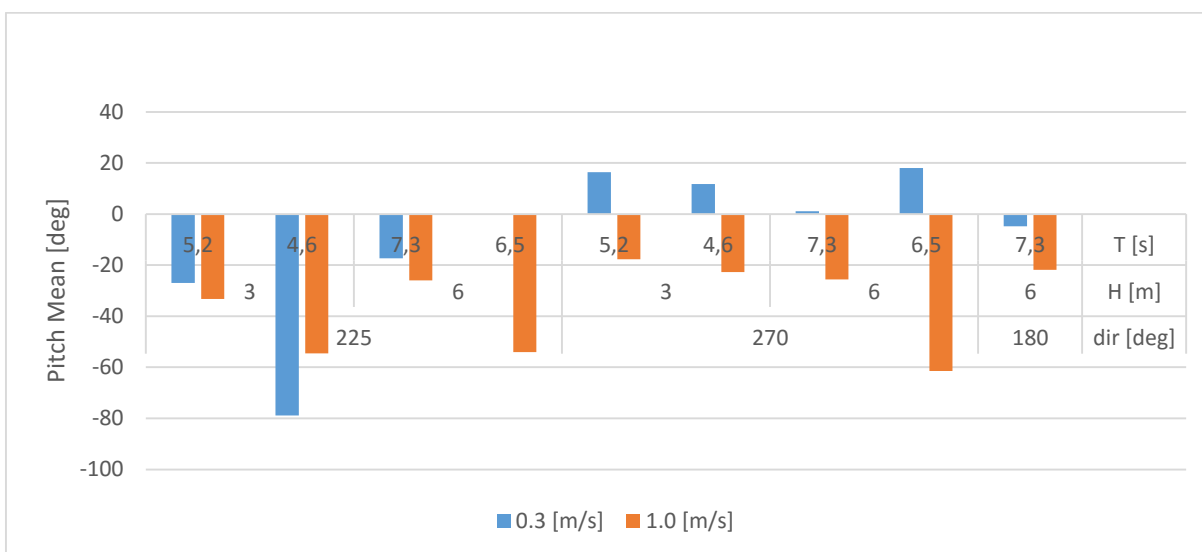


Figure 5-39: Mean pitch angle (low mooring, low pretension)

The wave and high frequent component are provided in Figure 5-40 and Figure 5-41 for the high mooring and low pretension cases. For all other setups the high frequent part of the pitch motion is shown in Figure 5-42 and Figure 5-43. It is observed that in one wave condition the high frequency pitch motion is significantly larger; in 6m and 7.3s 225 degree waves in 1.0 m/s current. It appears this condition excites a natural frequency, although similar behavior is not seen in 180 and 270 degree waves. In all configurations and current speeds high frequent pitch is observed, although the secondary mooring configuration has the smallest amplitude. No clear change in pitch with respect to pretension is observed.

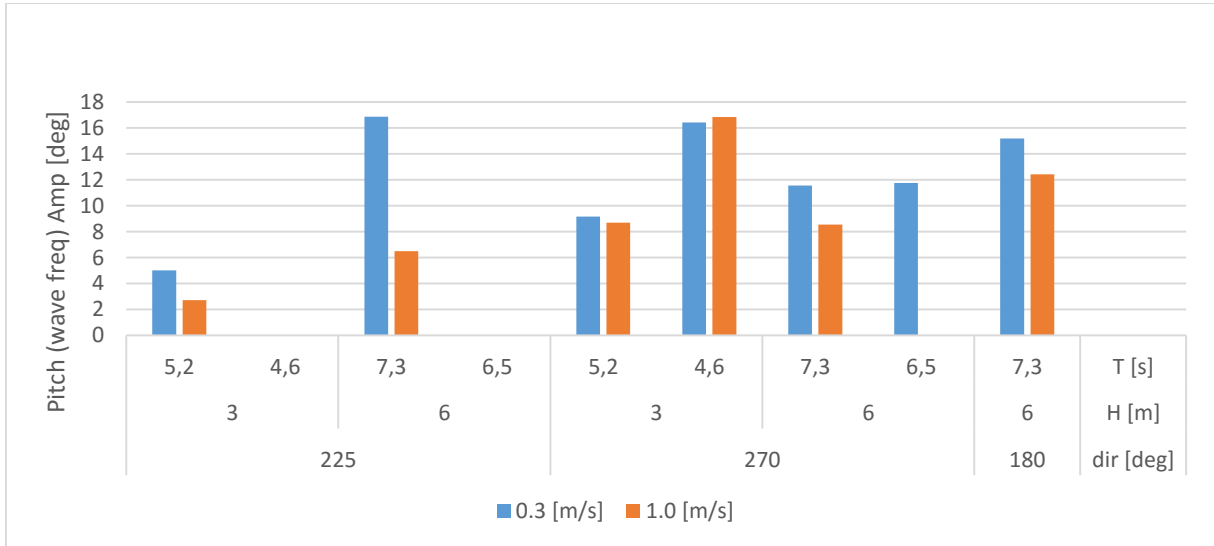


Figure 5-40: Wave frequent pitch amplitude (high mooring, low pretension)

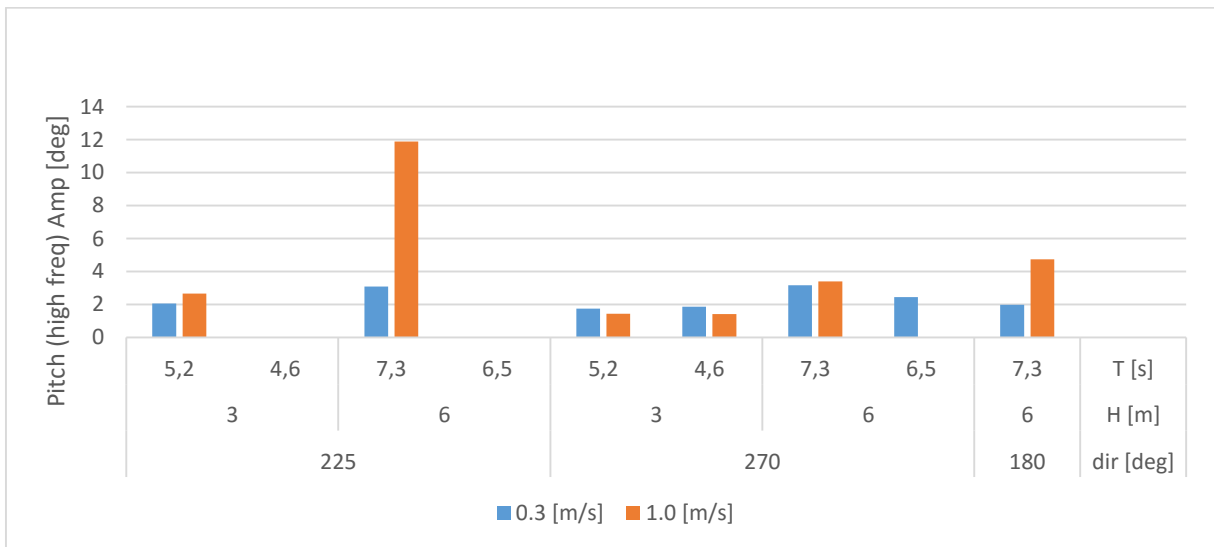


Figure 5-41: High frequent pitch amplitude (high mooring, low pretension)

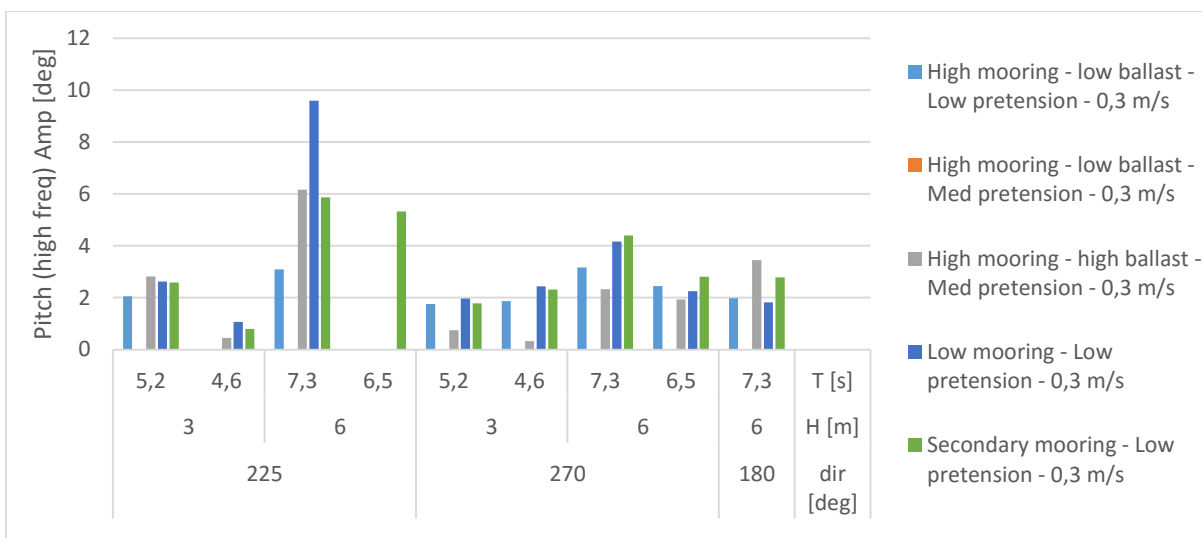


Figure 5-42: High frequent pitch amplitude for all configurations in 0.3m/s current

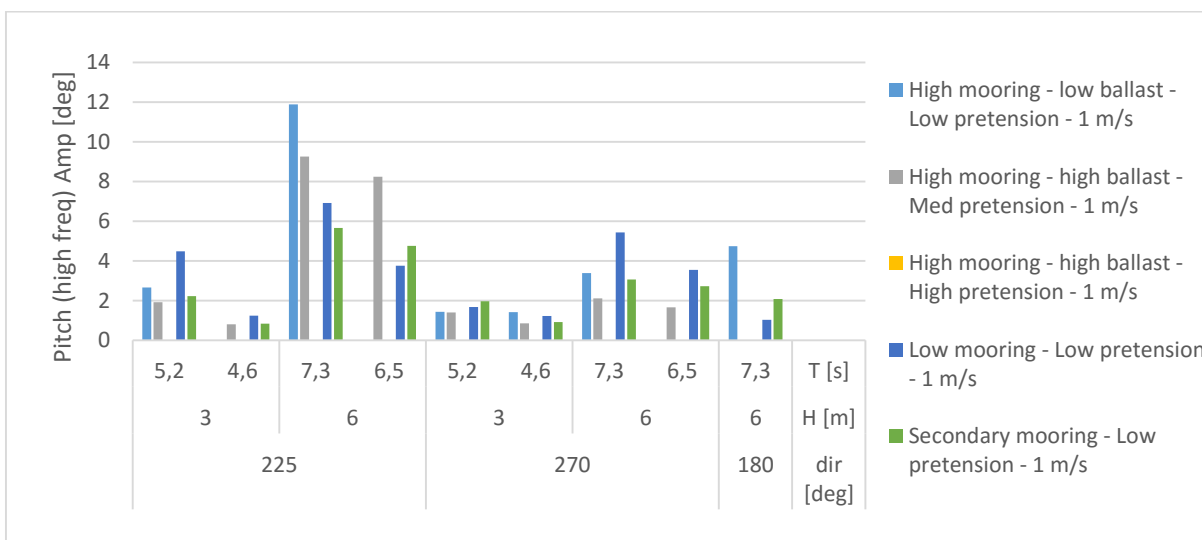


Figure 5-43: High frequent pitch amplitude for all configurations in 1m/s current

5.3.2 Loads

In this section the loads taking place in regular waves are analysed. The secondary mooring configuration is analysed separately, as loads are transferred from the boom to the tank in four locations—through the tension wire beneath the floater and the subsea mooring line. Furthermore, seven secondary mooring line loads are measured.

5.3.2.1 High & Low Mooring

First a look is taken to the low frequent loads. In Figure 5-45 and Figure 5-47 a low pass filter is applied to the tension and azimuth to compute the unit load. Note that the unit load is computed for the total



length (360m) and not the instantaneous length. The initial value is deducted from the time traces, for a better visual comparison. These figures look very similar to the centre position measurements, as shown in Section 5.3.1.1. Again an error is present in the 6m 6.5s wave from 225 deg in 0.3 m/s current in the high mooring low pretension case, from approximately 600s. The low mooring configuration has the same pretension as the low pretension high mooring cases. Low frequent motions are dominated by displacement (stiffness), with low influence of damping and mass/inertia.

In Section 5.3.1.1 it can be seen that in some cases the system moves transiently away from its initial position to a maximum offset, and then back again to a smaller offset than its initial deflection. This is reflected in a drop in unit load in Figure 5-45 and Figure 5-47, as the initial load in current has been set to zero.

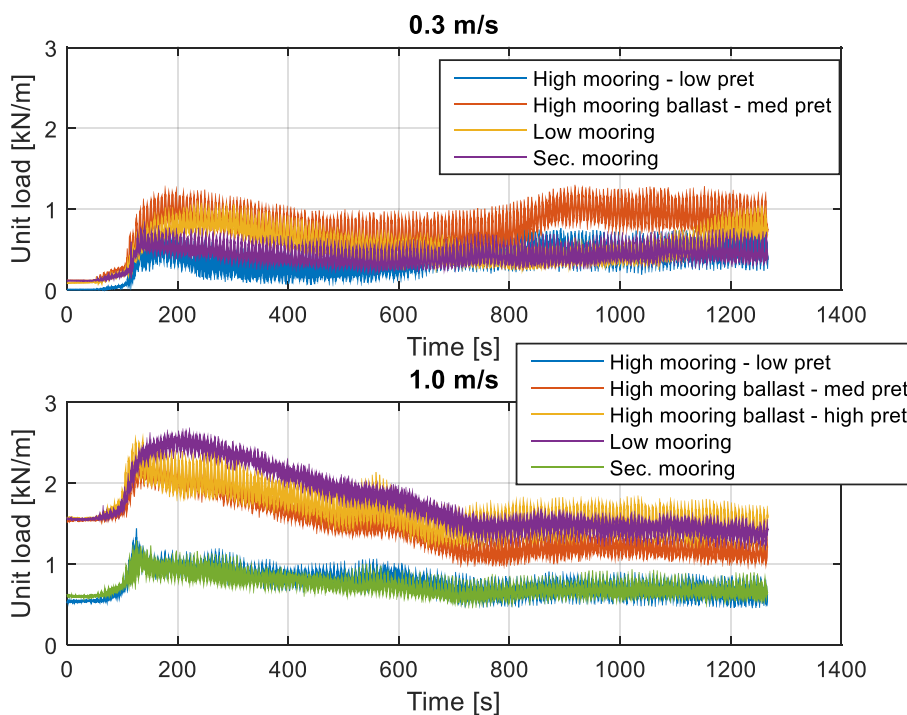


Figure 5-44: Unit load for H6 T6.5 deg225

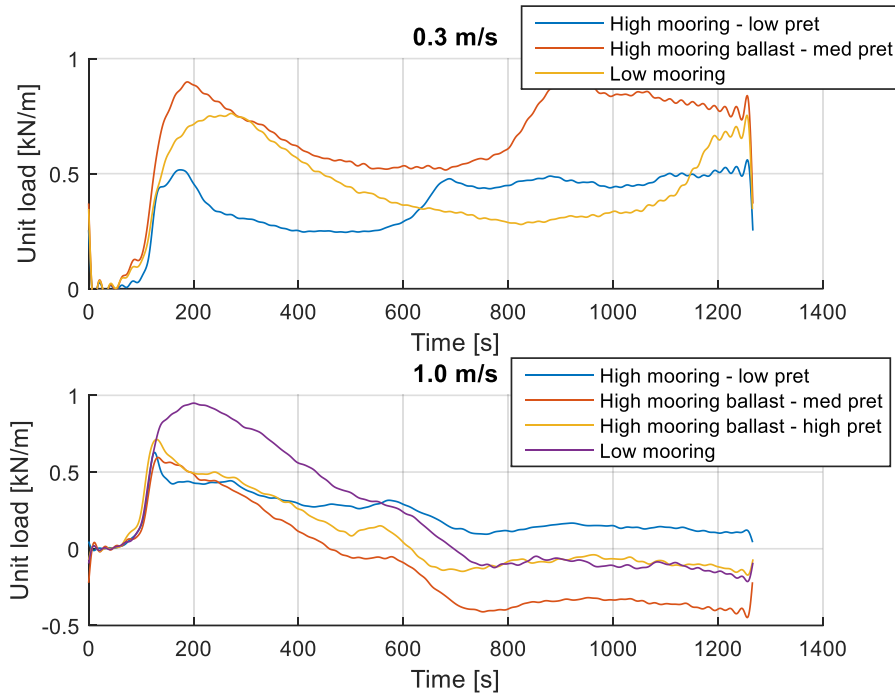


Figure 5-45: Unit load for H6 T6.5 deg225 (filtered and normalized to start at zero)

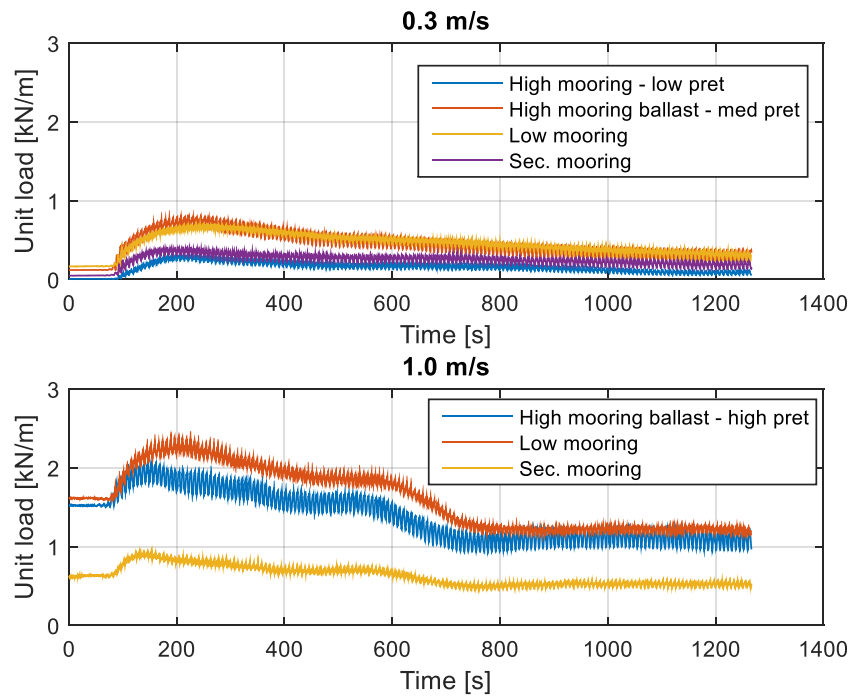


Figure 5-46: Unit load for H6 T7.3 deg180

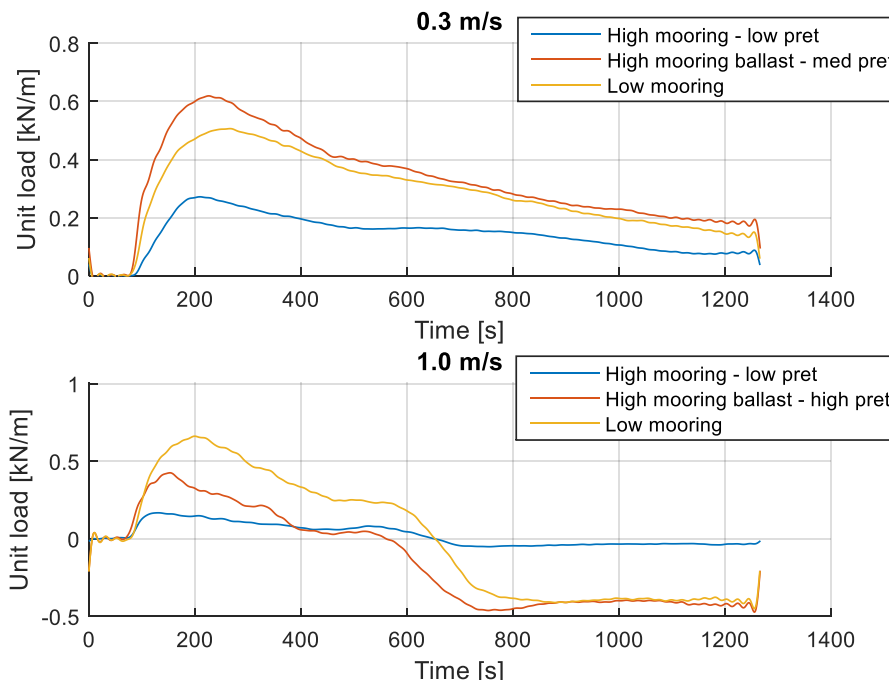


Figure 5-47: Unit load for H6 T7.3 deg180 (filtered and normalized to start at zero)

The transient loads are caused by the slow surge of the boom. It has been concluded in section 5.3.1.1 regarding the surge motion that this effect is caused by the build-up of the waves, forcing the boom first to move from its mean position, slowly returning or even overshooting from said position. Note that damping in the system is quadratic: leading to high damping in large frequencies (high velocities), as the square of a large number is even larger. However, the square of a number smaller than 1 becomes even smaller. In low frequencies velocities are low and consequently damping is low.

The wave frequent and second harmonic transversal force amplitude are shown in the Figure 5-48 and Figure 5-49. Wave and high frequent transversal load amplitudes are presented for various configurations in Figure 5-50 to Figure 5-53. In Figure 5-54 and Figure 5-55 the transient part of the transversal load is shown (initial value distracted from dynamic low frequent max). In Figure 5-51 and Figure 5-53 the transversal load is shown as a function of the square of the wave double amplitude divided by the period, which serves as an indication of the wave particle velocities—the wave period is related to the wave length. If the response is caused predominantly by drag, the response will be linear over the velocity squared.

The following is observed:

- Remarkably, the order of both response harmonics (wave and twice the wave frequency) is equal: the amplitudes are similar. The component at twice the wave frequency, which was

expected to be small, is significant. It is likely this component is caused by the pitching motion of the boom.

- The higher the wave velocity (related to amplitude and period), the higher the load.
- Even though the 270 degree waves are parallel to the boom, a very small transversal component is present.
- Wave loads for different configurations are equal for the low and high mooring configurations with a low pretension. As the pretension increases, the wave loading slightly increases. The cases with higher pretension were carried out with a higher ballast weight which surprisingly lowers the wave loading slightly.
- In 1.0 m/s the high pretension high mooring configuration cannot follow the waves well anymore, leading to higher wave frequent loads that stand out in terms of characteristics.
- Wave frequent loads are similar in terms of amplitude in 0.3 and 1.0 m/s current.
- If the system is flexible, the overall wave frequent loading is low with respect to the mean load.
- Wave and high frequent loads are generally larger in oblique waves than in
- In all configurations and currents transient peaks are observed in the loads. The 6m 6.5s wave at 225 degrees causes the highest transient loads.
- High frequency loads are present in all setups. In the low mooring the amplitude remain relatively lowest, whilst the high mooring with low pretension gives highest forcing.

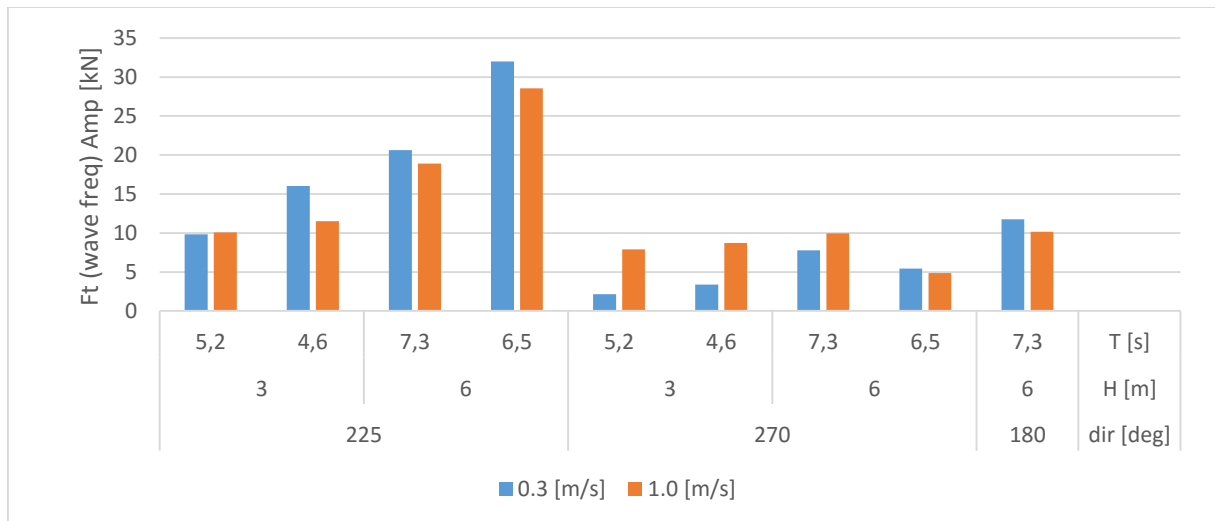


Figure 5-48: Transverse wave frequent load component (high mooring low pretension)

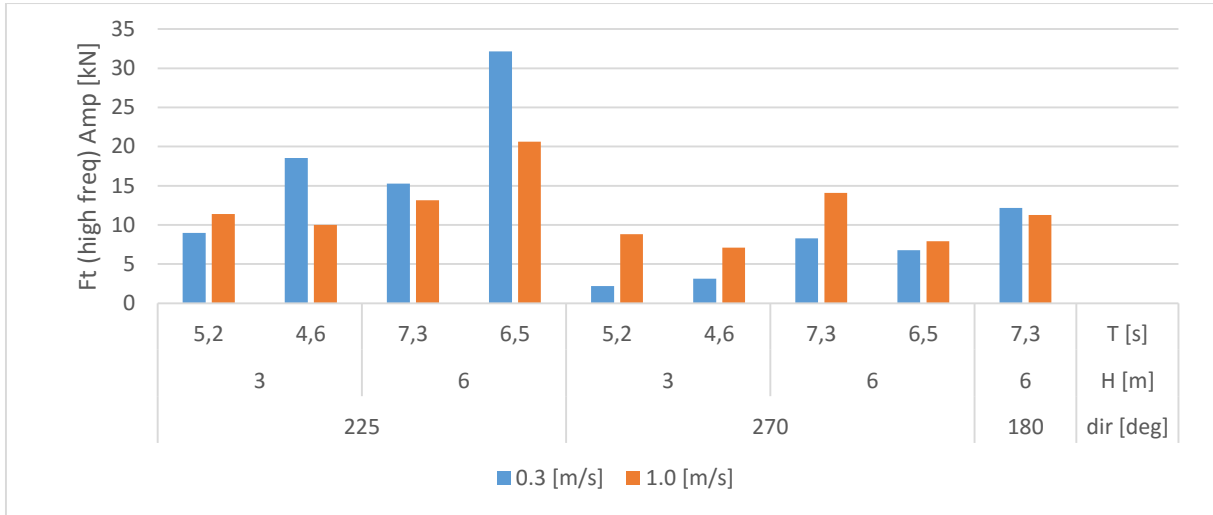


Figure 5-49: Transversal high frequent load component (twice the wave frequency, high mooring low pretension)

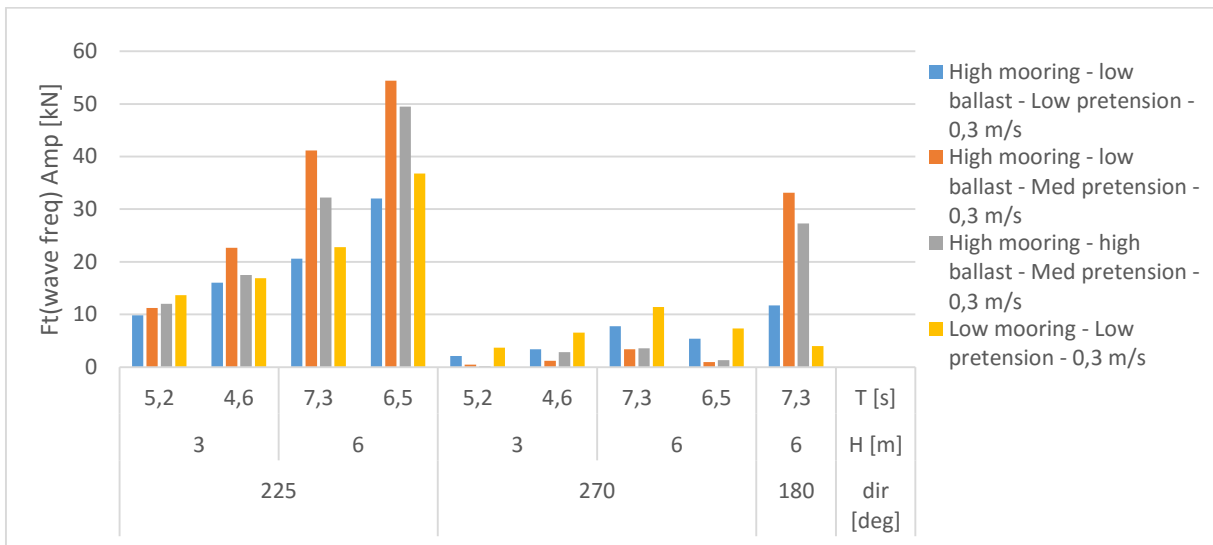


Figure 5-50: Wave frequent transverse load in 0.3 m/s current for various configurations

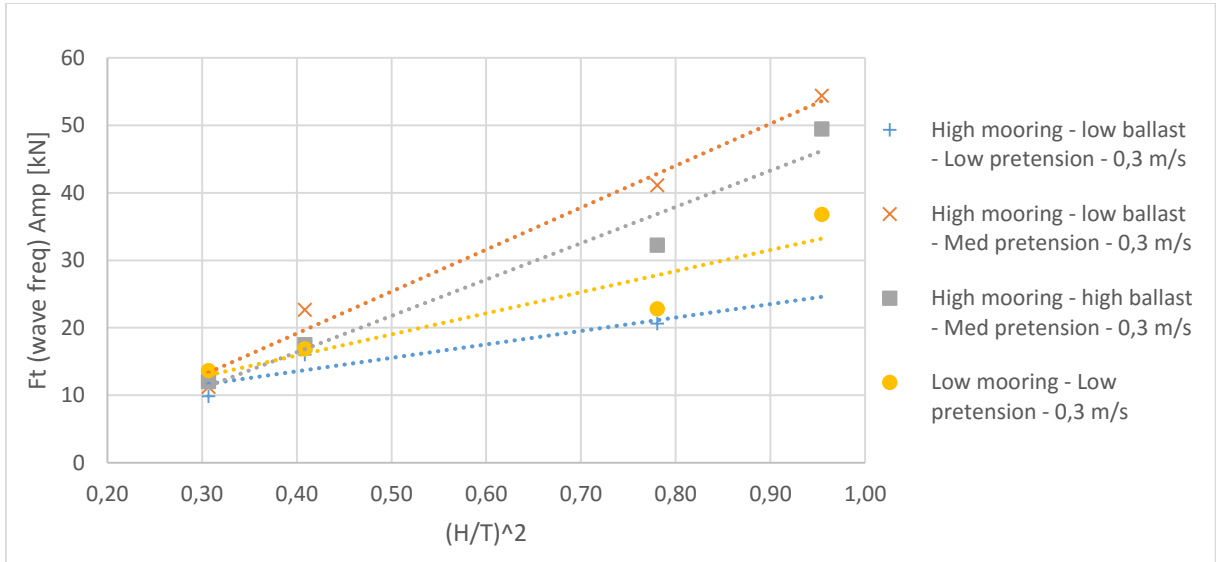


Figure 5-51: Transverse load in 0.3 m/s as a function of the relative wave velocity squared

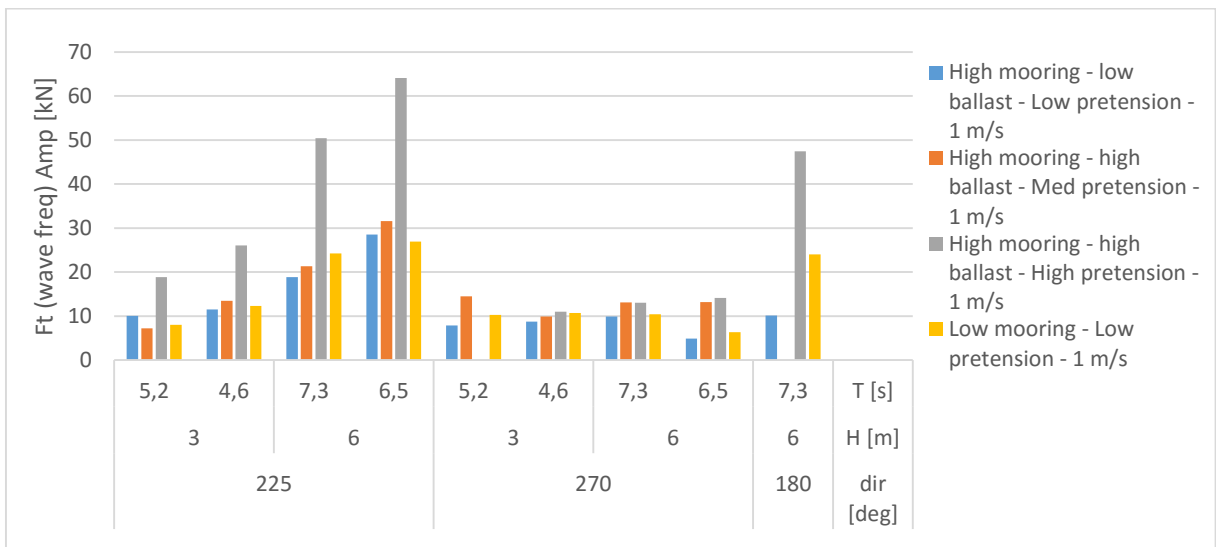


Figure 5-52: Wave frequent transverse load in 1.0 m/s current for various configurations

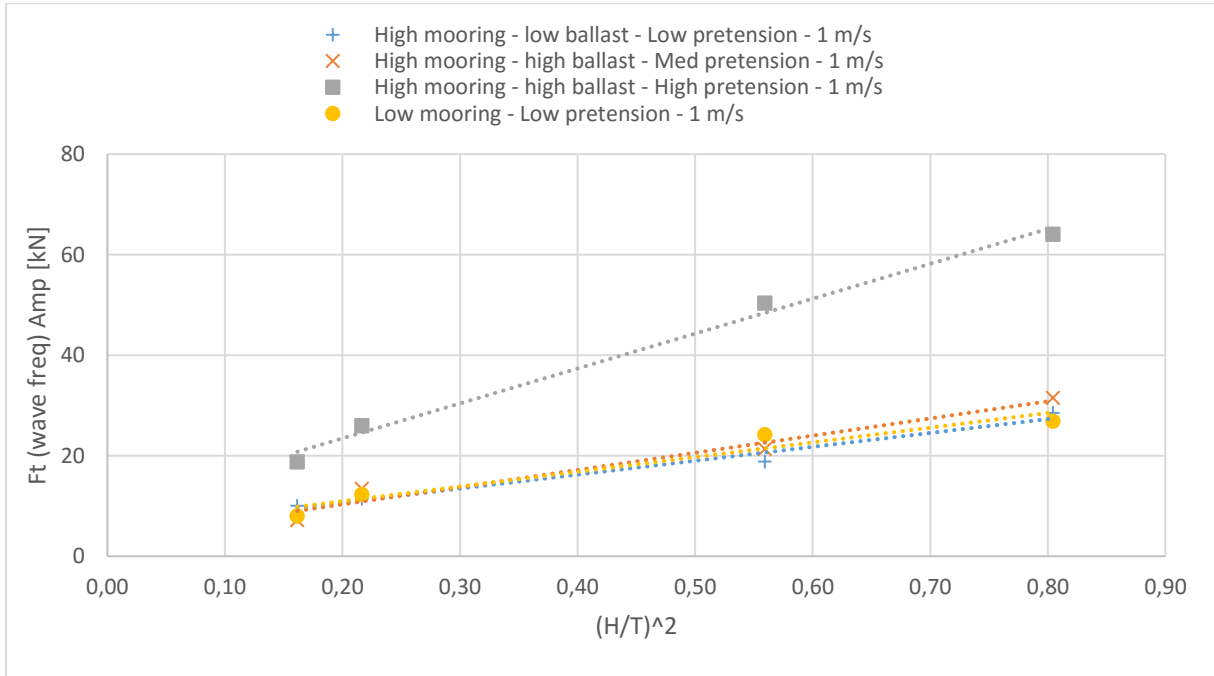


Figure 5-53: Transverse load in 1.0 m/s as a function of the relative wave velocity squared

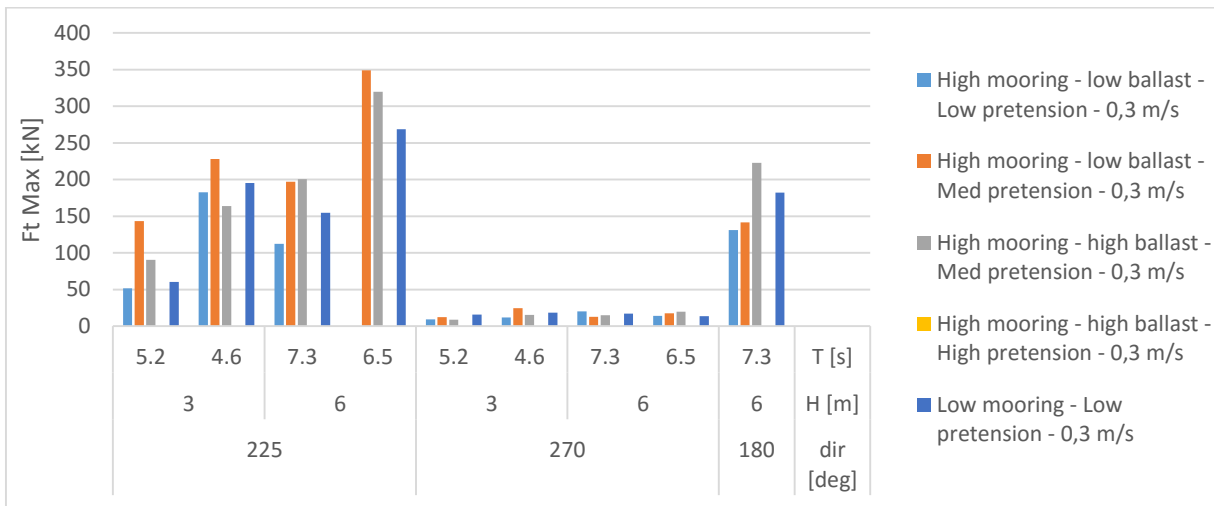


Figure 5-54: Transient transverse peak load in 0.3 m/s current

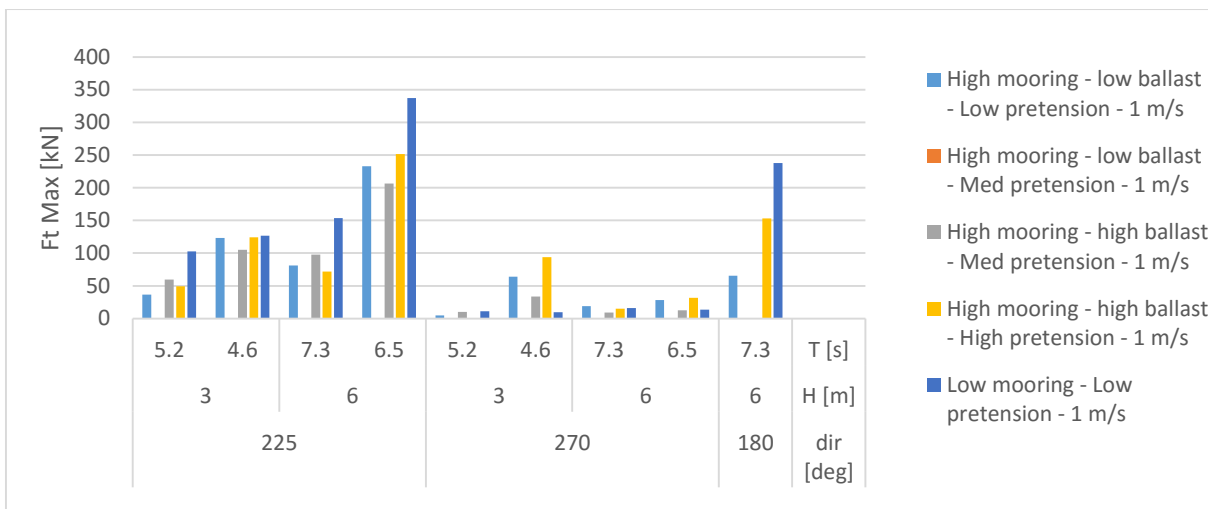


Figure 5-55: Transient transverse peak load in 1.0 m/s current

Unit load, or the transverse load per unit span of the system is shown in the following figures for 0.3 and 1.0 m/s current. Also here the high pretension high mooring case stands out. For this case the barrier is so stiff that it cannot move with the waves anymore.

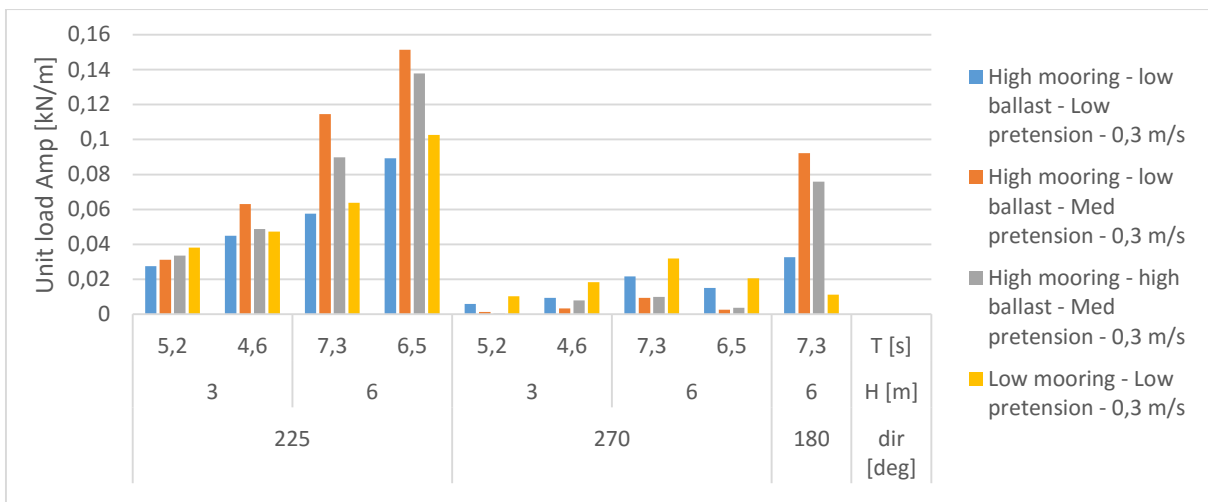


Figure 5-56: Wave frequent unit load amplitude in 0.3 m/s current for various configurations

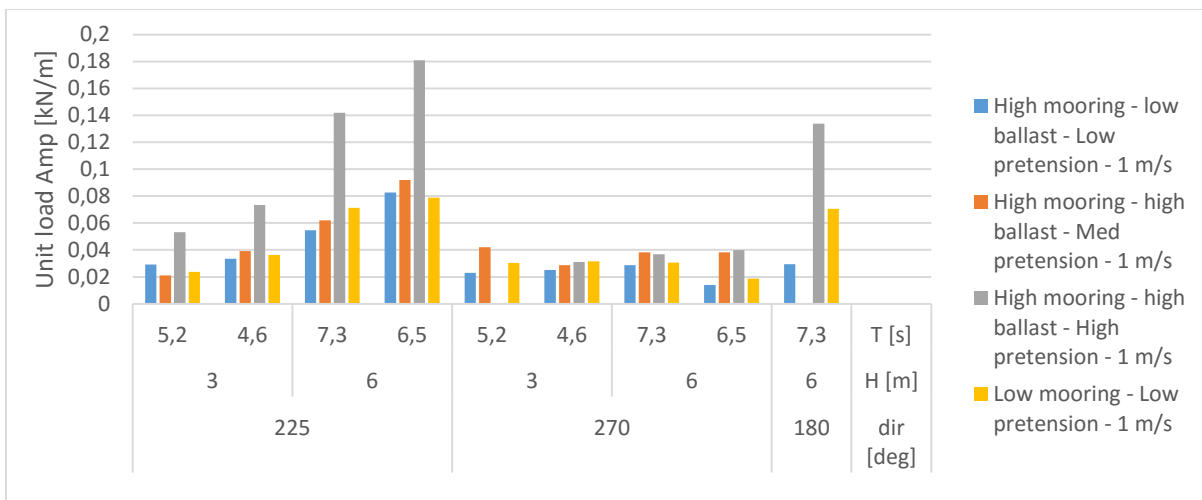


Figure 5-57: Wave frequent unit load amplitude in 1.0 m/s current for various configurations

A comparison of the high frequency loads (in the port side line) is provided for all configurations in Figure 5-58.

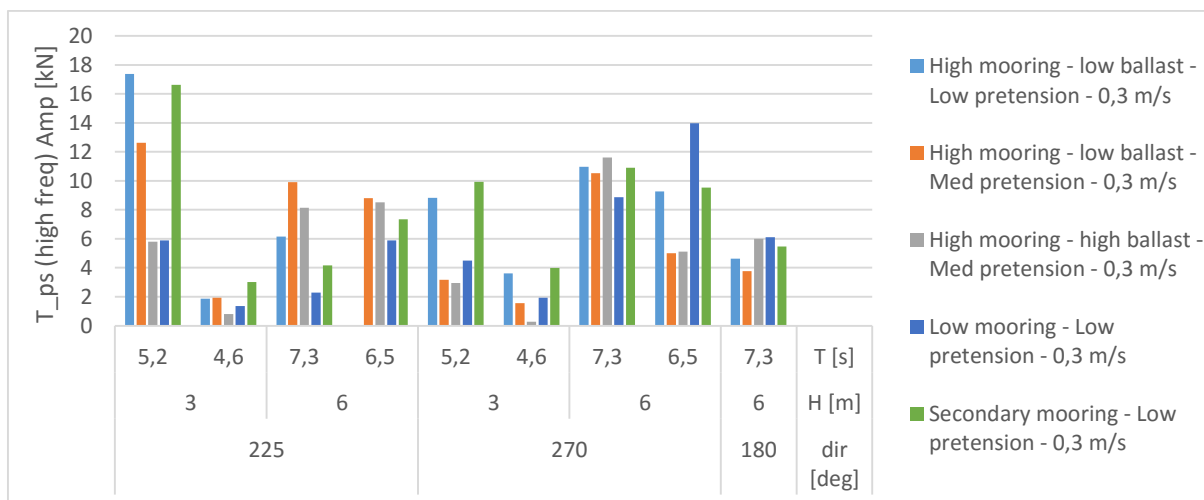


Figure 5-58: High frequency amplitude in port side mooring line

5.3.2.2 Secondary Mooring Lines

The wave and high frequent amplitude of the tension in the submerged mooring line is presented in Figure 5-60 and Figure 5-61. Results of the secondary tension wires are shown in Figure 5-62 to Figure 5-70. Snatching loads in these lines are of particular interest, where the line goes from slack to taut rapidly. The following is concluded based on these results:

- Similar to the high and low mooring large low frequent transient response is observed. It is likely that in most cases the system has not found a mean position yet in the test duration, as the loads are steadily decreasing in most cases up to the end of the test. In shorter periods the mean loads



remain higher than in the longer waves. In 0.3 m/s current the amplification with respect to the initial value is larger than in 1.0 m/s current.

- Overall wave dynamic loads remain low, except in the 180 deg case, where high loads are observed. High frequent loads are found in 6m oblique waves.
- The secondary mooring wires go from slack to taut in 0.3 m/s current. However, this does not lead to high loads.
- The load in the secondary mooring lines reaches a steady state during the test. The mean is equal to that in current, no additional loading is observed due to the waves.
- In 6m waves dynamic loads in the secondary mooring wires are much higher than in 3m. This is likely due to the length of the wires being such that the system cannot flexibly follow the waves but the secondary wires become taut and limit the movement, as orbital paths of the waves are larger in diameter in 6m waves.

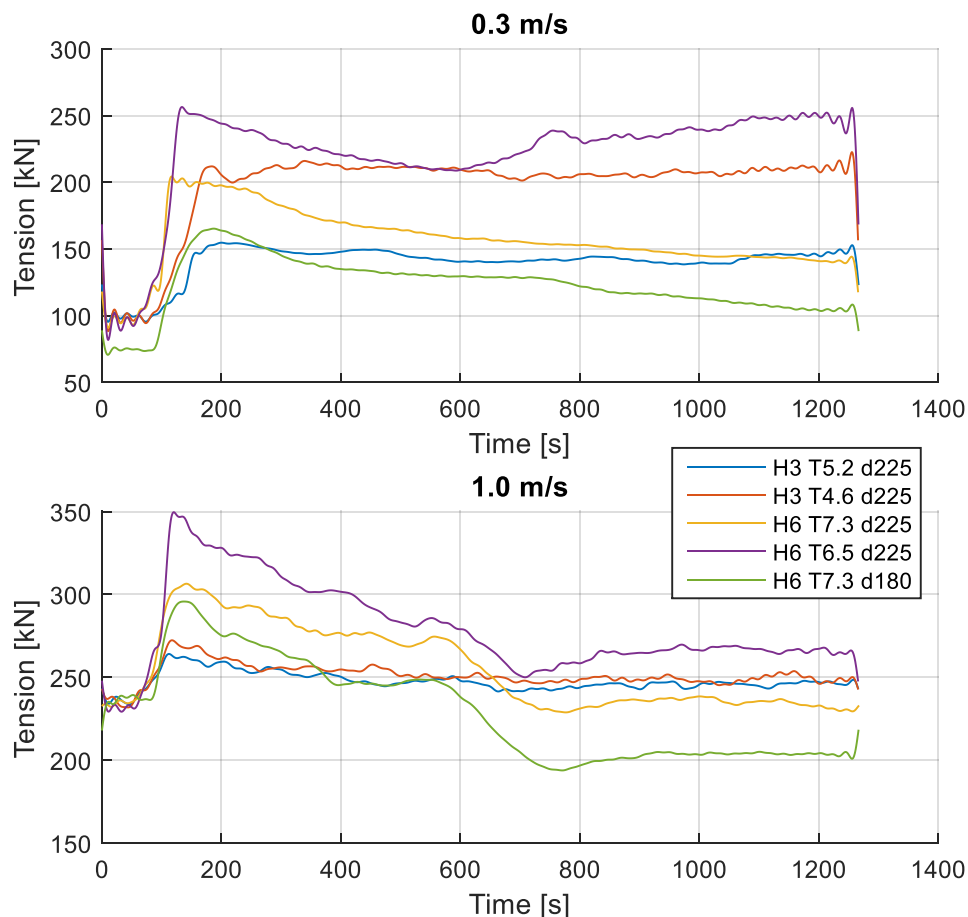


Figure 5-59: Low frequent subsea mooring wire load time traces (225&180 deg waves)

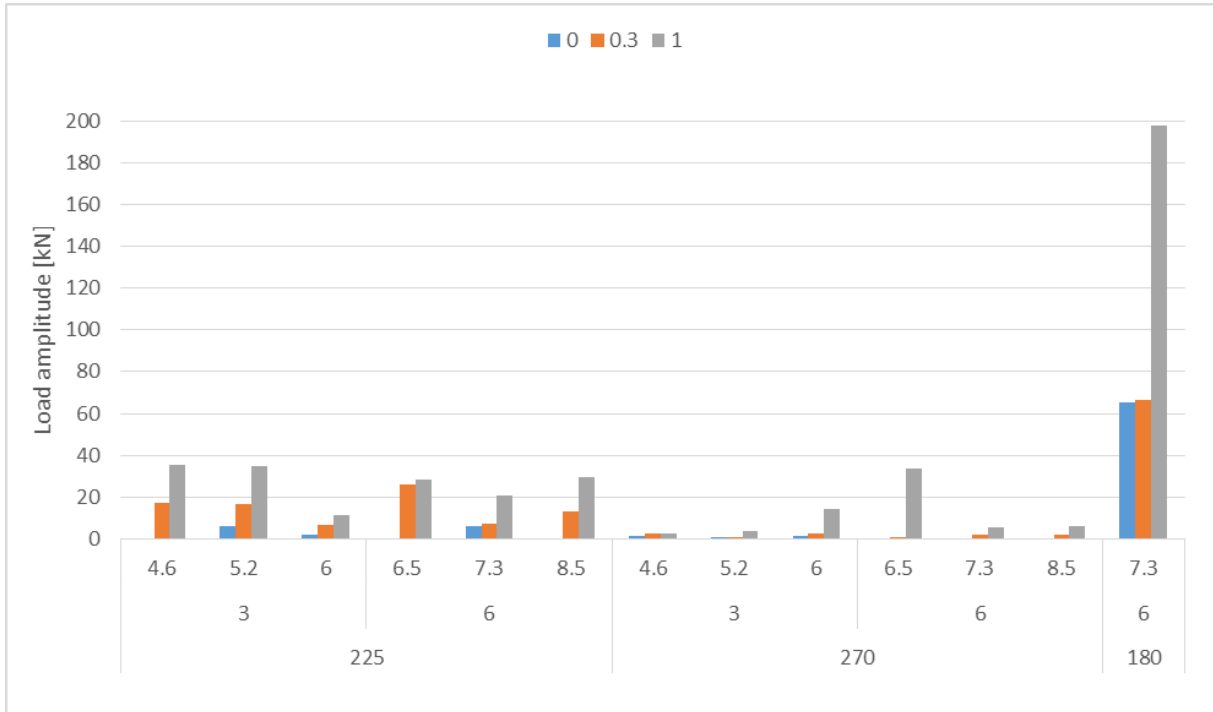


Figure 5-60: Wave frequent tension in port side part of submerged mooring line

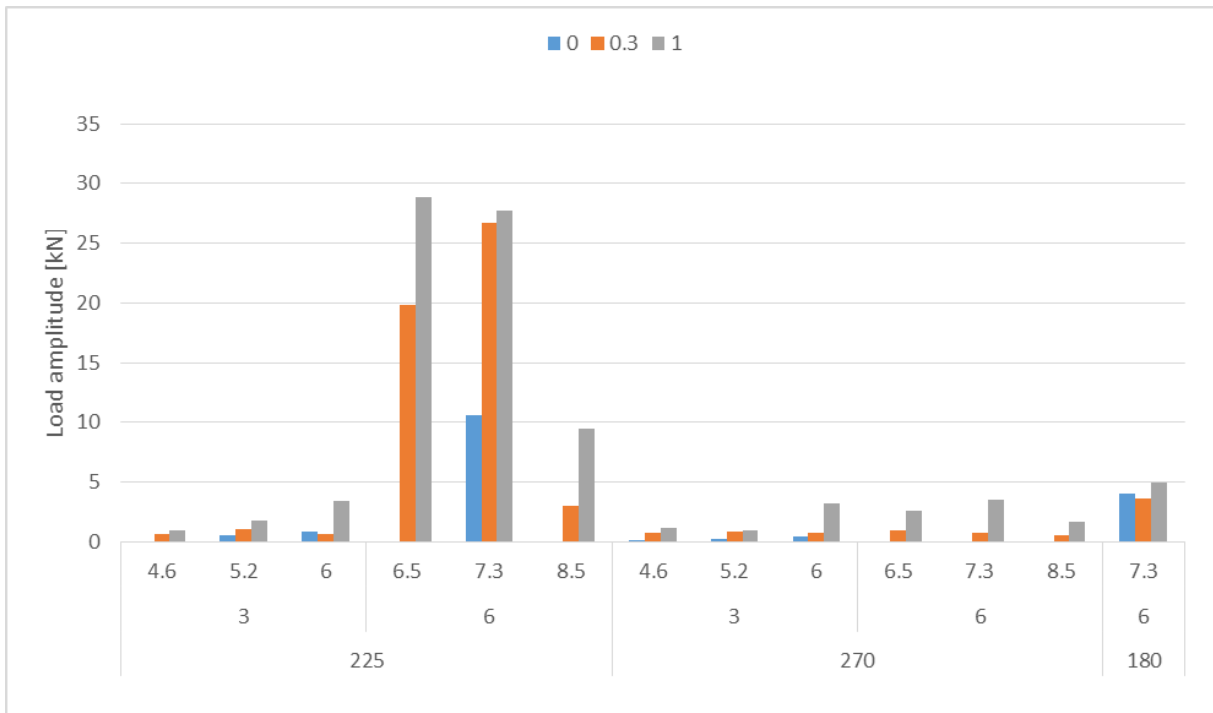


Figure 5-61: High frequent (twice wave frequency) tension in port side part of submerged mooring line

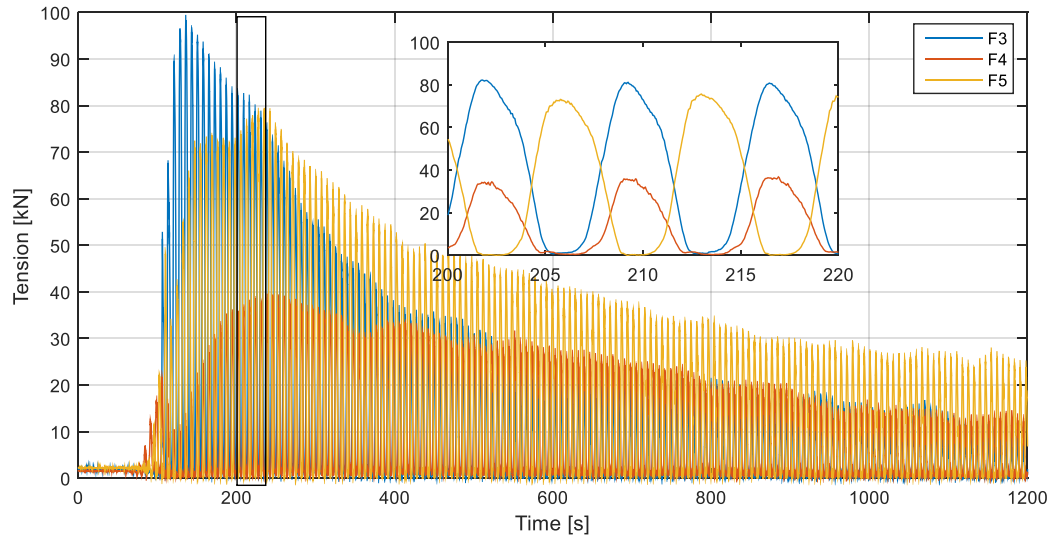


Figure 5-62: Time trace of secondary mooring lines tension (0.3 m/s current, 6m 7.3s 225 deg waves)

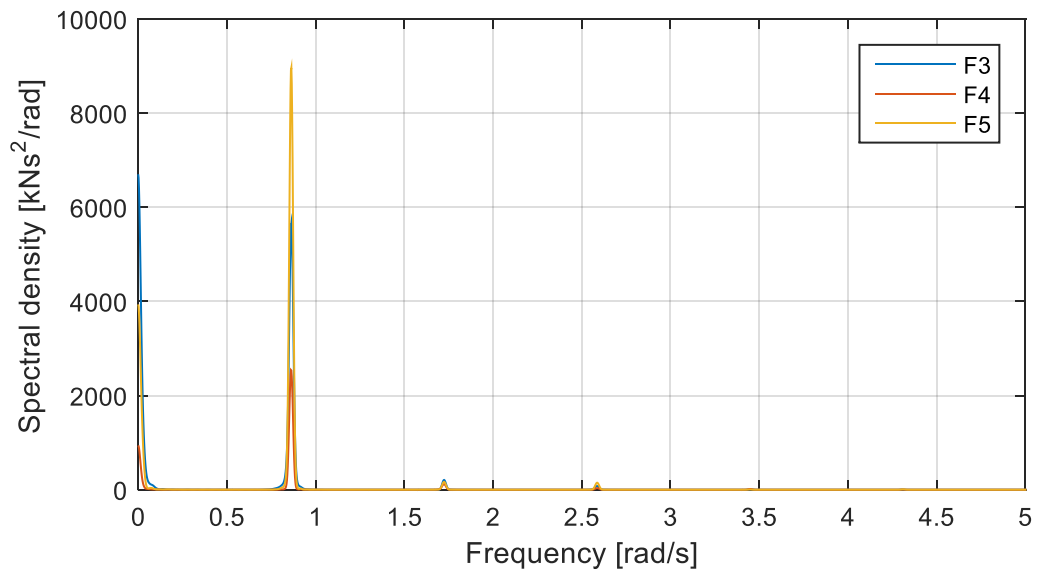


Figure 5-63: Spectral density load (0.3 m/s current, 6m 7.3s 225 deg waves)

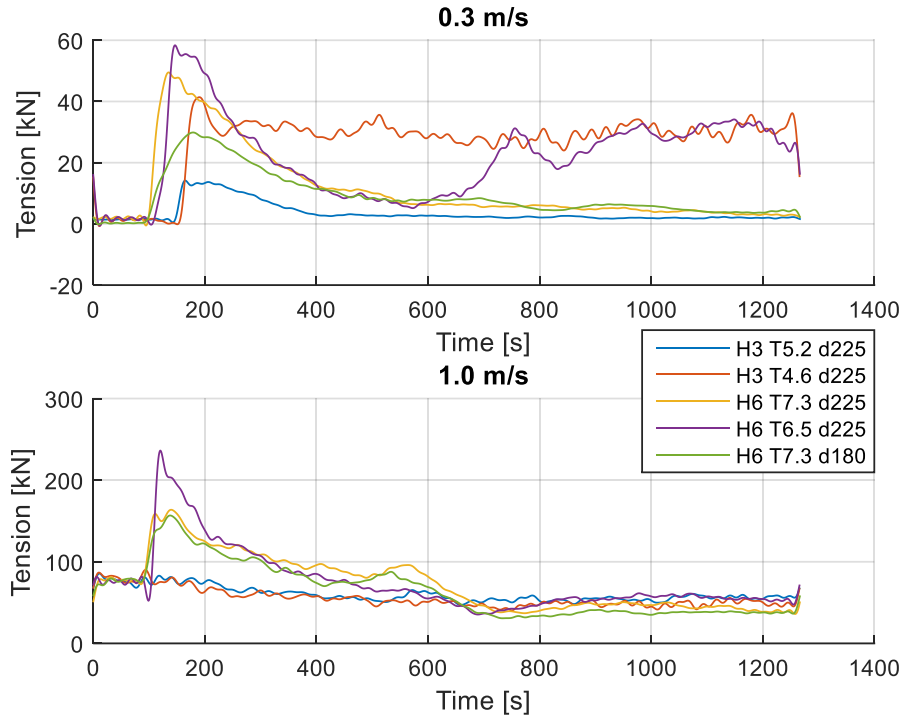


Figure 5-64: Low frequent load of secondary mooring line 5 time traces (225&180 deg waves)

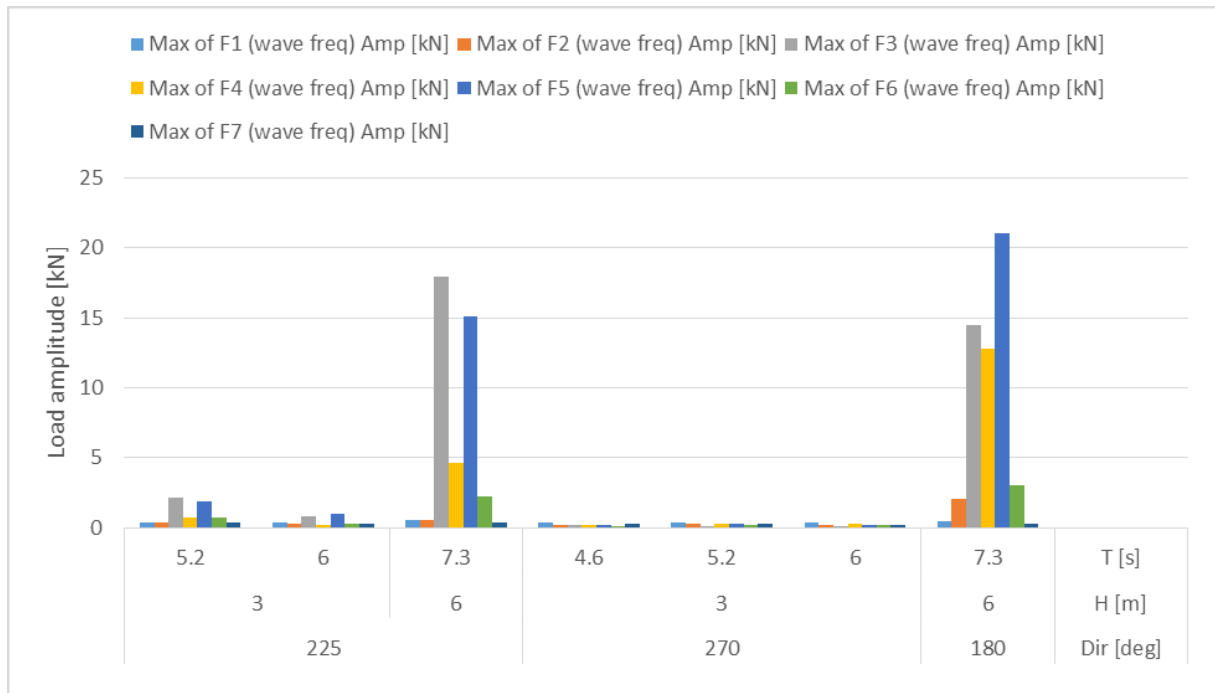


Figure 5-65: Secondary mooring line linear amplitude (0 m/s current)

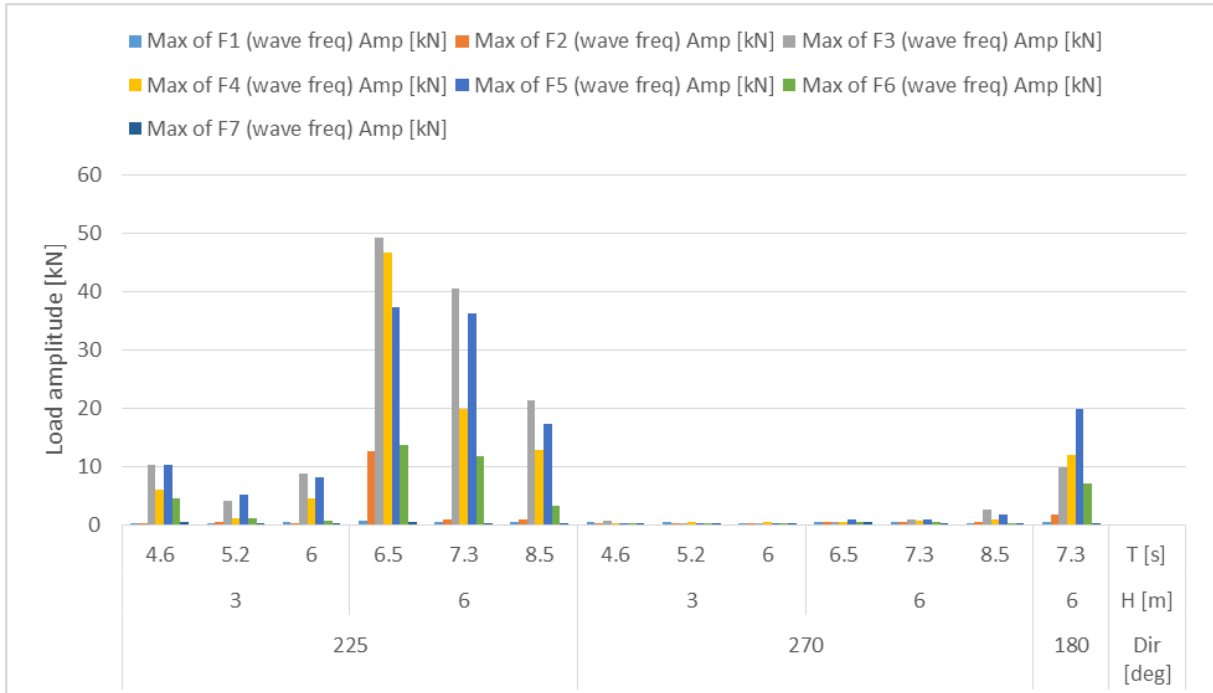


Figure 5-66: Secondary mooring line linear amplitude (0.3 m/s current)

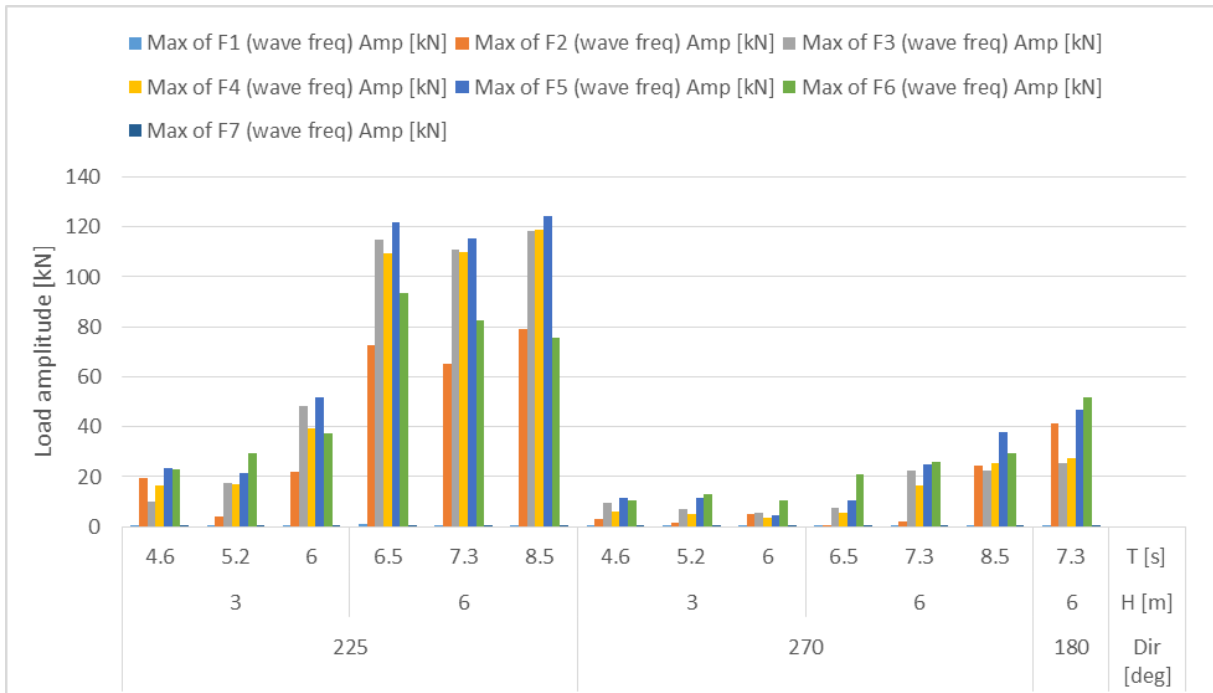


Figure 5-67: Secondary mooring line linear amplitude (1.0 m/s current)

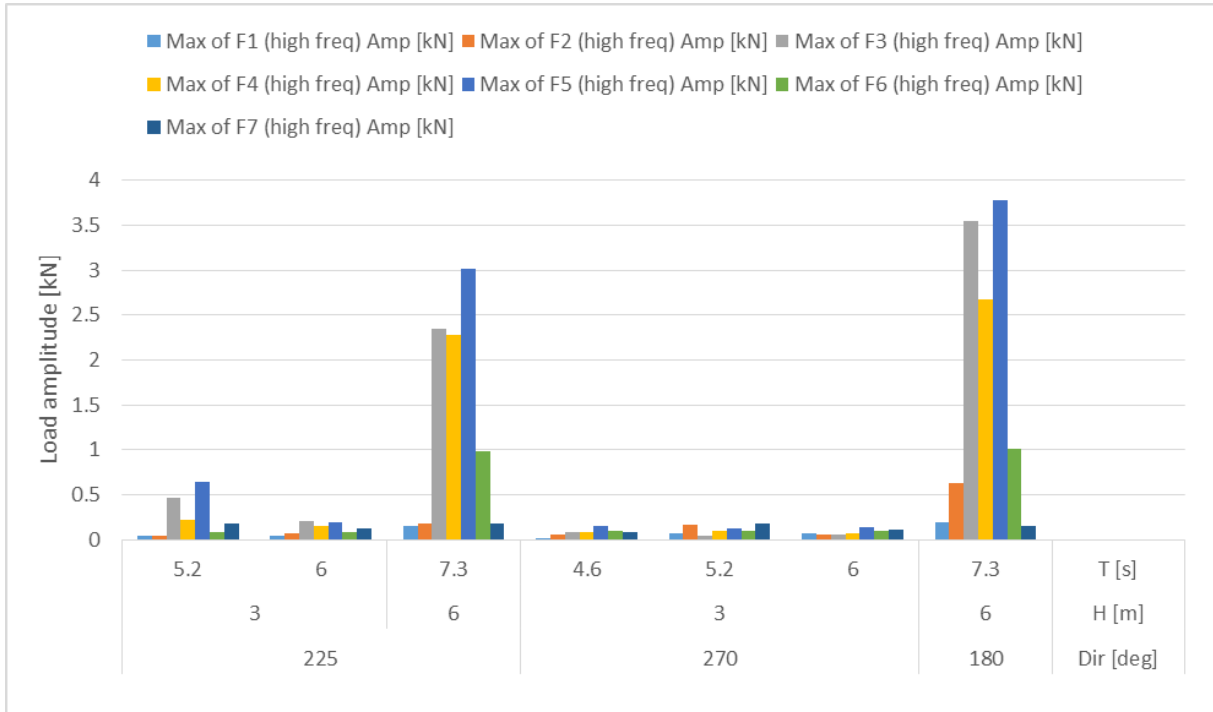


Figure 5-68: Secondary mooring high freq. amplitude (0 m/s current)

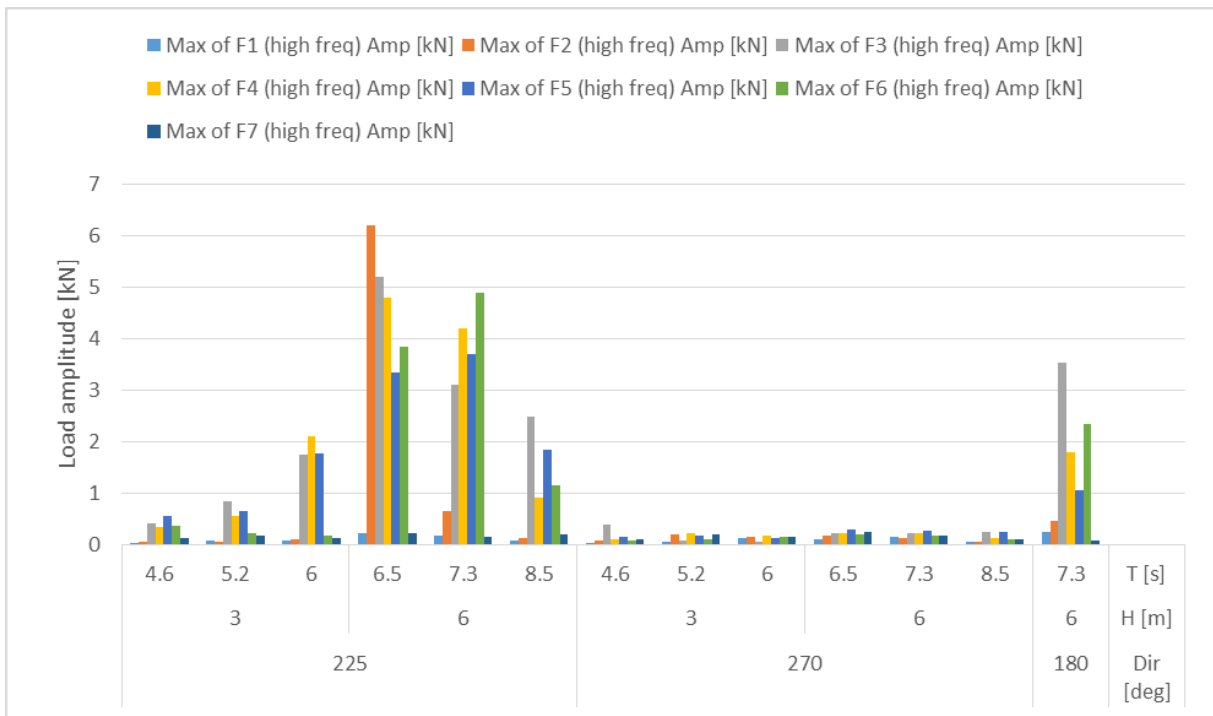


Figure 5-69: Secondary mooring high freq. amplitude (0.3 m/s current)

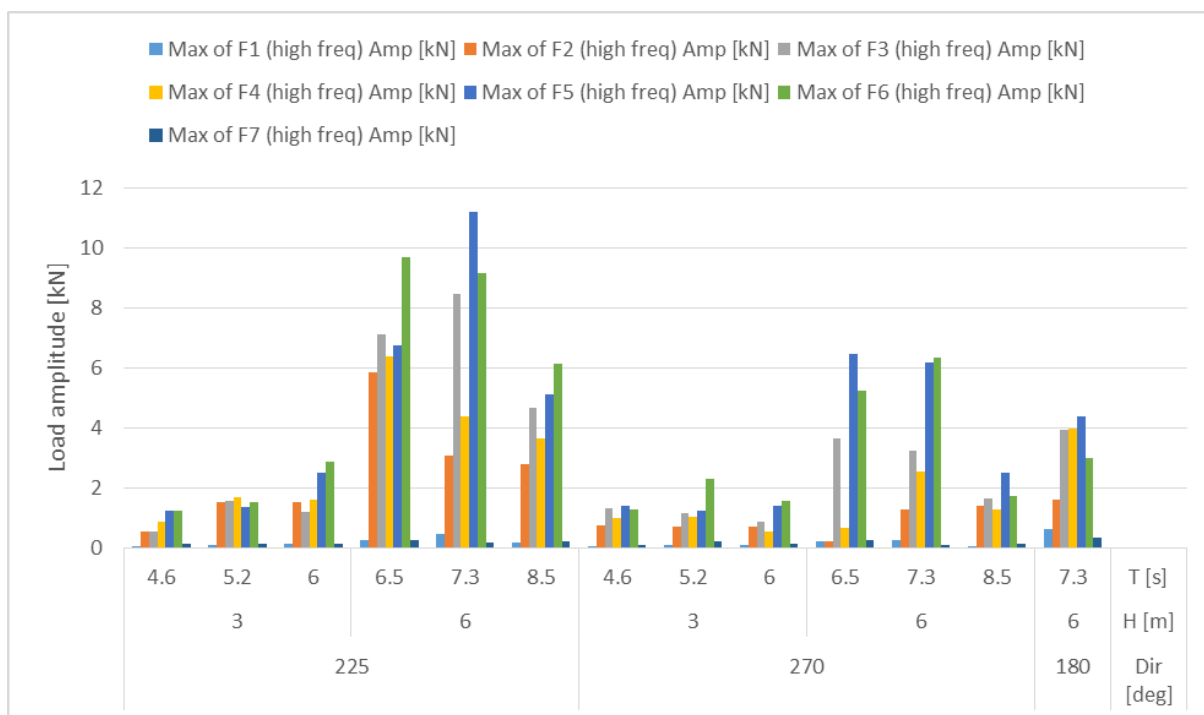


Figure 5-70: Secondary mooring high freq. amplitude (1.0 m/s current)

5.3.3 Bridging and overtopping

In the regular wave tests we see very little overtopping and bridging, which is remarkable and a positive result, as these cases have the most defined trough and crest, which does not happen often in an irregular sea state with a similar maximum wave height (which occurs only once in a three hour sea state). Furthermore, the periods were selected to be small, leading to short and steep waves. Overtopping and bridging events are extracted from the test videos, making it a subjective result. It was, however, impossible to quantify or measure during the test campaign.

Even though the bend stiffness of the system was minimized as much as was reasonably possible, due to the scaling laws it is much larger than what is expected full scale. The bend stiffness scales with the power five.

An overview of all overtopping and bridging interpretations can be found in Appendix C - .

Some overtopping is observed, most notable in the secondary mooring and high pretension high mooring configuration. In the medium pretension and high ballast cases in 1 m/s current overtopping is also observed, which is not the case in the 0.3 m/s current cases. Due to the current more tension is present in the system, leading to less flexibility.

Bridging is in only one case clearly visible (test number 802046, high mooring ballasted medium pretension 6m shortest wave, see Figure 5-71). In the high pretension and high mooring ballasted cases events that may be identified as bridging are observed.

In short:

- Overtopping is observed more than bridging (likely caused by the high weight of the floater with all the sensors (~160 kg/m without the ballast weight)).
- The higher the pretension, the more overtopping and bridging is found.
- Even in the lowest pretension in all mooring configurations overtopping is observed in 1.0 m/s current. No bridging is found. In the low and secondary mooring in more cases overtopping is found, evenly distributed over 225 and 270 degree wave headings. This includes cases with a 3m wave height, although with the 6m waves more often overtopping is observed.
- In only two cases in the medium pretension high mooring setup in 0.3 m/s current overtopping (no bridging) is observed. For the high pretension cases no runs with 0.3 m/s were performed.

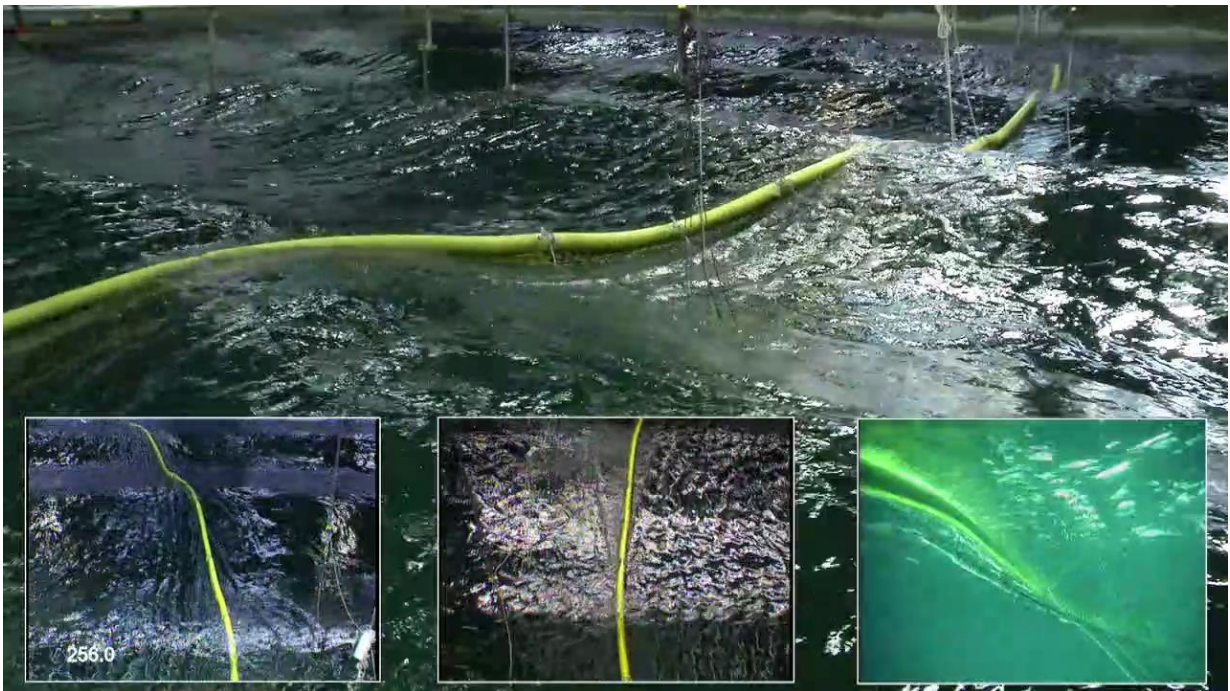


Figure 5-71: Snapshot of test showing both bridging and overtopping

5.4 Tests in Irregular Waves & Current

The response in irregular waves consists of multiple components:

- Mean current
- Mean wave
- Low frequency
- Wave frequency
- High frequency (>wave frequencies)

An example time trace can be found in Figure 5-72.

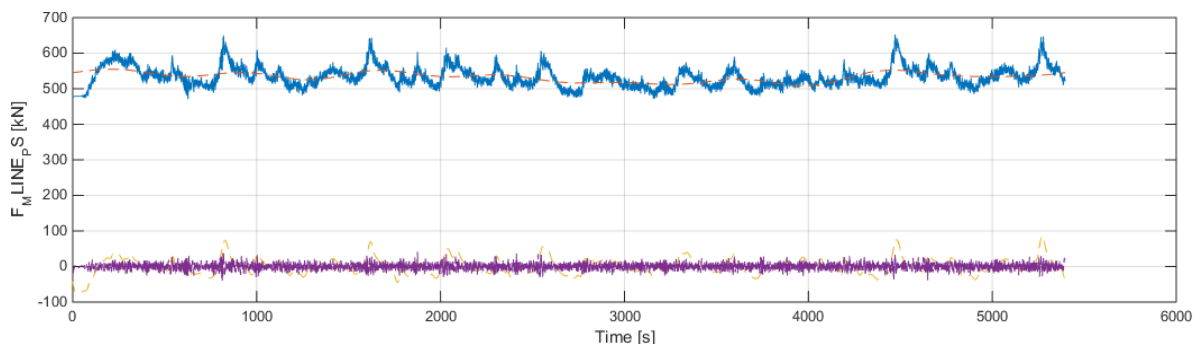


Figure 5-72: Typical time trace loads in springs

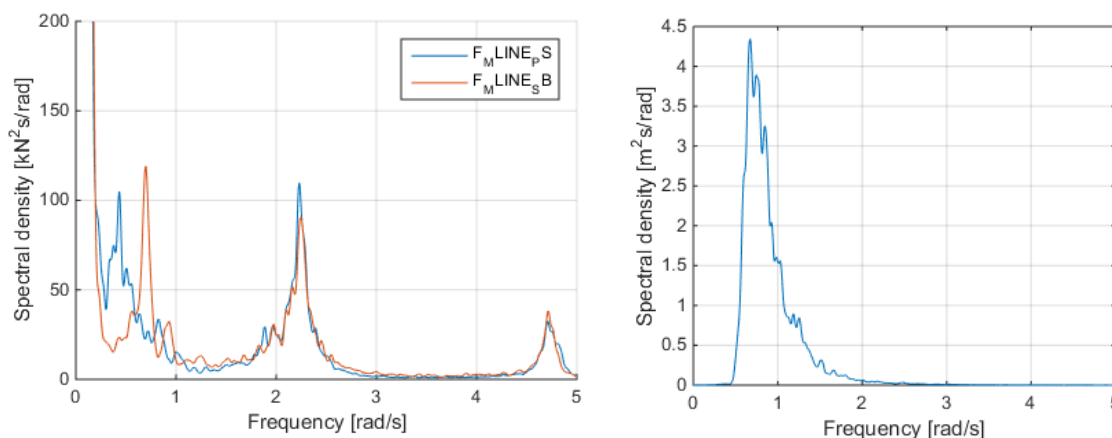


Figure 5-73: Spectral density of load signal (left) and input wave spectrum (right)—ULS 225 degrees high mooring setup

In Figure 5-73 the spectral density of the port and starboard side tensions is shown. Most of the energy is located in the lower frequencies, i.e. below 0.3 rad/s. Notice that equal to the regular waves a peak is seen at higher frequencies than the wave frequency. This peak is not at twice but three times the wave frequency. Note also that the wave frequent component differs for the port and starboard side sensors.

Also frequencies lower than 0.005 rad/s are filtered out, as some time traces show for instance a mean drop in the signal (see Figure 5-7).

We fit the MPM through the mean and low frequencies and fit a Generalized Pareto Distribution. As the high frequencies are filtered out, there is no need for declustering of extreme values exists. The following steps are taken:

1. Select time trace larger than 600s to get rid of any transient effects.
2. Filter out response over 0.3 rad/s and under 0.005rad/s.

3. Find extremes over a certain threshold (Peak Over Threshold method)
4. Fit Generalized Pareto distribution by maximizing the log-likelihood.
5. Estimate 3 hour most probable maximum

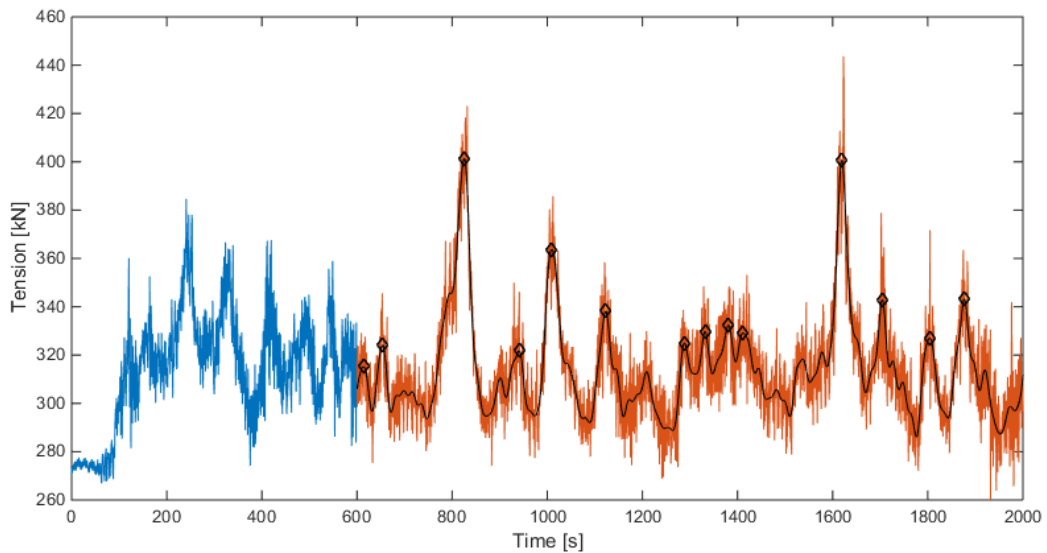


Figure 5-74: Time trace of starboard unfiltered load, on the left the transient ramp-up time and on the right the filtered signal including selected peaks

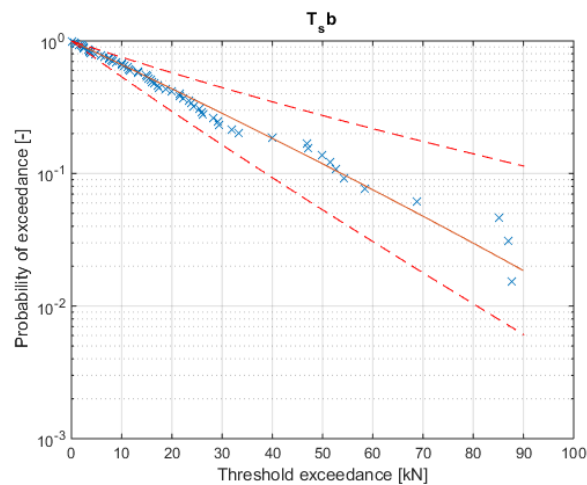


Figure 5-75: Extreme value fit with 95% confidence interval

5.4.1 Motions

The centre displacement is shown in Figure 5-77 and Figure 5-78. The following is observed:



- The displacement decreases as pretension increase.
- Displacement in the high mooring (low pretension) setup shows a large low-frequency contribution that is not seen in the other cases. In medium and high pretension the low-frequent part is approximately equal.
- Wave induced motions are approximately equal for the low and high moorings.
- Current is by far the largest contributor to the surge motion.

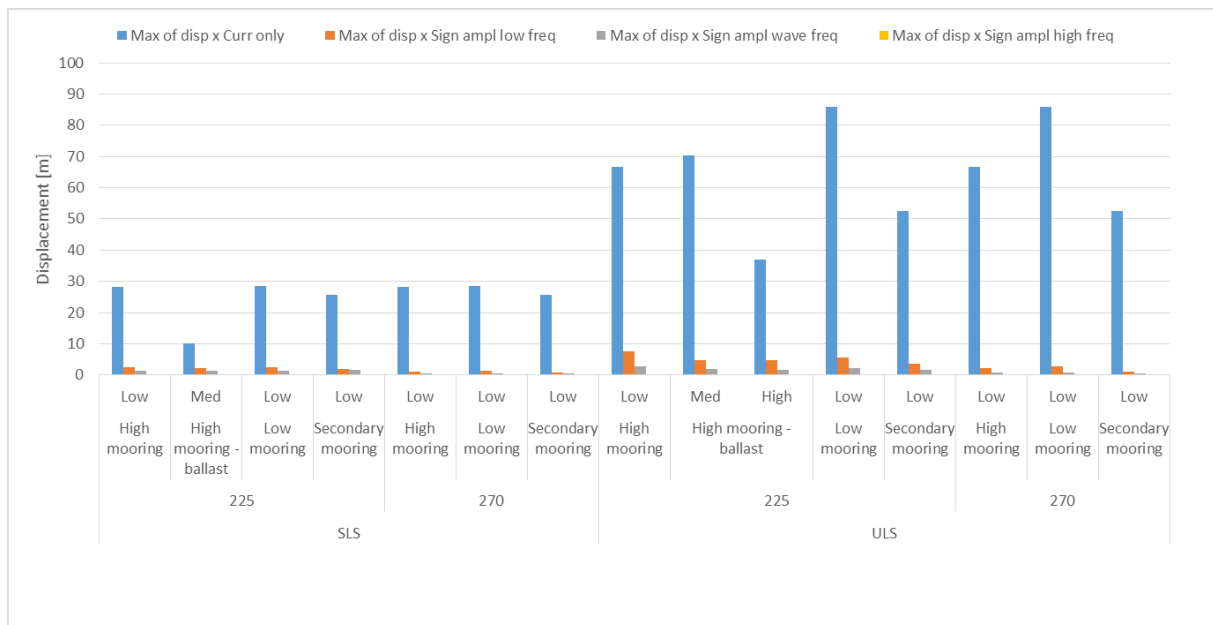


Figure 5-76: Surge motion significant values, including mean current contribution

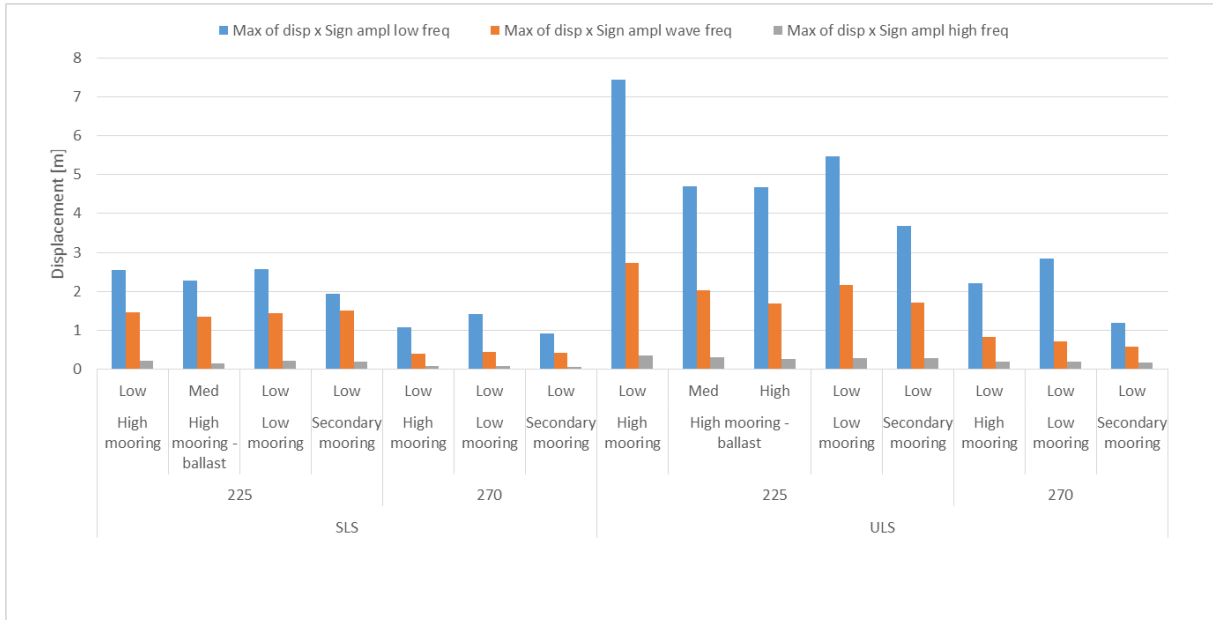


Figure 5-77: Surge motion significant values, current contribution removed

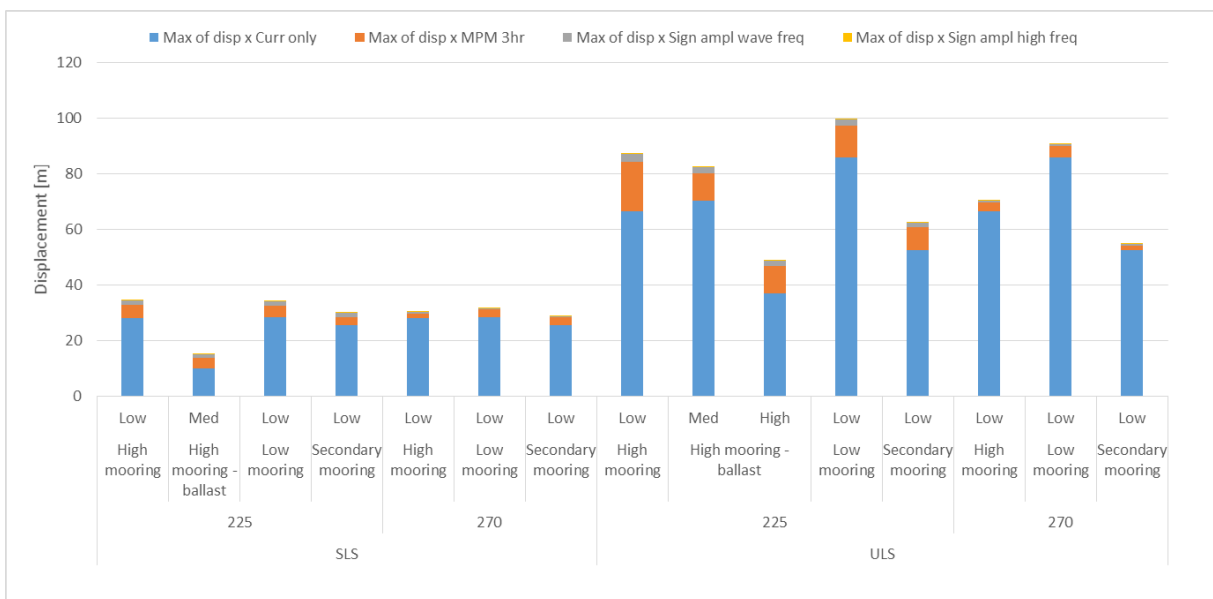


Figure 5-78: Comparison of displacement contributions: mean, low, wave and high frequency

A time trace of the pitch motions of test 803004 (high mooring ballasted, medium pretension ULS 225 degrees) is shown in Figure 5-79. A mean pitch angle of maybe -10 degrees is present, but in some instances the angle almost reaches -90 degrees (smaller values than ~-80 degrees are not measured and recorded as the max value). This likely means that the system switches between two equilibriums: a small negative pitch angle (equilibrium in current), or a very large one (close to -90 degrees). The pitch

goes from the mean value to a large peak and back in approximately 30s, which means it is not wave frequent related. Unfortunately for many irregular wave cases the pitch measurement is not usable and consequently it cannot be presented in this document.

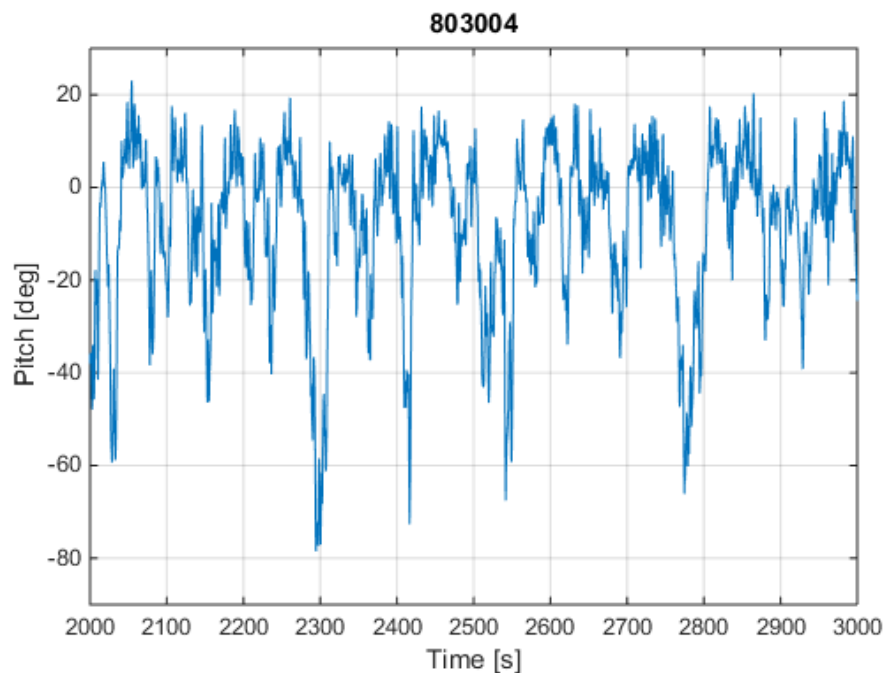


Figure 5-79: Time trace of pitch motion of test 803004 (high mooring, high ballast, medium pretension, ULS 225 deg)

In the swell cases extreme pitch angles such as the ones mentioned above are not observed.

5.4.2 Loads

In this section the loads taking place in irregular seas are analysed. The secondary mooring configuration is analysed separately, as loads are transferred from the boom to the tank in four locations—through the tension wire beneath the floater and the subsea mooring line. Furthermore, seven secondary mooring line loads are measured.

5.4.2.1 High & Low Mooring

The loads in the two springs on the sides of model are studied in this section. Furthermore, the transversal part of the load is investigated as well.

With respect to the tensions shown in Figure 5-80, Figure 5-81 and Figure 5-82 the following is learned:

- Loads in parallel irregular seas are significantly lower than in oblique seas (as opposed to regular waves, where smaller differences are observed).
- The long SLS case yields very small wave induced loads. This is due to the relatively low wave particle velocity.
- A significant low-frequency response is observed in the tensions, which also is observed in the displacement, for the high mooring and low pretension set-up. What excites this motion



remains unclear. Drift is not expected to occur, as wave drift requires diffraction of waves which is highly unlikely for the flexible boom. Stokes drift is expected to be observed in all cases. The low natural period of the system is likely caused by the low stiffness of the springs and a very large amount of added mass (water moving with the screen in lower frequencies). The resonance does not occur when larger pretensions are present.

- Starboard loads are lower than port side, as the waves either come from port side or partially come from that direction (oblique).
- The wave and high frequency wave loads are presented in significant value, as the maxima are smaller than extrema in the slow motions (adding all MPM together would yield a much larger extreme, as it is unlikely that they occur at the same time). The significant values are small and difficult to recognize in the figures.
- Tensions in the low mooring set-up are larger for the current only load (as expected, since the screen isn't able to fold away in higher currents). However, the dynamic loads are approximately equal.

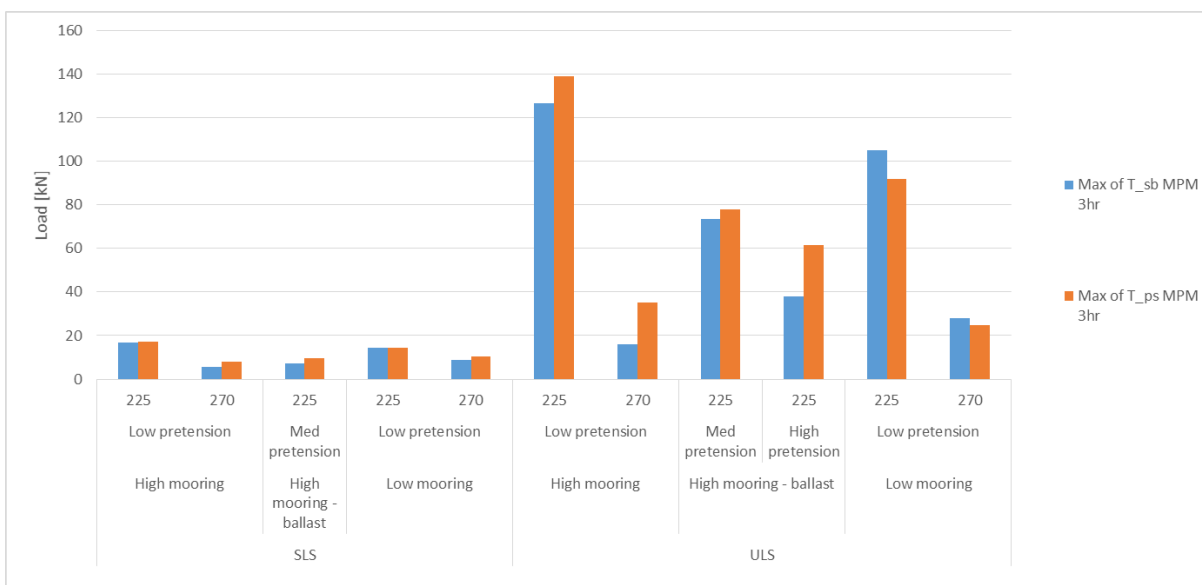


Figure 5-80: 3hr MPM (low frequency) of port and starboard side loads

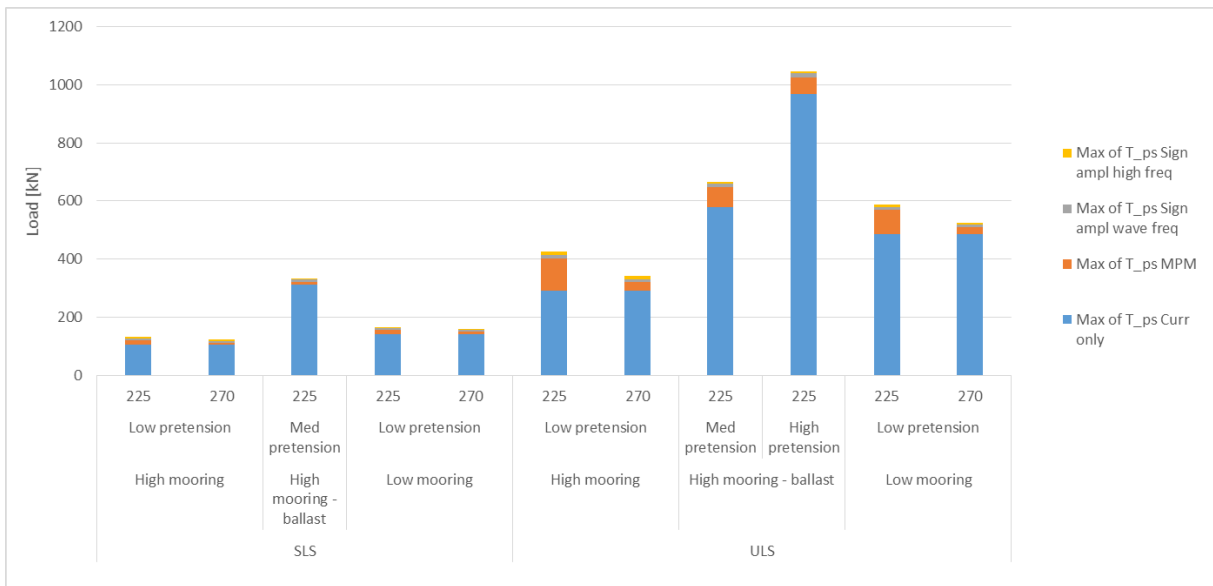


Figure 5-81: Load contributions (port side)

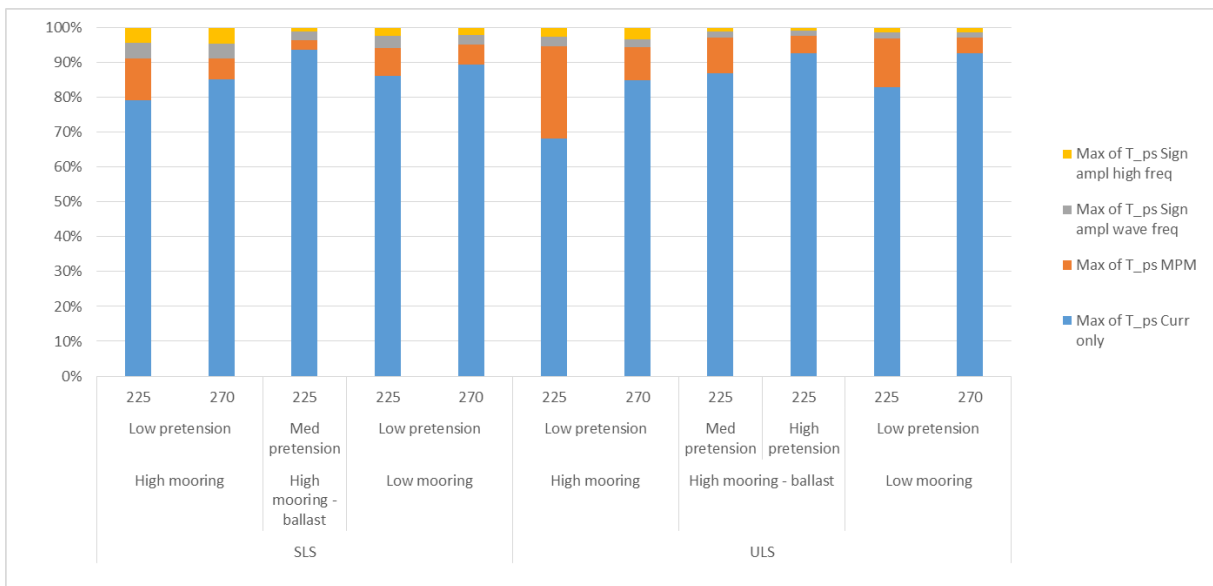


Figure 5-82: Normalized loads (port side)

With respect to the transversal load, see Figure 5-83, Figure 5-84 and Figure 5-85, the following is observed:

- The transversal load increases as the pretension increases, which is also seen in regular waves (except for the resonance seen in the high mooring, low pretension case)
- In the low mooring configuration the transversal load is approximately equal to the high mooring ballasted cases.



- Wave induced loads are much lower for the longer waves, although their relative contribution to the total load increases (higher daf).

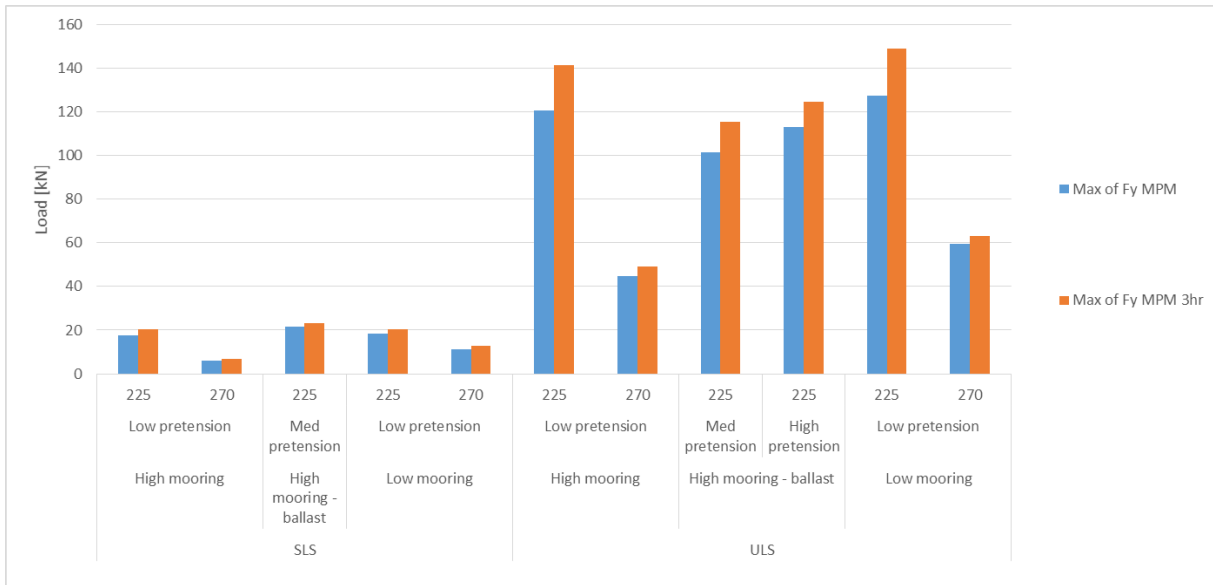


Figure 5-83: Fitted MPM and extrapolated 3hr MPM of low frequent transverse load

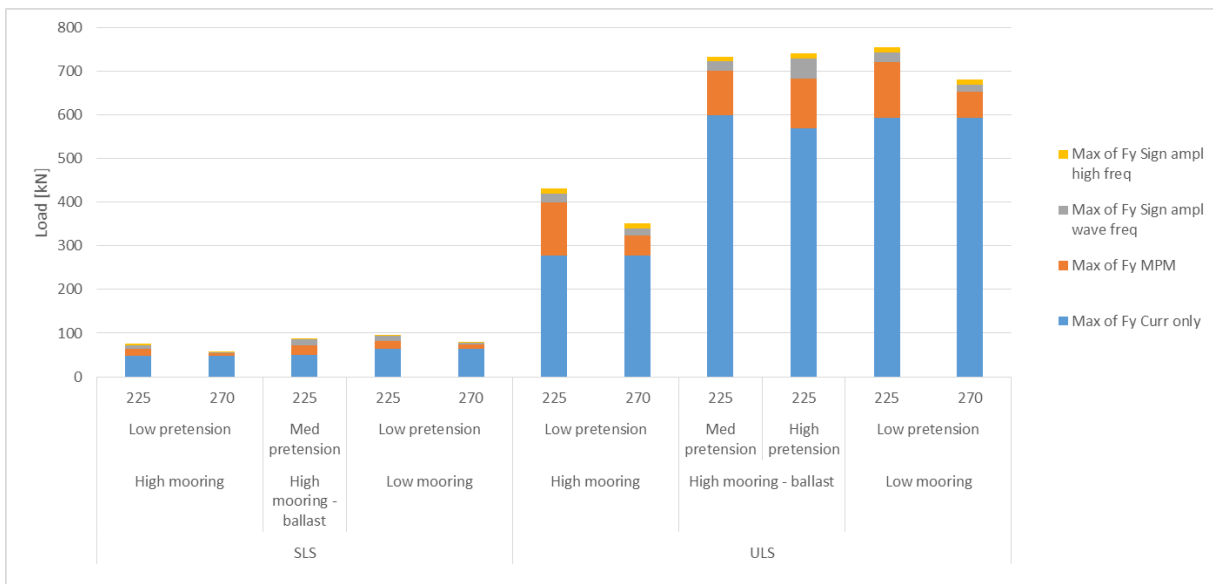


Figure 5-84: Transverse load contributions

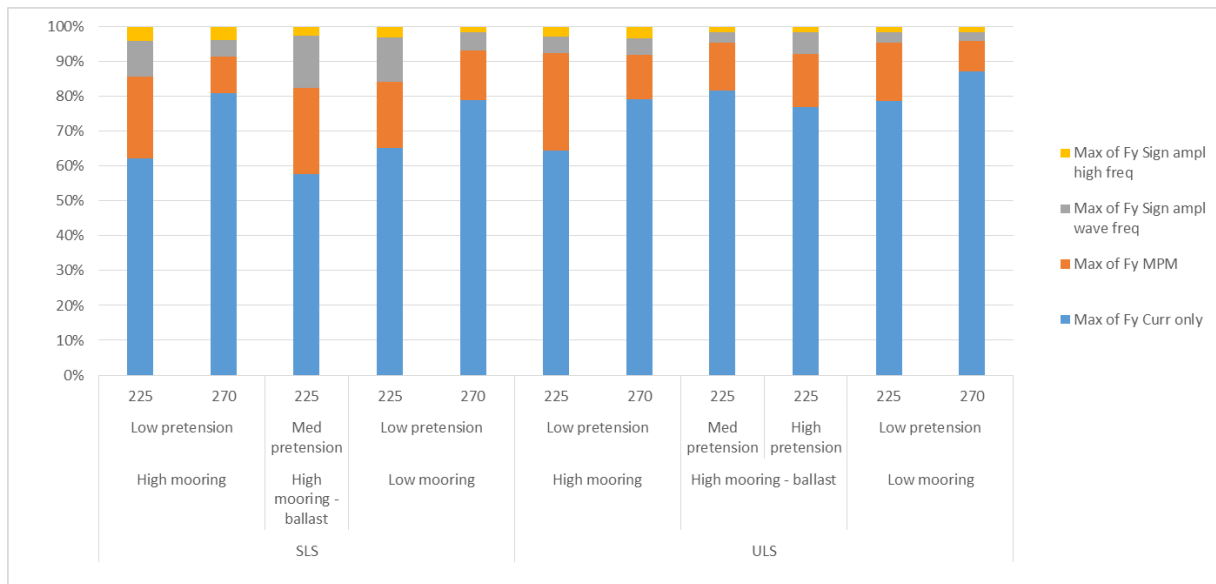


Figure 5-85: Relative transverse loads

5.4.2.2 Secondary Mooring

Measurements of the loading were taken in the secondary mooring wires and in the subsea tension line on both sides of the basin. Statistical and spectral results of these measurements are shown in Figure 5-86 to Figure 5-90.

The following can be concluded:

- Snatching of the secondary mooring lines occurs, but no sharp peaks are observed. The largest part of the total load in the lines is wave frequent.
- Due to the low frequency motion of the barrier low frequency loads are found in the secondary mooring lines.
- In the SLS cases the loads in the secondary mooring lines can be neglected.
- In the subsea tension wire large low frequent loads are measured in the 225 deg ULS. In all other cases this load is lower.

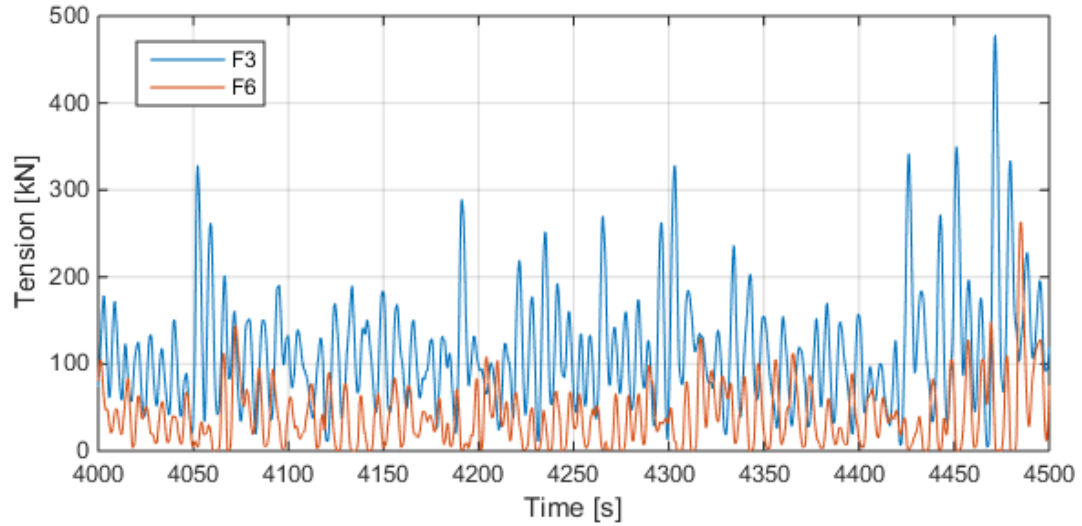


Figure 5-86: Time trace of secondary mooring line 3 and 6 in 225deg ULS

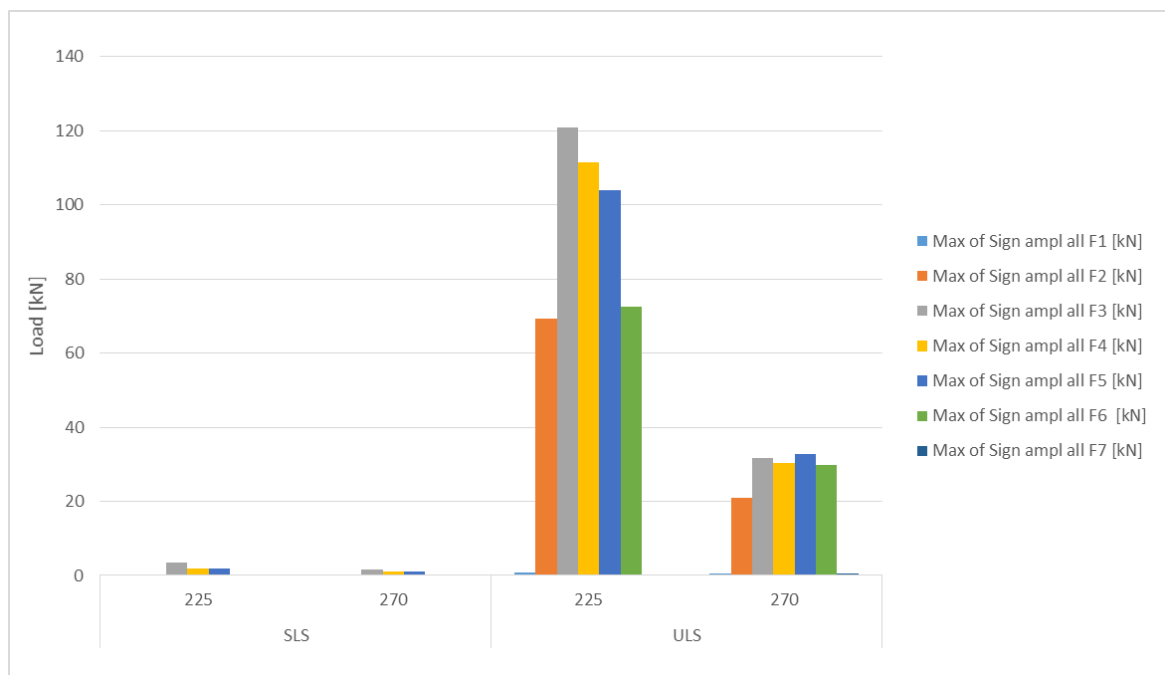


Figure 5-87: Significant amplitude of secondary mooring lines

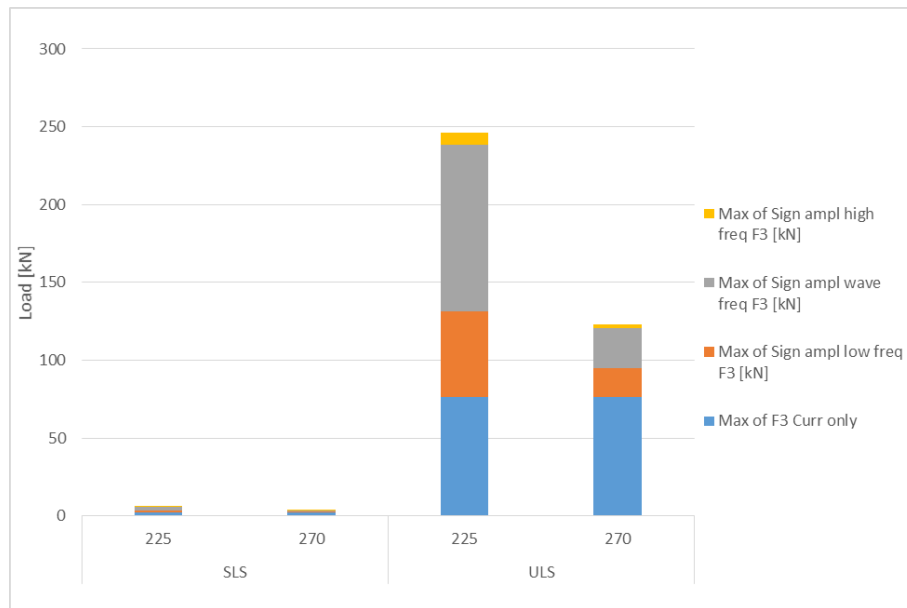


Figure 5-88: Load components of highest loaded line (number 3)

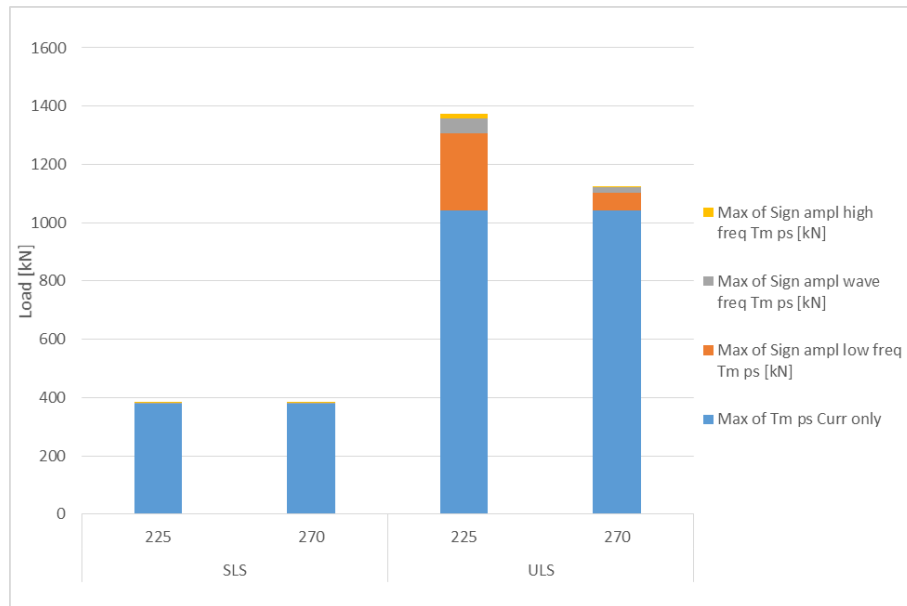


Figure 5-89: Load components of port side subsea tension line

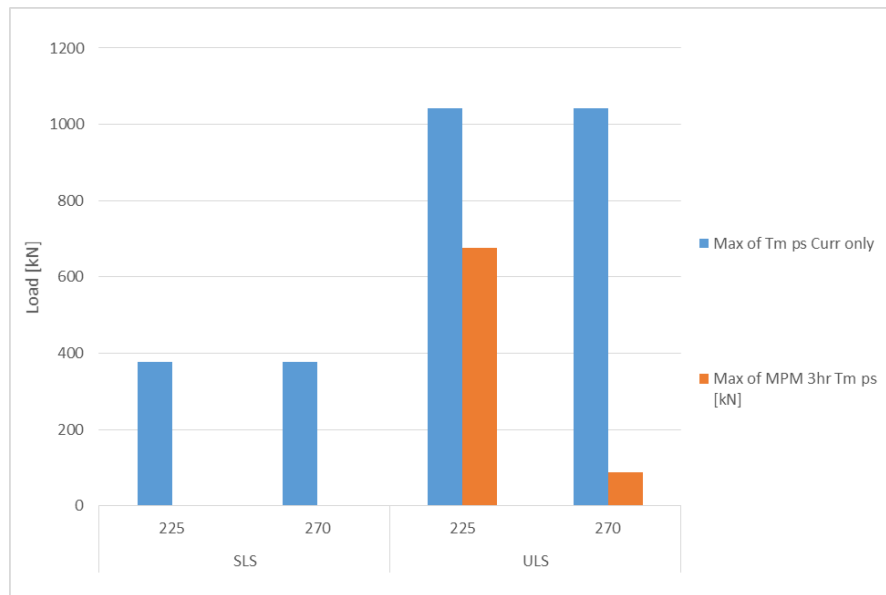


Figure 5-90: Comparison of mean (including pretension) and low frequent 3 hour MPM of subsea mooring line tension

5.4.3 Overtopping and bridging

An overview of bridging and overtopping events, which have been obtained visually from video footage of the model tests, is provided in Table 5-4.

Little bridging is observed in the irregular wave tests, overtopping is found more often. This is due to two main reasons: the skirt is longer than the floater is high and the bending stiffness of the barrier upwards in vertical direction is higher due to the presence of the screen and more important the axially stiff tension wire.

In the SLS cases for both wave headings in no case significant overtopping and bridging was found. Even though the significant wave height is 4m, with a maximum wave height of approximately 7m, due to the long waves the system is able to follow the waves well. As in the ULS breaking waves were present, often washing over the floater takes place.

In Figure 5-91 to Figure 5-93 snap shots during the same time in the tests are shown of the three configurations during the 270 degree wave heading ULS. In all three photos the checkerboard pattern is well visible, indicating bridging or close to bridging. In appendix B photos from the 225 degree (oblique) ULS condition are shown.



Table 5-4: Overtopping and bridging events in irregular waves

Type	Pretension	Wave			Current Velocity	Marin Test No.	Data	
		H	T	Dir			Overtopping	Bridging
[-]	[kN]	[m]	[s]	[deg]	[m/s]	[-]	[-]	
Low mooring	Low	6.25	8.45	225	1	703001	yes	no
	Low	6.25	8.45	270	1	704001	yes	yes
	Low	4	13	225	0.3	705001	no	no
	Low	4	13	270	0.3	706001	no	no
High mooring	Med	6.25	8.45	225	1	803004	yes	no
	Low	6.25	8.45	225	1	803002	yes	no
	Low	4	13	225	0.3	805001	no	no
	High	6.25	8.45	225	1	803005	yes	no
	Low	6.25	8.45	270	1	804001	yes	probably
	Med	4	13	225	0.3	805002	no	no
Secondary mooring	Low	4	13	270	0.3	806001	no	no
	Low	6.25	8.45	225	1	903001	yes	no
	Low	6.25	8.45	270	1	904001	yes	no
	Low	4	13	225	0.3	905001	no	no
Low	4	13	270	0.3	906001	no	no	

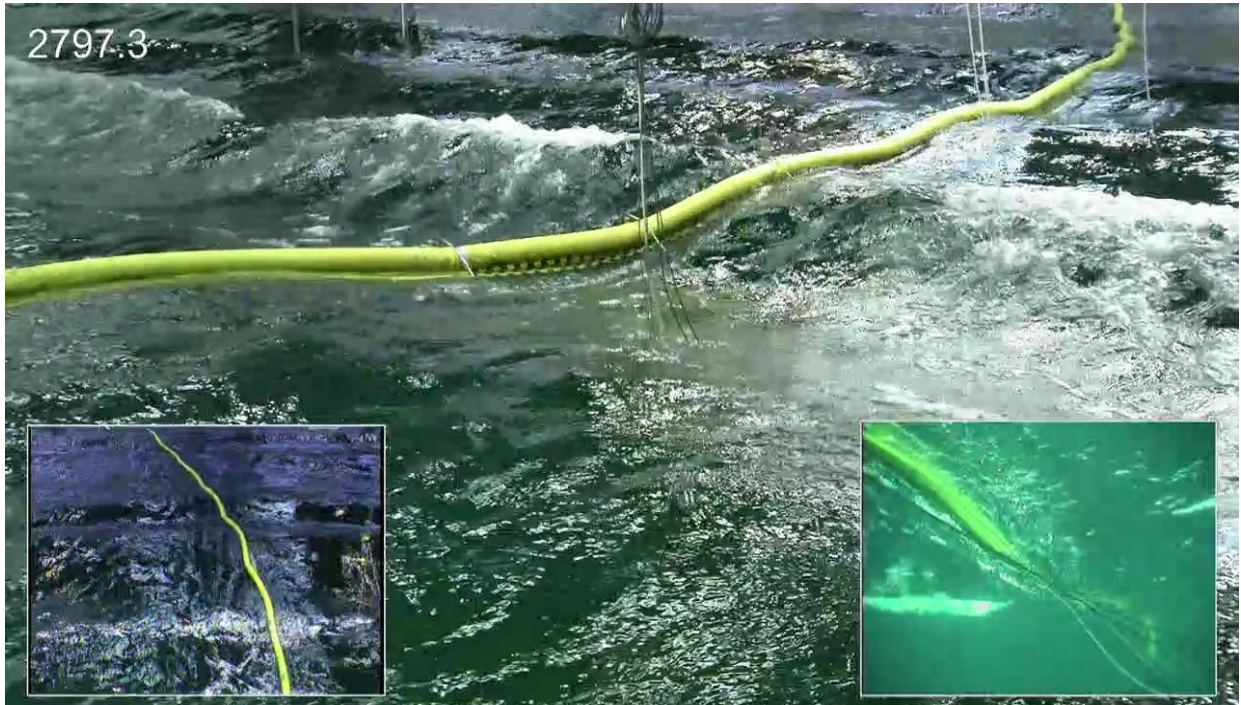


Figure 5-91: High mooring (low pretension) 270 deg ULS

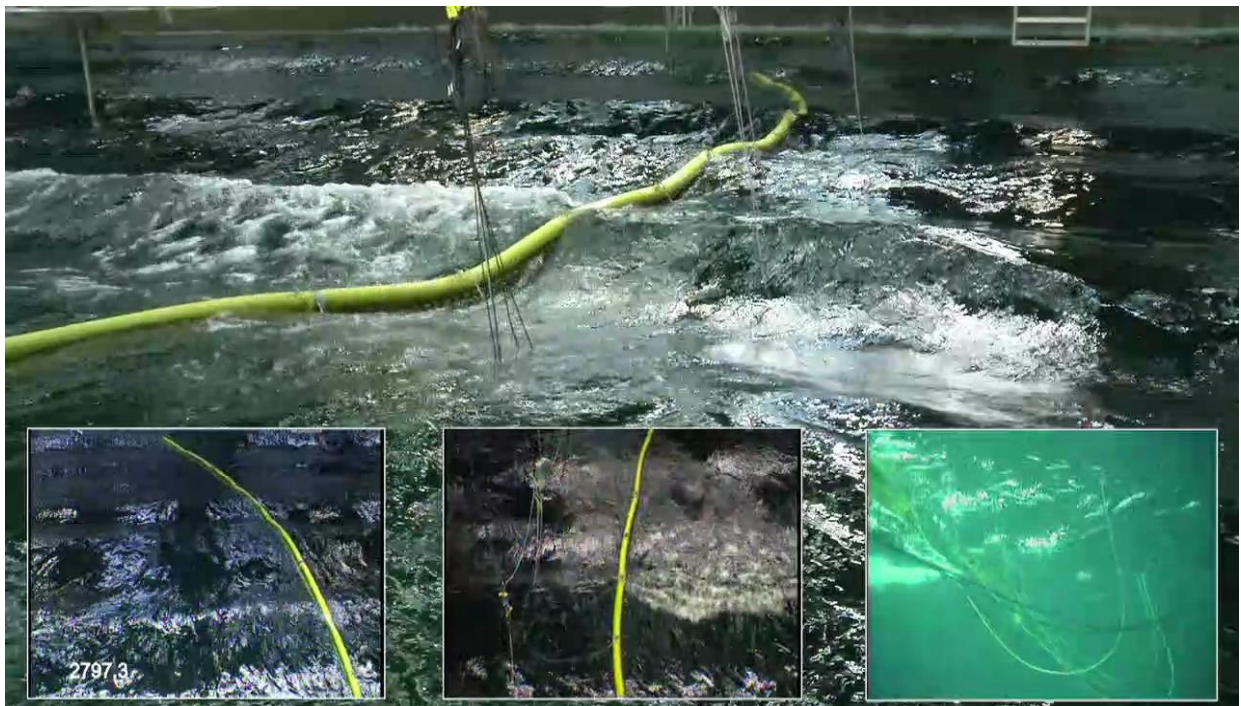


Figure 5-92: Low mooring 270 deg ULS

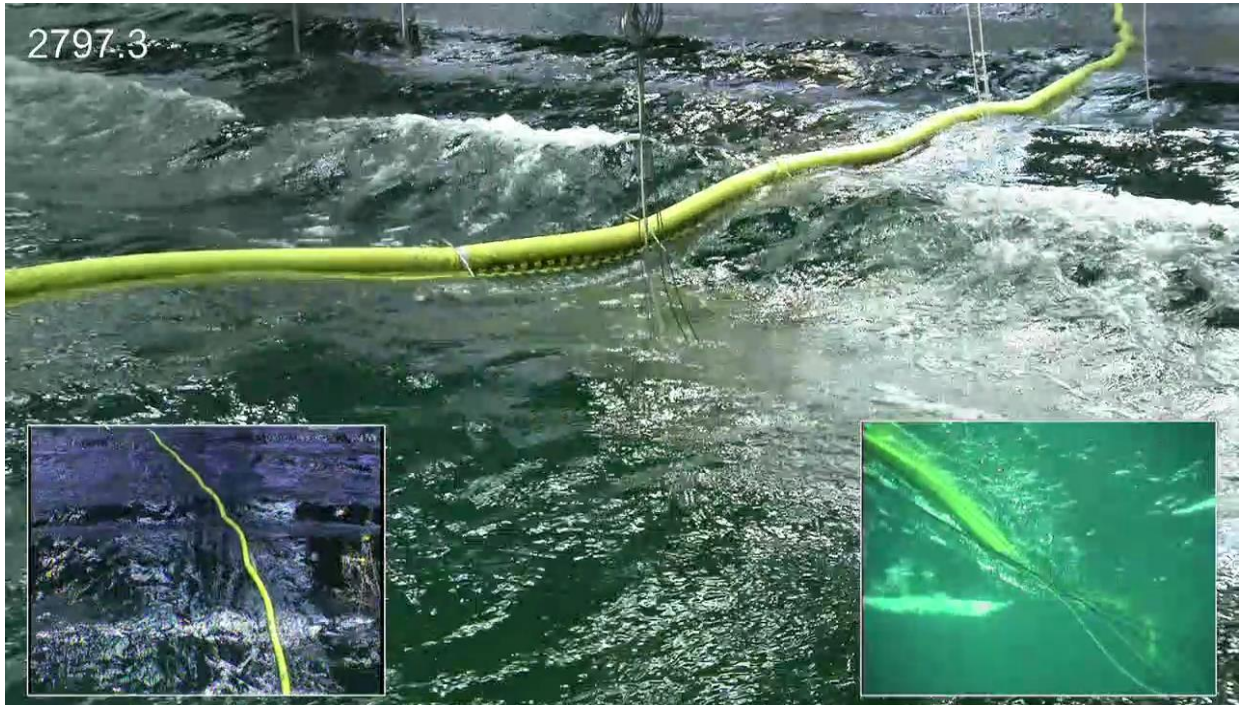


Figure 5-93: Secondary mooring 270 deg ULS

6 Performance of Configurations

During the test three suspension configurations were tested: low, high and secondary mooring. Furthermore, the influence of pretension on the system has been tested. In this chapter a qualitative comparison is made based on the following performance parameters:

1. Hydrodynamic response
 - a. Current
 - b. Waves
2. Plastic holding
 - a. Flexibility with respect to waves (bridging/overtopping)
 - b. Screen orientation

The loading on the system due to current and waves is given as follows (note that this holds for the sea states and current velocities used in the basin tests; for lower current velocity and steeper high waves loading these ratios change):

1. Current induced load (can be expected to be ~60-80% of the total load in a steady state situation)
2. Transient (can be as large as the current component but slowly fades)
3. Irregular: low frequent component in steady state irregular seas (~10-20% of the total load in an extreme event)
4. Wave frequent (a few percent of the total load)
5. High frequent (a few percent of the total load)

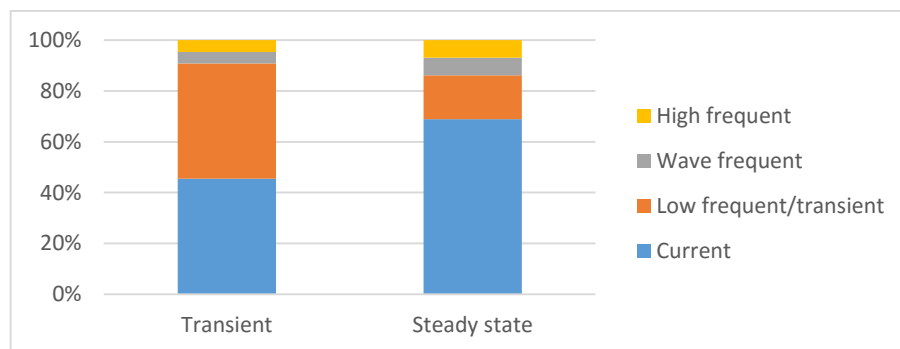


Figure 6-1: Rough load component ratio in a transient and steady state (irregular seas 1m/s and 6m Hs) condition

The hydrodynamic performance of the three configurations is compared in Table 6-1 using Harvey balls: if the balls is fully coloured, the results is positive (i.e. a low response, or high flexibility).



Table 6-1: Configuration hydrodynamic response performance

		Mooring		
		High	Low	2nd
Current				
Wave	Mean			
	Transient			
	Irregular			
	Wave frequent			
	High frequent			

For all cases the current load is dominant. In extreme cases current loading is lower for the high mooring, in daily conditions they are highly similar, almost equal. The mean loading due to waves is for all cases low and consequently equal. Transient motion is the motion at the beginning of the test, when the waves are ramped. All configurations are susceptible to transient motions, although the secondary mooring is relatively limited in this motion due to the subsea mooring wire. Wave frequent loads is in all systems low. However, the secondary mooring line loading is predominantly wave frequent with a significant amplitude. Lastly, all systems experience high frequency loading, albeit with a low amplitude (slightly lower than wave frequent loads). This loading is likely caused by a pitch motion, which may be limited by adding an extra tension member on top of the system.

The plastic holding performance for the three configurations is presented in Table 6-2. Note that the position of the screen is not measured and quantitatively estimated.

Table 6-2: Configuration plastic holding performance

		Mooring		
		High	Low	2nd
Flexibility in waves				
Screen orientation				

No large differences in flexibility, or ability to follow waves, have been observed between the three configurations: all systems followed the waves well. The high mooring configuration was better able to follow waves in 1.0 m/s current than the other configurations.

The pretension has been varied for the high mooring setup only. The influence of pretension on hydrodynamic performance is shown in Table 6-3.

Table 6-3: Pretension hydrodynamic performance

		Pretension		
		Low	Medium	High
Current		-	-	-
Wave	Mean	●	●	●
	Transient	○	◐	◑
	Irregular	○	◑	◐
	Wave frequent	●	●	◑
	High frequent	◑	◑	◑

Pretension does not significantly influence the current loading, a slight increase in span may be observed, but this was found to be of relative small influence. As mentioned before, the mean load is for all cases low. For all pretensions transient behaviour leading to a peak load is observed. However, for the medium pretension even a drop in the load below the mean load due to current occurs, whilst the high pretension moves back to its initial position. Low frequency motions in irregular waves are reduced by the pretension. In high pretension the wave frequent loads become relatively higher, but are still small compared to the current induced load. Similarly to the comparison of configurations, all pretensions show high frequent loading.

Finally the plastic holding performance is compared for the carried out pretensions in Table 6-4.

Table 6-4: Pretension plastic holding performance

	Pretension		
	Low	Medium	High
Flexibility in waves	●	◐	◑
Screen orientation	-	-	-

As expected, the system in low pretension can follow waves the best. However, differences between flexibility in medium and high pretension are small. Furthermore, in 0.3 m/s for all configurations and pretensions the barrier is better able to follow the waves (in the SLS conditions no overtopping and bridging is observed for any condition; unfortunately this case was not carried out for high pretension). The screen orientation is likely not influenced by pretension.

7 Conclusion & Recommendations

7.1 Conclusions

Model tests have been carried out to study the following: hydrodynamics of a floating boom with a screen attached and limiting characteristics for plastic capturing (overtopping/bridging). With respect to the first the following can be concluded:

- Loading is dominated by current. In the 0.3 m/s cases approximately 50-60% of the load is caused by the current, and in 1.0 m/s it ranges from 60-80%, depending on the sea state. Even in waves that run parallel to the system wave loading is observed, caused by the effective shortening of the path that the boom follows.
- The three mooring configurations behave in terms of hydrodynamics highly similar, especially in waves. In high current velocities the low mooring and secondary mooring boom are subjected to higher loads than the high mooring.
- The wave loading can be subdivided in a low, wave and high frequent component. The first causes the highest loads and is more dominant in low pretensions. It varies with a much lower frequency than the wave frequency.
- Wave frequent loads remain low, even in higher pretensions. At a certain threshold the system cannot flexibly follow the waves anymore and wave frequent loads increase. Even though these loads were found to be higher for the highest pretension, relative to the current load they are small.
- A high frequent component (at twice or three times the wave frequency) is observed in all configurations. It is thought to be caused by a pitching motion of the floater. The magnitude of this component is relatively low: in some cases equal to the wave frequent component, but in most lower. Even though the magnitude is low, due to the high frequency it may cause fatigue damage.
- The system should be engineered such that it has sufficiently low axial flexibility and bending stiffness to deform with the waves. If this is the case, loads and structural stress will remain low. This is also limited by the amount of tension that runs through the system, which also acts as a stiffness. A numerical model can be calibrated with the results of these tests and extrapolated to a design for the Pacific array.

With regards to the plastic capturing capability the following can be stated:

- Bridging and overtopping is not quantified but dealt with visually based on the videos of the tests.
- In the longer sea states no bridging and overtopping is observed. Only in the steep sea states or with high current especially overtopping is seen, and less bridging.

- In the low and secondary mooring configurations in 1.0 m/s the current induced load is higher than that of the high mooring, and consequently the ability to follow the waves is worse. However, this is likely not an operational current velocity.

7.2 Recommendations

- Low frequent/transient motions should be investigated: in combination with the current induced load, which is understood well, these will define the governing loads. A numerical model is required that can predict low frequent and transient motions on a large scale.
- The plastic capturing efficiency difference between a high mooring and low/secondary mooring needs to be quantified (entrainment). The load mitigation of the high mooring configuration is very beneficial in keeping loads low in extreme events, but this configuration will likely loose plastic more often.
- Mitigation options for the high frequency pitch should be investigated, as this may cause local fatigue damage to the permanent system.
- Debris induced load should be investigated, as this is left outside the scope of this report (it was not possible to test this on this model scale, due to the strong effects of surface tension). Plastics may accumulate and at some point disturb the flow, leading to different loads on the barrier.

Appendix A - Stiffness & Weight of the Model

Axial stiffness:

Axial stiffness can be represented as:

$$F = \frac{EA}{L} \Delta x = 2k\Delta x$$

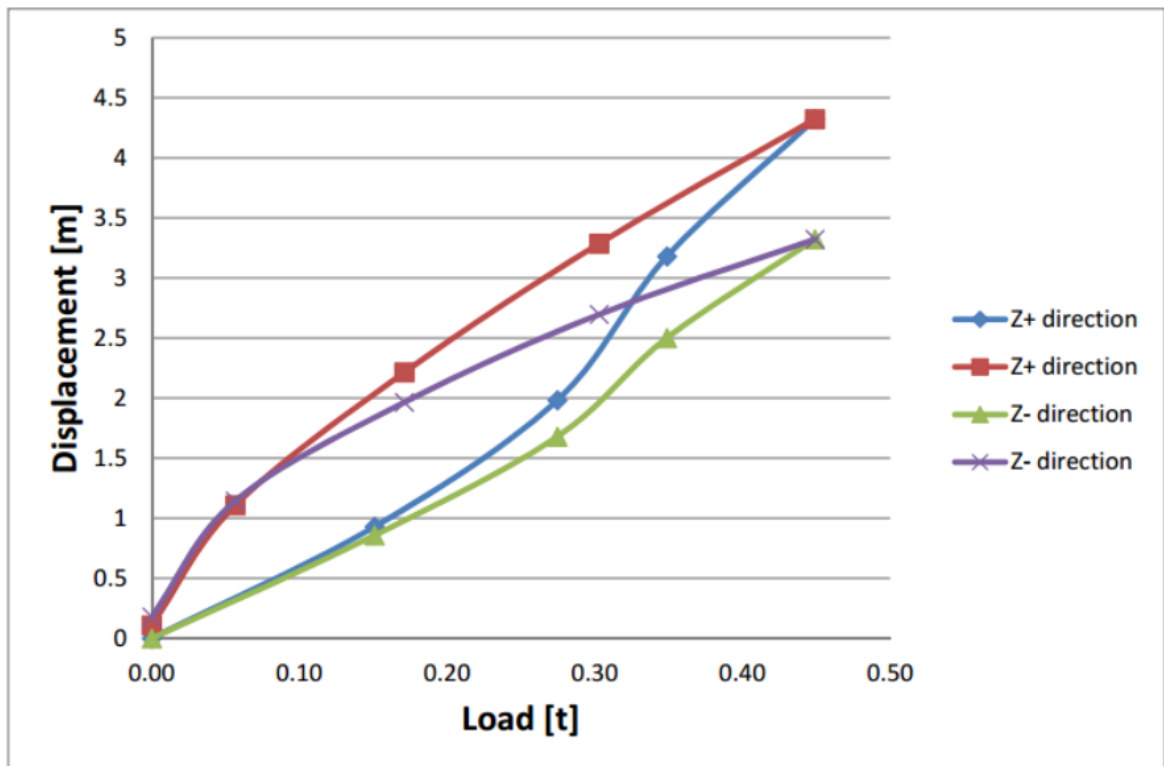
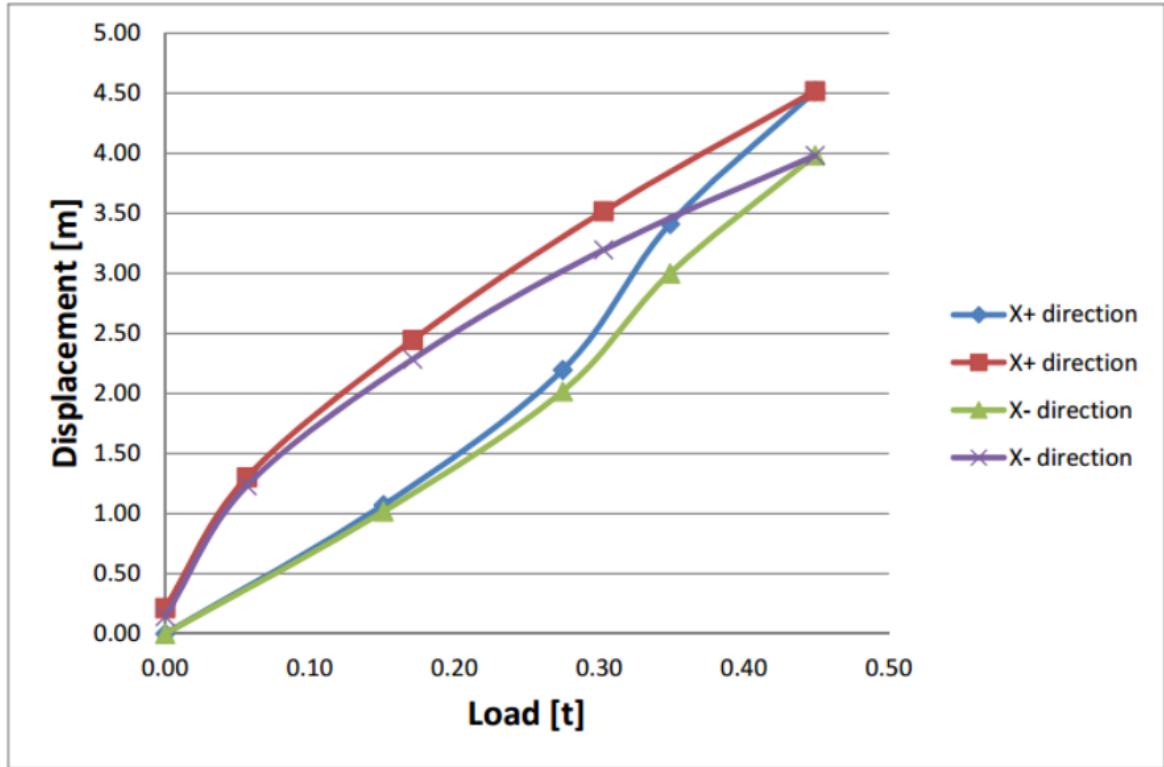
Where k is the spring stiffness of the springs in the model tests, EA is the axial stiffness of the material used to keep the system in place (tension wire for instance), and L denotes the length of the material being subjected to a load F and is consequently stretched with Δx .

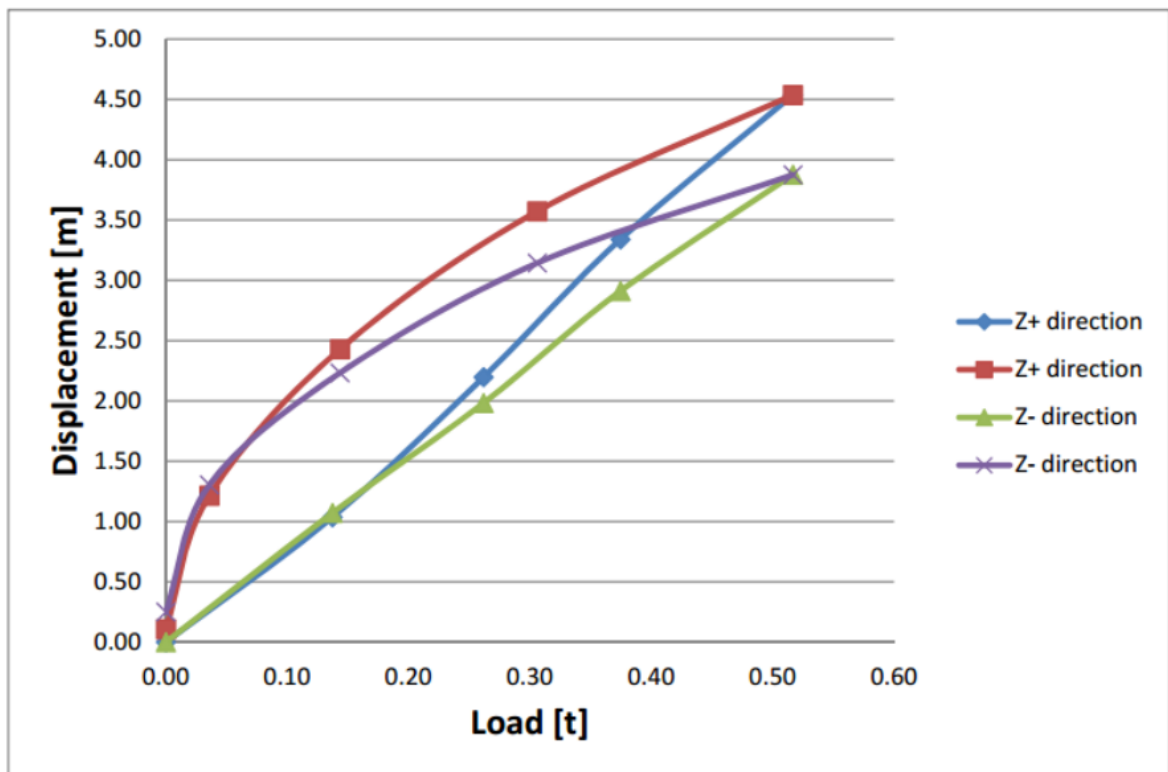
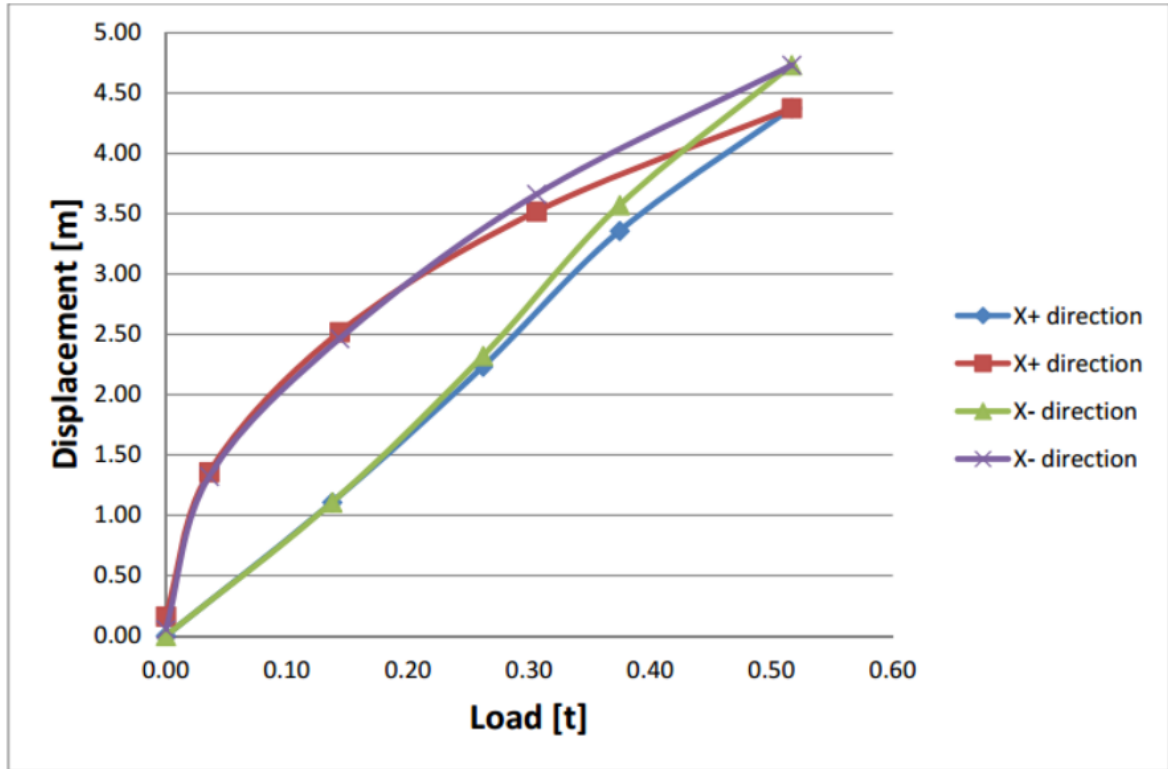
According to this equation, a longer length of the same wire (or section) will lead to overall a more flexible system. However, on a longer section the load per unit length is equal and will thus lead to a larger load that needs to be taken by this wire. A higher load means a higher required MBL and consequently a larger and stiffer wire. It was found that this scales approximately linear with the section length. In short, as longer sections are used also stiffer wires are required. The ultimate consequence is that the stiffness k is *equal* for a system with a section length of 100m, 200m or even 2km.

Two spring stiffness's are given; the most flexible one corresponds to a nylon rope and the high value is closer to polyester/aramid. Note that for the calculation of these values a unit load of 1kN/m is subjected to the system in order to find a maximum tension in the wire. In the ultimate state an angle of 45 degrees is utilized with 5% system stretch. A conservative safety factor of 1.5 is taken into account (the stiffer the system, the higher the loads and the easier it bridges).

Bending stiffness:

Apart from the model tests dedicated tests were conducted to determine the bending stiffness of the model. Two model segments were assessed by pulling with a known load in the model fixed X and Z directions. In both the X and Z direction positive and negative oriented loads were applied to make sure that the asymmetry due to the tension line was also taken into account. Please see [ER.1] for detailed information regarding the procedure and for the exact values.

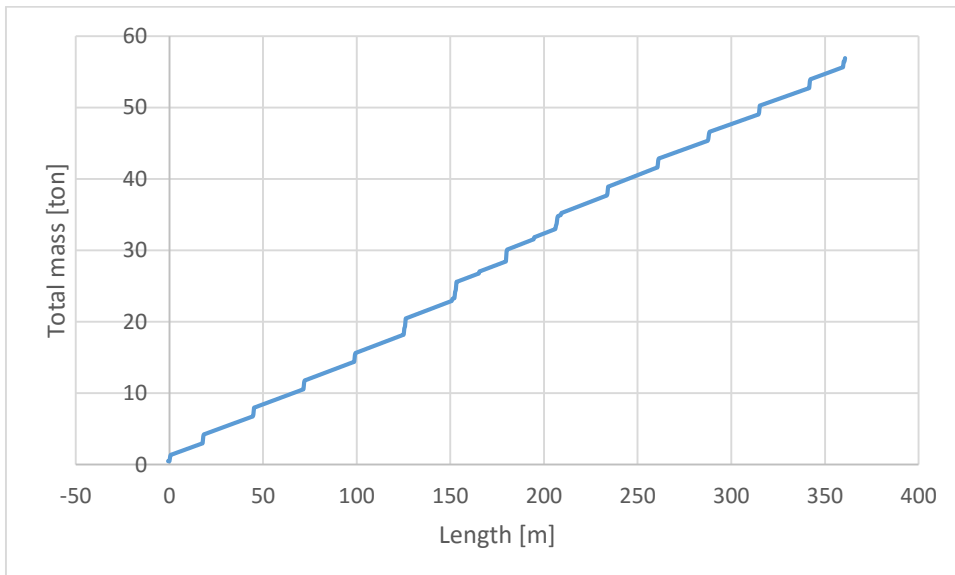
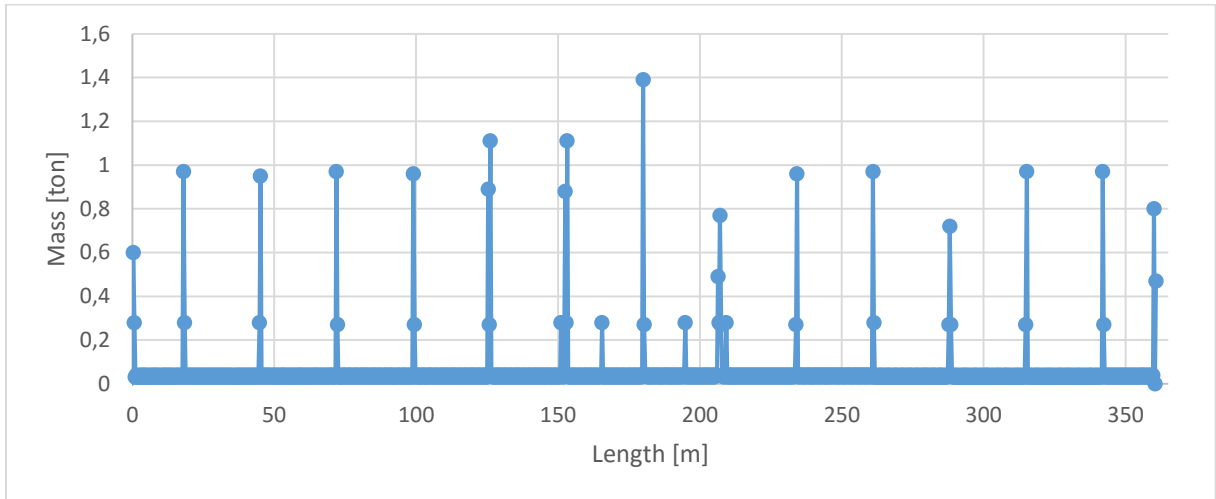






Weight distribution:

The dry weight distribution over the length is shown in the following figures. The spikes represent the connection points and sensors. Please see [ER.1] for detailed information regarding the procedure and for the exact values.





Appendix B - Load Cases (Carried Out)

Mooring (end connections)			Wave				Current	Marin Test No.
Type	Pretension		Type	H	T	Direction	Velocity	
[-]	[-]	[kN]	[-]	[m]	[s]	[deg]	[m/s]	
Low mooring	Low	58.4	Regular	6	7.3	225	0.3	702001
	Low	58.4	Regular	6	6.5	225	0.3	702002
	Low	58.4	Regular	3	5.2	225	0.3	702003
	Low	58.4	Regular	3	4.6	225	0.3	702004
	Low	58.4	Regular	3	5.2	270	0.3	702005
	Low	58.4	Regular	3	4.6	270	0.3	702006
	Low	58.4	Regular	6	7.3	270	0.3	702007
	Low	58.4	Regular	6	6.5	270	0.3	702008
	Low	58.4	Regular	6	7.3	180	0.3	702010
	Low	58.4	None	0	20	0	1	702011
	Low	58.4	Regular	3	5.2	270	1	702012
	Low	58.4	Regular	3	4.6	270	1	702013
	Low	58.4	Regular	6	7.3	270	1	702014
	Low	58.4	Regular	6	6.5	270	1	702015
	Low	58.4	Regular	3	5.2	225	1	702016
	Low	58.4	Regular	3	4.6	225	1	702017
	Low	58.4	Regular	6	7.3	225	1	702018
	Low	58.4	Regular	6	6.5	225	1	702019
	Low	58.4	Regular	6	7.3	180	1	702020
	High Mooring	Low	58.4	JONSWAP	6.25	8.45	225	1
Low		58.4	JONSWAP	6.25	8.45	270	1	704001
Low		58.4	JONSWAP	4	13	225	0.3	705001
Low		58.4	JONSWAP	4	13	270	0.3	706001
Low		58.4	None	0	20	0	0.3	706002
Low		58.4	Regular	3	5.2	270	0.3	802001
Low		58.4	Regular	3	4.6	270	0.3	802002
Low		58.4	Regular	3	5.2	225	0.3	802003
Low		58.4	Regular	3	4.6	225	0.3	802004
Low		58.4	Regular	6	7.3	225	0.3	802005
Low		58.4	Regular	6	6.5	225	0.3	802006
Low	58.4	Regular	6	7.3	180	0.3	802007	
Low	58.4	Regular	6	7.3	270	0.3	802008	
Low	58.4	Regular	6	6.5	270	0.3	802009	
Low	58.4	None	0			0.3	802010	
Low	58.4	None	0			1	802011	



Mooring (end connections)			Wave				Current	Marin Test No. [-]	
Type	Pretension		Type	H	T	Direction	Velocity		
[-]	[-]	[kN]	[-]	[m]	[s]	[deg]	[m/s]		
High mooring	Low	58.4	Regular	3	5.2	270	1	802012	
	Low	58.4	Regular	3	4.6	270	1	802013	
	Low	58.4	Regular	6	7.3	270	1	802014	
	Low	58.4	Regular	6	6.5	270	1	802015	
	Low	58.4	Regular	3	6	225	1	802016	
	Low	58.4	Regular	3	5.2	225	1	802017	
	Low	58.4	Regular	6	7.3	225	1	802019	
	Low	58.4	Regular	3	4.6	225	1	802020	
	Low	58.4	Regular	6	6.5	225	1	802021	
	Low	58.4	Regular	6	7.3	180	1	802022	
	Med	300	None	0				0.3	802023
	Med	300	Regular	3	5.2	270		0.3	802024
	Med	300	Regular	3	4.6	270		0.3	802025
	Med	300	Regular	3	5.2	225		0.3	802026
	Med	300	Regular	3	4.6	225		0.3	802027
	Med	300	Regular	6	7.3	225		0.3	802028
	Med	300	Regular	6	6.5	225		0.3	802029
	Med	300	Regular	6	7.3	270		0.3	802030
	Med	300	Regular	6	6.5	270		0.3	802031
	Med	300	Regular	6	7.3	180		0.3	802032
	Med	300	None	0				0.3	802033
	Med	300	Regular	3	5.2	270		0.3	802034
	Med	300	Regular	3	4.6	270		0.3	802035
	Med	300	Regular	3	5.2	225		0.3	802036
	Med	300	Regular	3	4.6	225		0.3	802037
	Med	300	Regular	6	7.3	270		0.3	802038
	Med	300	Regular	6	6.5	270		0.3	802039
	Med	300	Regular	6	7.3	225		0.3	802040
	Med	300	Regular	6	6.5	225		0.3	802041
	Med	300	Regular	6	7.29	180		0.3	802042
	Med	300	Regular	3	5.2	270		1	802043
	Med	300	Regular	3	4.6	270		1	802044
Med	300	Regular	6	7.3	270		1	802045	
Med	300	Regular	6	6.5	270		1	802046	
Med	300	Regular	3	5.2	225		1	802047	
Med	300	Regular	3	4.6	225		1	802048	
Med	300	Regular	6	7.3	225		1	802049	



Mooring (end connections)			Wave				Current	Marin Test No. [-]
Type	Pretension		Type	H	T	Direction	Velocity	
[-]	[-]	[kN]	[-]	[m]	[s]	[deg]	[m/s]	
High mooring	Med	300	Regular	6	6.5	225	1	802050
	High	878.3	Regular	6	6.5	225	1	802051
	High	878.3	Regular	6	7.3	225	1	802052
	High	878.3	Regular	3	4.6	225	1	802053
	High	878.3	Regular	3	5.2	225	1	802054
	High	878.3	Regular	6	6.5	270	1	802055
	High	878.3	Regular	6	7.3	270	1	802056
	High	878.3	Regular	3	4.6	270	1	802057
	High	878.3	Regular	6	7.3	180	1	802058
	High	878.3	None			180	1	802059
	Low	58.4	JONSWAP	6.25	8.45	225	1	803002
	Med	300	None	0			1	803003
	Med	300	JONSWAP	6.25	8.45	225	1	803004
	High	878.3	JONSWAP	6.25	8.45	225	1	803005
	Low	58.4	JONSWAP	6.25	8.45	270	1	804001
	Low	58.4	JONSWAP	4	13	225	0.3	805001
	Med	300	JONSWAP	4	13	225	0.3	805002
	Low	58.4	JONSWAP	4	13	270	0.3	806001
Secondary mooring	Low	58.4	Regular	3	6	225	0	902004
	Low	58.4	Regular	3	6	270	0	902005
	Low	58.4	Regular	3	5.2	270	0	902006
	Low	58.4	Regular	3	4.6	270	0	902007
	Low	58.4	Regular	6	7.3	80	0	902009
	Low	58.4	Regular	3	5.2	225	0	902010
	Low	58.4	Regular	6	7.3	225	0	902011
	Low	58.4	None	0			0.3	902012
	Low	58.4	Regular	3	6	270	0.3	902013
	Low	58.4	Regular	3	5.2	270	0.3	902014
	Low	58.4	Regular	3	4.6	270	0.3	902015
	Low	58.4	Regular	3	6	225	0.3	902016
	Low	58.4	Regular	3	5.2	225	0.3	902017
	Low	58.4	Regular	3	4.6	225	0.3	902018
	Low	58.4	Regular	6	8.5	270	0.3	902019
Low	58.4	Regular	6	7.3	270	0.3	902020	



Mooring (end connections)			Wave				Current	Marin Test No. [-]
Type	Pretension		Type	H	T	Direction	Velocity	
[-]	[-]	[kN]	[-]	[m]	[s]	[deg]	[m/s]	
Secondary Mooring	Low	58.4	Regular	6	6.5	270	0.3	902021
	Low	58.4	Regular	6	7.3	225	0.3	902023
	Low	58.4	Regular	6	8.5	225	0.3	902024
	Low	58.4	Regular	6	6.5	225	0.3	902025
	Low	58.4	Regular	6	7.3	180	0.3	902026
	Low	58.4	None	0			1	902027
	Low	58.4	Regular	3	6	270	1	902028
	Low	58.4	Regular	3	5.2	270	1	902029
	Low	58.4	Regular	3	4.6	270	1	902030
	Low	58.4	Regular	3	6	225	1	902031
	Low	58.4	Regular	3	5.2	225	1	902032
	Low	58.4	Regular	3	4.6	225	1	902033
	Low	58.4	Regular	6	8.5	270	1	902034
	Low	58.4	Regular	6	7.3	270	1	902035
	Low	58.4	Regular	6	6.5	270	1	902036
	Low	58.4	Regular	6	7.3	225	1	902038
	Low	58.4	Regular	6	8.5	225	1	902039
	Low	58.4	Regular	6	6.5	225	1	902040
	Low	58.4	Regular	6	7.3	180	1	902041
	Low	58.4	JONSWAP	6.25	8.45	225	1	903001
Low	58.4	JONSWAP	6.25	8.45	270	1	904001	
Low	58.4	JONSWAP	4	13	225	0.3	905001	
Low	58.4	JONSWAP	4	13	270	0.3	906001	



Appendix C - Overtopping & Bridging

Overtopping in regular waves:

Type	Pretension	Wave			Current Velocity	Marin Test No.	Data	
		H	T	Dir			Overtopping	Bridging
[-]	[kN]	[m]	[s]	[deg]	[m/s]	[-]	[-]	
Low mooring	Low	6	7,3	225	0,3	702001	no	no
	Low	6	6,5	225	0,3	702002	no	no
	Low	3	5,2	225	0,3	702003	no	no
	Low	3	4,6	225	0,3	702004	no	no
	Low	3	5,2	270	0,3	702005	no	no
	Low	3	4,6	270	0,3	702006	no	no
	Low	6	7,3	270	0,3	702007	no	no
	Low	6	6,5	270	0,3	702008	no	no
	Low	6	7,3	180	0,3	702010	no	no
	Low	3	5,2	270	1	702012	no	no
	Low	3	4,6	270	1	702013	probably	probably
	Low	6	7,3	270	1	702014	no	no
	Low	6	6,5	270	1	702015	probably	probably
	Low	3	5,2	225	1	702016	no	no
	Low	3	4,6	225	1	702017	yes	no
	Low	6	7,3	225	1	702018	no	no
Low	6	6,5	225	1	702019	yes	no	
Low	6	7,3	180	1	702020	no	no	
High Mooring	Low	3	5,2	270	0,3	802001	no	no
	Low	3	4,6	270	0,3	802002	no	no
	Low	3	5,2	225	0,3	802003	no	no
	Low	3	4,6	225	0,3	802004	no	no
	Low	6	7,3	225	0,3	802005	no	no
	Low	6	6,5	225	0,3	802006	no	no
	Low	6	7,3	180	0,3	802007	no	no
	Low	6	7,3	270	0,3	802008	no	no
	Low	6	6,5	270	0,3	802009	no	no
	Low	3	5,2	270	1	802012	no	no
	Low	3	4,6	270	1	802013	no	probably
	Low	6	7,3	270	1	802014	no	no



Type	Pretension	Wave			Current	Marin Test No.	Data	
		H	T	Dir			Velocity	Overtopping
[-]	[kN]	[m]	[s]	[deg]	[m/s]	[-]	[-]	
Low	6	6,5	270	1	802015	no	no	
Low	3	6	225	1	802016	no	no	
Low	3	5,2	225	1	802017	no	no	
Low	6	7,3	225	1	802019	no	no	
Low	3	4,6	225	1	802020	no	no	
Low	6	6,5	225	1	802021	yes	no	
Low	6	7,3	180	1	802022	no	no	
Med	3	5,2	270	0,3	802024	no	probably	
Med	3	4,6	270	0,3	802025	no	probably	
Med	3	5,2	225	0,3	802026	no	no	
Med	3	4,6	225	0,3	802027	no	no	
Med	6	7,3	225	0,3	802028	probably	no	
Med	6	6,5	225	0,3	802029	yes	no	
Med	6	7,3	270	0,3	802030	no	no	
Med	6	6,5	270	0,3	802031	no	no	
Med	6	7,3	180	0,3	802032	no	no	
Med	3	5,2	270	0,3	802034	no	no	
Med	3	4,6	270	0,3	802035	no	no	
Med	3	5,2	225	0,3	802036	no	no	
Med	3	4,6	225	0,3	802037	probably	no	
Med	6	7,3	270	0,3	802038	no	no	
Med	6	6,5	270	0,3	802039	no	no	
Med	6	7,3	225	0,3	802040	no	no	
Med	6	6,5	225	0,3	802041	yes	no	
Med	6	7,29	180	0,3	802042	no	no	
Med	3	5,2	270	1	802043	no	no	
Med	3	4,6	270	1	802044	no	probably	
Med	6	7,3	270	1	802045	probably	no	
Med	6	6,5	270	1	802046	yes	yes	
Med	3	5,2	225	1	802047	no	no	
Med	3	4,6	225	1	802048	yes	probably	
Med	6	7,3	225	1	802049	no	no	
Med	6	6,5	225	1	802050	yes	no	



Type	Pretension	Wave			Current	Marin Test No.	Data	
		H	T	Dir			Velocity	Overtopping
[-]	[kN]	[m]	[s]	[deg]	[m/s]	[-]	[-]	
	High	6	6,5	225	1	802051	yes	no
	High	6	7,3	225	1	802052	no	no
	High	3	4,6	225	1	802053	probably	probably
	High	3	5,2	225	1	802054	no	no
	High	6	6,5	270	1	802055	yes	probably
	High	6	7,3	270	1	802056	probably	probably
	High	3	4,6	270	1	802057	probably	probably
	High	6	7,3	180	1	802058	no	no
Secondary mooring	Low	3	6	225	0	902004	no	no
	Low	3	6	270	0	902005	no	no
	Low	3	5,2	270	0	902006	no	no
	Low	3	4,6	270	0	902007	no	no
	Low	6	7,3	180	0	902009	no	no
	Low	3	5,15	225	0	902010	no	no
	Low	6	7,3	225	0	902011	no	no
	Low	3	6	270	0,3	902013	no	no
	Low	3	5,2	270	0,3	902014	no	no
	Low	3	4,6	270	0,3	902015	no	no
	Low	3	6	225	0,3	902016	no	no
	Low	3	5,2	225	0,3	902017	no	no
	Low	3	4,6	225	0,3	902018	no	no
	Low	6	8,5	270	0,3	902019	no	no
	Low	6	7,3	270	0,3	902020	no	no
	Low	6	6,5	270	0,3	902021	no	no
	Low	6	7,3	225	0,3	902023	no	no
	Low	6	8,5	225	0,3	902024	no	no
	Low	6	6,5	225	0,3	902025	no	no
	Low	6	7,3	180	0,3	902026	no	no
	Low	3	6	270	1	902028	no	no
	Low	3	5,2	270	1	902029	no	no
Low	3	4,6	270	1	902030	no	no	
Low	3	6	225	1	902031	no	no	
Low	3	5,2	225	1	902032	no	no	



Type	Pretension	Wave			Current	Marin Test No.	Data	
		H	T	Dir			Velocity	Overtopping
[-]	[kN]	[m]	[s]	[deg]	[m/s]	[-]	[-]	
	Low	3	4,6	225	1	902033	no	no
	Low	6	8,5	270	1	902034	no	no
	Low	6	7,3	270	1	902035	no	no
	Low	6	6,5	270	1	902036	yes	no
	Low	6	7,3	225	1	902038	yes	no
	Low	6	8,5	225	1	902039	no	no
	Low	6	6,5	225	1	902040	yes	no
	Low	6	7,3	180	1	902041	no	no

Overtopping in irregular waves:

Type	Pretension	Wave			Current	Marin Test No.	Data	
		H	T	Dir			Velocity	Overtopping
[-]	[kN]	[m]	[s]	[deg]	[m/s]	[-]	[-]	
Low mooring	Low	6.25	8.45	225	1	703001	yes	no
	Low	6.25	8.45	270	1	704001	yes	yes
	Low	4	13	225	0.3	705001	no	no
	Low	4	13	270	0.3	706001	no	no
High mooring	Med	6.25	8.45	225	1	803004	yes	no
	Low	6.25	8.45	225	1	803002	yes	no
	Low	4	13	225	0.3	805001	no	no
	High	6.25	8.45	225	1	803005	yes	no
	Low	6.25	8.45	270	1	804001	yes	probably
	Med	4	13	225	0.3	805002	no	no
	Low	4	13	270	0.3	806001	no	no
Secondary mooring	Low	6.25	8.45	225	1	903001	yes	no
	Low	6.25	8.45	270	1	904001	yes	no
	Low	4	13	225	0.3	905001	no	no
	Low	4	13	270	0.3	906001	no	no

Appendix D - Photos



Figure 7-1: High mooring low pretension 225 deg ULS

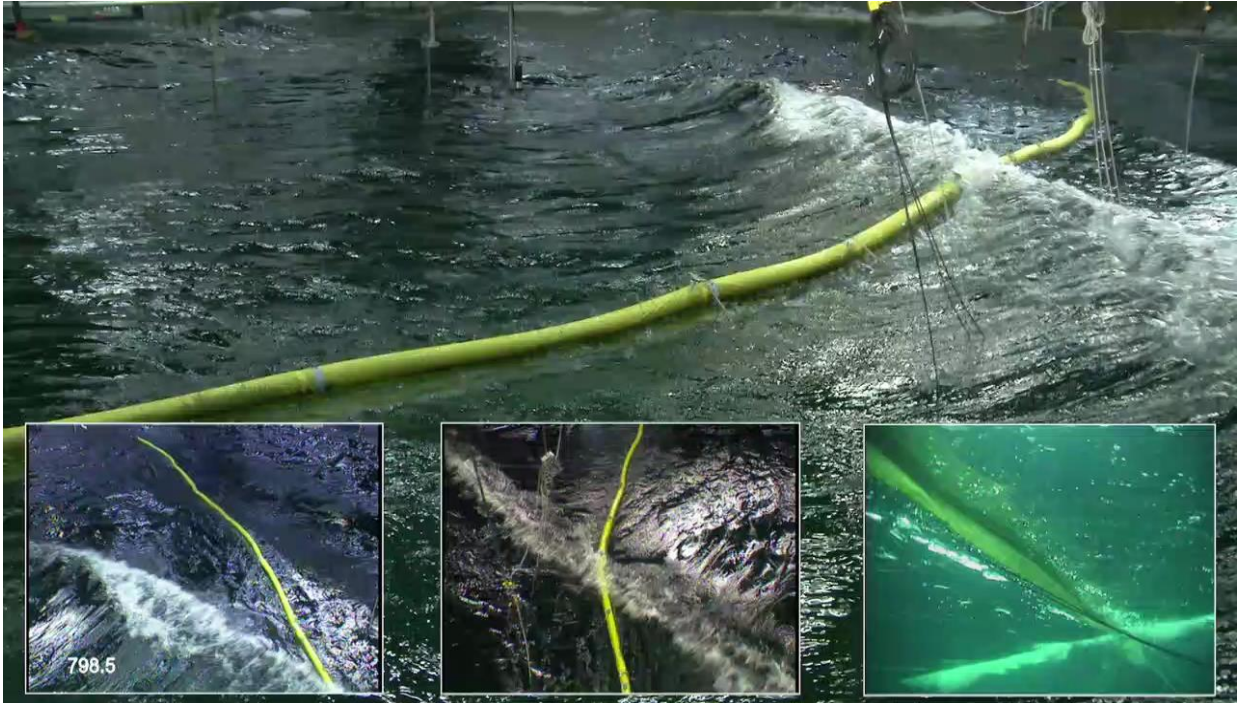


Figure 7-2: High mooring med pretension 225 deg ULS

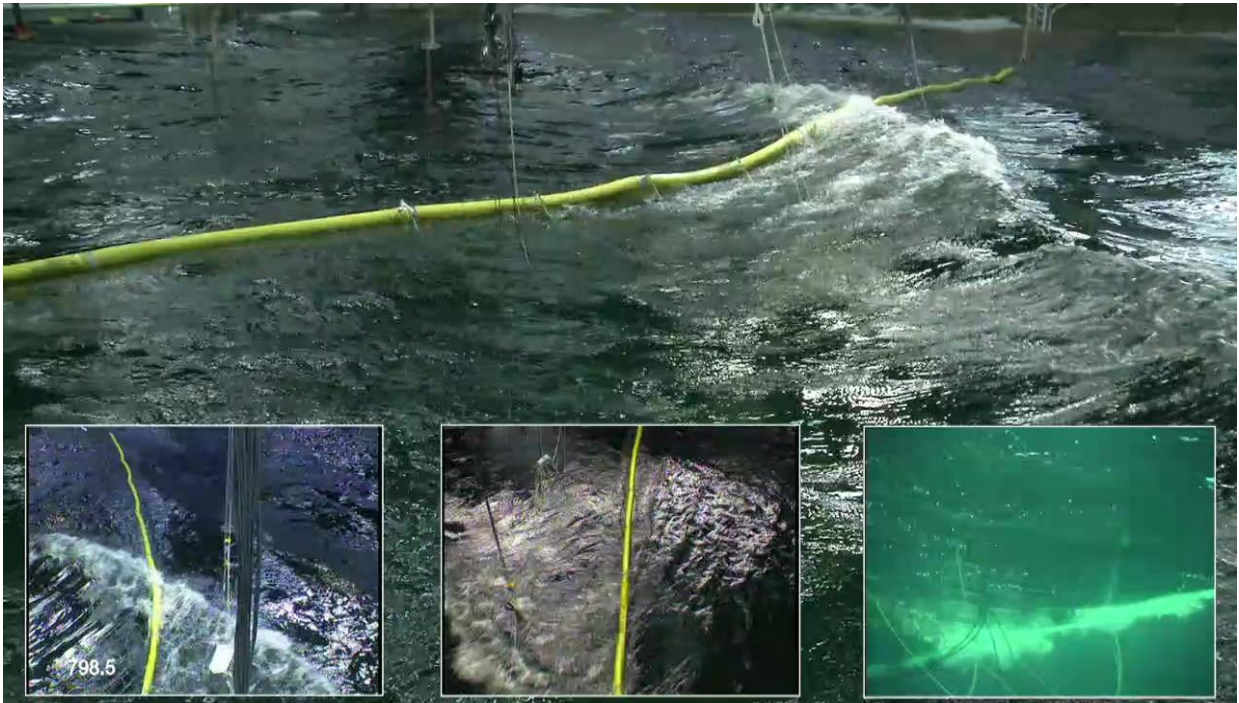


Figure 7-3: High mooring high pretension 225 deg ULS

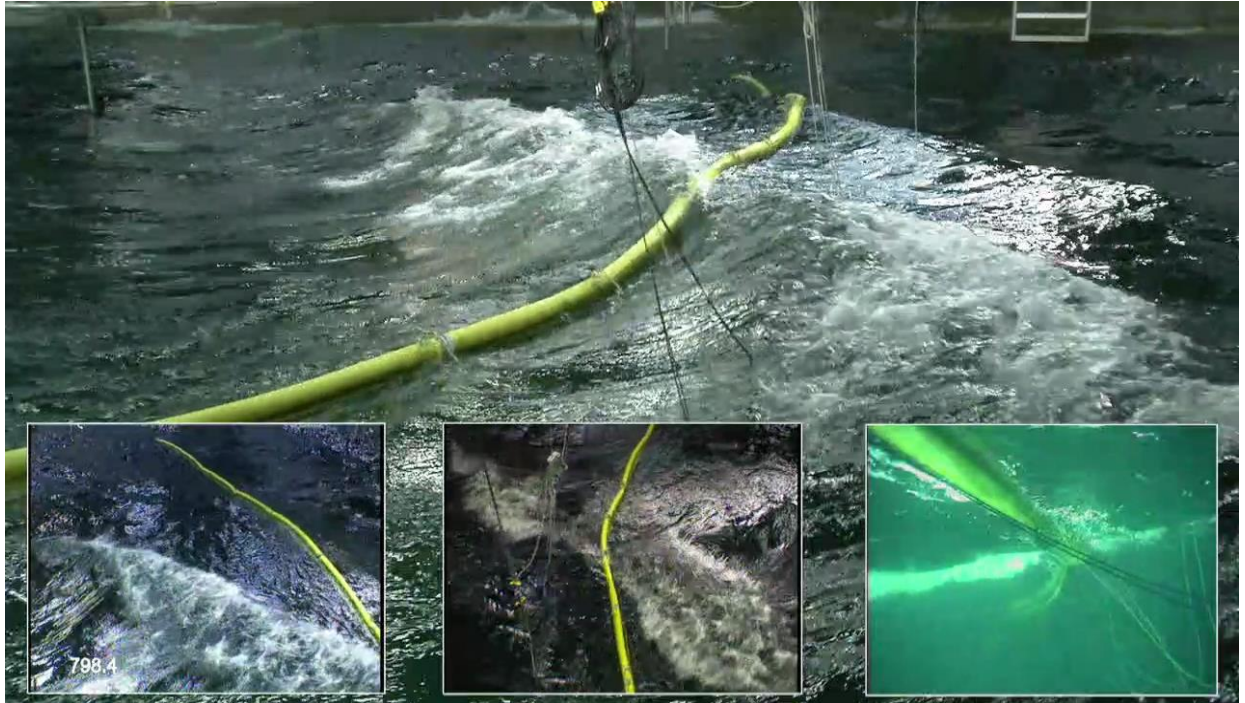


Figure 7-4: Low mooring 225 deg ULS

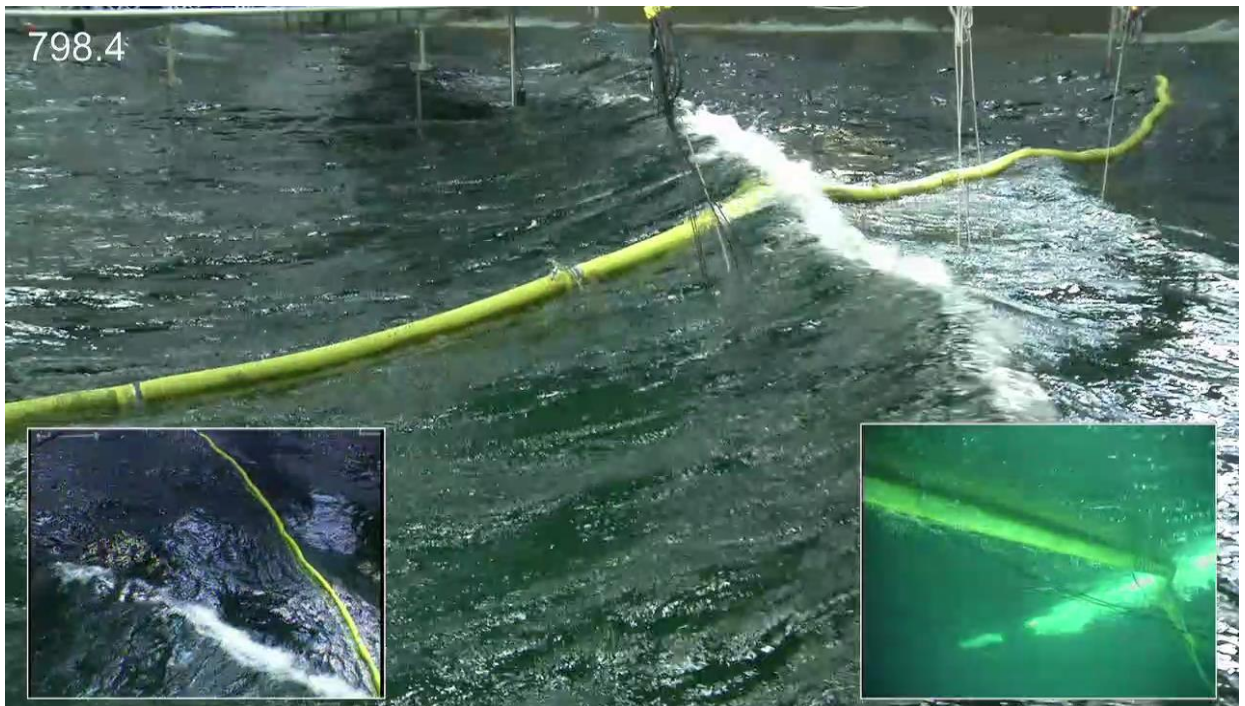


Figure 7-5: Secondary mooring 225 deg ULS

